Microbiology of Barrier Component Analogues of a Deep Geological Repository

by

Rachel Beaver

A thesis
presented to the University of Waterloo
in fulfillment of the
thesis requirement for the degree of
Master of Science
in
Biology

Waterloo, Ontario, Canada, 2020

Author's Declaration

This thesis consists of material all of which I authored or co-authored: see Statement of Contributions included in the thesis. This is a true copy of the thesis, including any required final revisions, as accepted by my examiners.

I understand that my thesis may be made electronically available to the public.

Statement of Contributions

Chapter 2

The Tsukinuno bentonite sampling was coordinated by Erik Kremmer (NWMO). The Opalinus core was received from Niels Burzan and Rizlan Bernier-Latmani (École Polytechnique Fédérale de Lausanne, Switzerland). The Northern Ontario crystalline rock core sampling was coordinated by Jeff Binns (Nuclear Waste Management Organization). Sian Ford (McMaster University) swabbed the outer layer of the Northern Ontario crystalline rock core and crushed the inner layer. Melody Vachon (University of Waterloo) assisted with the cultivation of anaerobic heterotrophs and SRB.

Abstract

Many countries are in the process of designing and implementing long-term storage solutions for used nuclear fuel. Like many of these countries, Canada is considering a deep geological repository (DGR) wherein used fuel bundles will be placed in copper-coated carbon steel used fuel containers encased in bentonite buffer boxes. Previously published research has simulated aspects of a DGR experimentally to identify DGR conditions that would prevent microbial activity. Although such microcosm-type experiments can observe microbial growth and activity over relatively limited time frames, a DGR will remain functional for at least a million years, and will be exposed to fluctuating environmental conditions. To address these temporal limitations, there is value to examining ancient natural barrier components that serve as analogues for future DGR components. My research explored the abundance, viability, and composition of microorganisms in ancient natural DGR barrier component analogues using a combination of cultivation- and DNA-based approaches. Samples were obtained from the Tsukinuno bentonite deposit (Japan) that formed in the late Miocene (~10 million years ago), the Opalinus clay formation (Switzerland) that formed approximately 174 million years ago, and Canadian shield crystalline rock from Northern Ontario. Given sample logistics and site-access considerations, most cultivation and molecular analyses focussed on the Tsukinuno bentonite clay samples, although the other site samples were included for comparison using a subset of techniques.

Aerobic heterotroph abundances were relatively low for all Tsukinuno bentonite samples, ranging from 4.1×10^1 to 1.1×10^4 colony forming units per gram dry weight (CFU/gdw). Anaerobic heterotrophs were only detected in half of the Tsukinuno bentonite samples and ranged in abundance from 4.5×10^1 CFU/gdw to 9.9×10^2 CFU/gdw. Sulfate-reducing bacteria were only detected in one sample by cultivation, with a very low estimate of 5 MPN/gdw. Overall, culturable microbial abundances were lower than nucleic acid targets detected by quantitative PCR (Wilcoxon signed ranks test; $p < 0.05$). A range of 3.2×10^1 to 7.2×10^7 (average of 5.7×10^6) 16S ribosomal RNA (16S rRNA) gene copies/gdw was

detected in the Tsukinuno bentonite samples, and averages of 1.2 x 10^3 16S rRNA gene copies/gdw and 1.1 x 10^3 16S rRNA gene copies/gdw were measured for the Opalinus clay and Northern Ontario crystalline rock (NOCR) core samples, respectively. Because this research did not use cultivation-based approaches for Opalinus clay and NOCR samples, and PCR-based technique cannot distinguish DNA from cells and extracellular DNA, future research would be required to determine whether the detected DNA was associated with viable microorganisms.

Analysis of 16S rRNA gene amplicons revealed that three of the Tsukinuno bentonite samples were dominated by putative aerobic heterotrophs and fermenting bacteria from the *Actinobacteria* phylum, whereas five of the Tsukinuno bentonite samples were dominated by sequences similar to those from acidophilic chemolithoautotrophs capable of sulfur reduction. The remaining two Tsukinuno bentonite samples had nucleic acid profiles below reliable detection limits, generating inconsistent replicate 16S rRNA gene profiles and probable contaminant sequences. The NOCR and Opalinus clay samples also yielded inconsistent replicate 16S rRNA gene profiles, implying undetectable nucleic acids in those rock samples and profiles indistinguishable from contaminant sequences.

Total genomic DNA from Tsukinuno clay cultures was extracted and 16S rRNA genes were amplified and sequenced. Representatives of the phyla *Bacteroidetes*, *Proteobacteria*, *Actinobacteria*, and *Firmicutes* were identified in the aerobic heterotroph cultures, and additional bacteria from the phyla *Actinobacteria* and *Firmicutes* were isolated in the cultures of anaerobic heterotrophs and fermenting bacteria. Only one nucleic acid sequence detected from a culture was also detected in its corresponding clay sample, suggesting that nucleic acids from culturable bacteria were relatively rare within the clay samples. Sequencing of DNA extracted from the sulfate reducing bacteria culture revealed that the taxon present in the culture was affiliated with the *Desulfosporosinus* genus, which was not detected in the corresponding clay sample.

Acknowledgements

I would like to thank everyone who helped and supported me throughout the completion of this degree. First, I would like to thank my supervisor, Josh Neufeld, for his continued support and enthusiasm, and for providing the resources necessary to complete this research. I would also like to thank the remainder of my committee, Barb Butler and Trevor Charles, for their opinions and insight.

Thank you to the Neufeld lab members for their continued input and for making the lab such an enjoyable place to spend the last two years. I would like to specifically thank Katja Engel for her continued input and help with troubleshooting throughout this project, and Daniel Min and Jackson Tsuji for technical support with QIIME2, R, and Python.

Thank you to the people who collected the clay and rock samples, without which this research would not have been possible, and to the Nuclear Waste Management Organization, Ontario Research Fund, and the Natural Sciences and Engineering Research Council for funding this research.

Finally, I would like to thank my family and friends for their ongoing support.

Table of Contents

List of Figures

List of Tables

List of Abbreviations

Acetyl-CoA	Acetyl-coenzyme A
ANME	Anaerobic methanotrophic
AOM	Anaerobic oxidation of methane
APM	Adaptive phased management
ASV	Amplicon sequence variant
ATP	Adenosine triphosphate
BSA	Bovine serum albumin
CANDU	CANada Deuterium Uranium
CFU	Colony forming units
CH_4	Methane
Cl^-	Chloride
CO_2	Carbon dioxide
DGR	Deep geological repository
Fe^{2+}	Iron(II)
Fe^{3+}	Iron(III)
gdw	Gram dry weight
H_2	Dihydrogen
HS^-	Bisulfide
MAG	Metagenome assembled genome
MIC	Microbiologically influenced corrosion
MPN	Most probable number
N_2	Dinitrogen
NH_4^+	Ammonium
NO_2^-	Nitrite
NO_3^-	Nitrate
NOCR	Northern Ontario crystalline rock
NWMO	Nuclear Waste Management Organization
OTU	Operational taxonomic unit

PCR	Polymerase chain reaction
PLFA	Phospholipid fatty acid
qPCR	Quantitative polymerase chain reaction
QIIME2	Quantitative Insights into Microbial Ecology 2
r	Pearson correlation
r_s	Spearman correlation
R2A	Reasoner's 2A
rRNA	Ribosomal RNA
S^0	Elemental sulfur
S^{2-}	Sulfide
$S_2O_3^{2-}$	Thiosulfate
SO_4^{2-}	Sulfate
SRB	Sulfate reducing bacteria
TCA	Tricarboxylic acid
UFC	Used fuel container

Chapter 1

Introduction and literature review

1.1 Canadian used nuclear fuel

Canadian nuclear reactors, also known as CANDU reactors, use solid uranium dioxide as fuel. Uranium dioxide powder is pressed to form small fuel pellets, which are stacked together and housed in a zirconium alloy casing to form fuel pencils that are then welded together within bundles, which is the "battery" that fuels a nuclear reactor (Figure 1.1) [2]. After a fuel bundle has served its purpose in a nuclear reactor and is removed, it remains radioactive and must be stored safely for approximately one million years until it returns to the radioactivity level of naturally occurring uranium (Figure 1.2) [4]. Considering both the existing used nuclear fuel and an additional 90,000 used fuel bundles that are produced every year from use in Canadian reactors, projections suggest that 5.5 million used fuel bundles must be stored by the end of current Canadian nuclear reactor lifetimes [5].

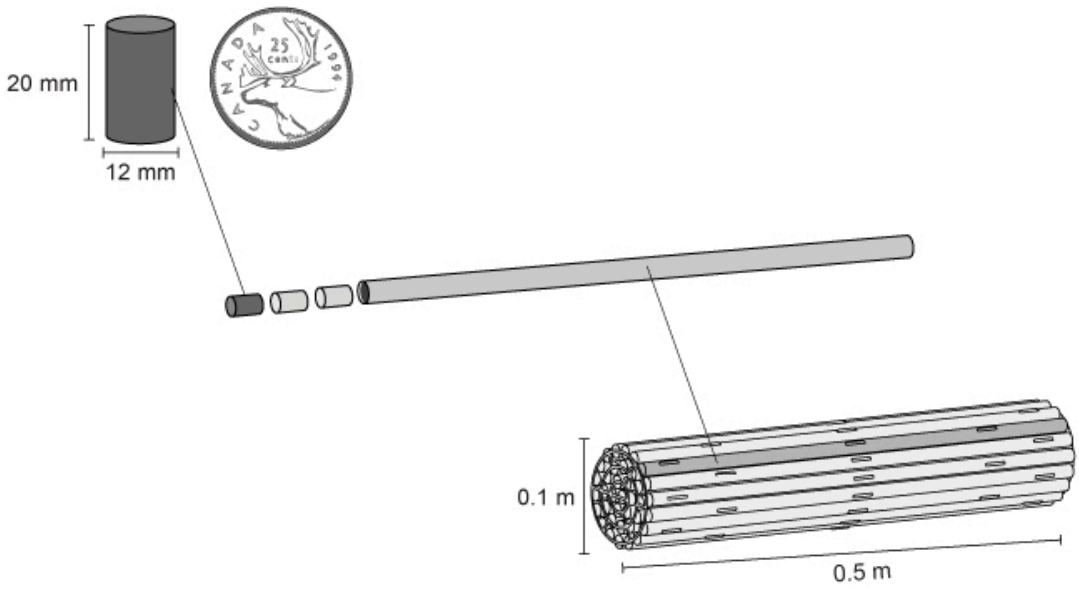

Figure 1.1 Nuclear fuel pellets stacked to form "pencils" that are welded into fuel bundles [1].

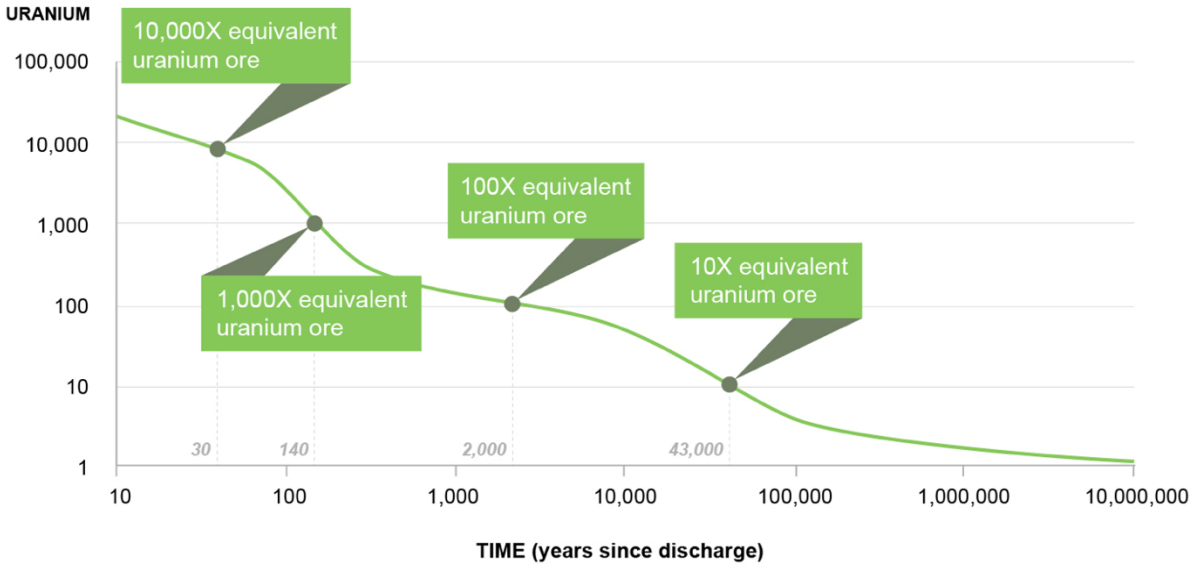

Figure 1.2 Radioactivity of irradiated uranium over time compared to the radioactivity of uranium ore [3].

1.2 Storage of used nuclear fuel

Currently, used nuclear fuel bundles are stored in water-filled pools for the first seven to ten years after removal from a nuclear reactor while their heat and radioactivity decreases [6]. After removal from the pools, used fuel bundles are stored in dry storage containers, silos, or vaults, made of reinforced high-density concrete, lined inside and outside with steel plates. To ensure continued isolation of the used nuclear fuel, dry storage containers must be assessed and potentially replaced after 50 years. In addition, in the absence of a deep geological repository, the facilities that house the dry storage containers would require rebuilding or refurbishing many times over the next million years through multiple glaciation cycles [6].

The Nuclear Waste Management Organization (NWMO) was established in 2002 with the goal of designing and implementing a long-term storage plan for Canada's used nuclear fuel. The NWMO proposes a plan called adaptive phased management, which will end in the storage of Canada's used nuclear fuel in a deep geological repository (DGR) located 500-1000 m belowground in a stable host rock [7] (Figure 1.3). Deep geological repositories are

widely accepted to be the best option for the long-term storage of used nuclear fuel, and their design and implementation is underway in many countries. The proposed DGR design incorporates a multibarrier system to ensure the continued protection of the used nuclear fuel even in the event of a barrier failure [8]. The first two barriers are innate to the nuclear fuel itself, because it is a stable solid, and the zirconium alloy that houses the fuel is corrosion resistant. Used fuel bundles will be packed into used fuel containers (UFCs), made of structurally stable steel, coated in copper for corrosion resistance (Figure 1.3) [8]. Next, UFCs will be encased in buffer boxes made of highly compacted bentonite clay with a dry density of at least 1700 kg/m^3 and initial water content of approximately 20% (Figure 1.3). Once placement of bentonite buffer boxes in the DGR is complete, void spaces will be filled in with additional bentonite clay backfill [9].

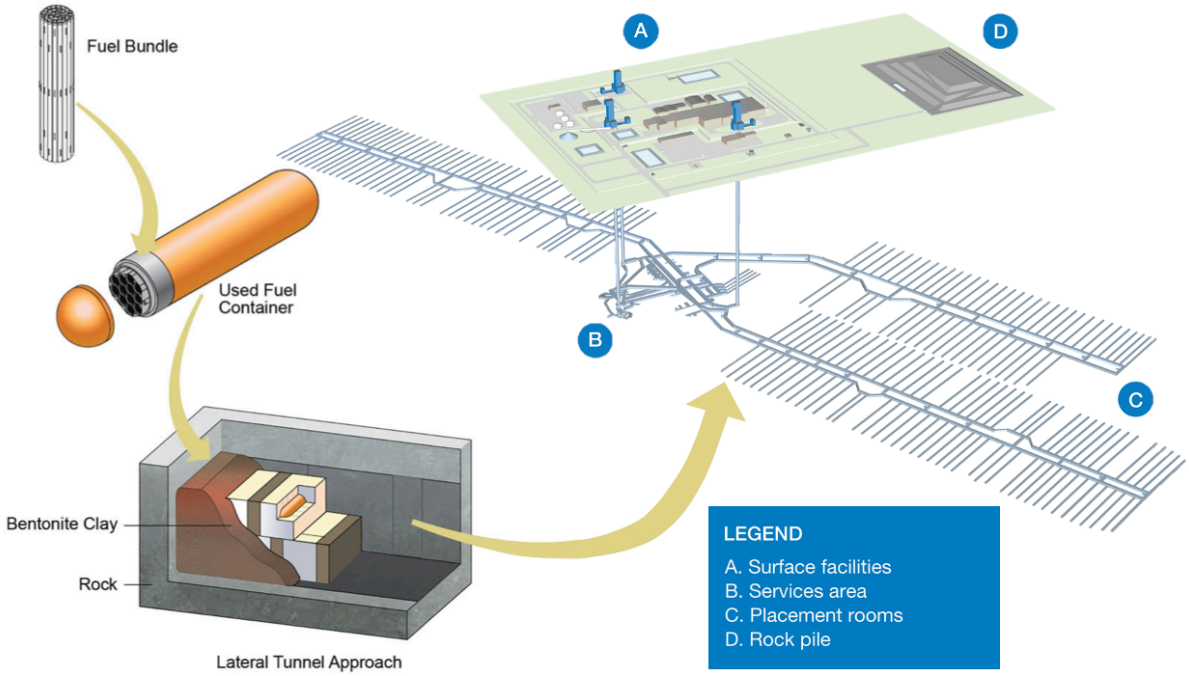

Figure 1.3 Theoretical design of a deep geological repository. Modified from [10, 11].

1.3 Bentonite clay

Bentonite is a type of clay formed by the weathering of volcanic tuff, porous rock created by the consolidation of volcanic ash, and is defined by the presence of montmorillonite, the most

abundant mineral of the water-absorbing smectite clay minerals [12, 13]. A structural unit of montmorillonite consists of a sheet of tetrahedrally coordinated silica on either side of an octahedrally coordinated sheet of aluminum ions [14]. This structure repeats, with exchangeable cation layers between structural units, and weak van der Waals forces holding structural units together to form montmorillonite particles with an average size of 0.5 μm [13, 14]. There are two main classifications of bentonites: sodium and calcium. When the exchangeable cation layer consists primarily of sodium ions, the attraction between sodium ions and the negatively charged structural units of montmorillonite is weak, and the hydration of sodium ions with water results in an increase in the distance between structural units, which is observed as clay swelling. In contrast, calcium ions are more strongly attracted to the montmorillonite structural units, and when water hydrates calcium-dominated exchangeable cation layers, the water does not push structural units apart, thus swelling is not observed [12, 13]. In addition to montmorillonite, bentonite clays can contain variable amounts of other minerals such as quartz and feldspar [12].

It is the swelling capacity of bentonite clays that make them an ideal buffer material in a DGR. High swelling creates a small pore size that can prevent microbial growth and stabilizes the material mechanically. Additionally, bentonite has a low hydraulic permeability, which prevents flow path formation to and from the host rock [15]. This would interfere with transport of gases and fluids that could result in UFC corrosion and increased microbial activity, and, in combination with bentonite's adsorptive properties, would immobilize radionuclides in the case of a container failure [15].

1.4 Environmental conditions of a DGR

Once placement is complete, the environment of the DGR is expected to change temporally due to the high amounts of heat that will be generated initially by radioactive decay of the used nuclear fuel. These temperature-related changes will involve three main stages. During the first stage, the temperature will be at its highest, which will cause drying and shrinking of the bentonite buffer [7]. Models predict that a maximum container surface temperature of

84°C will be achieved after 45 years [16]. Although the rate of transport of dissolved species to and from the UFC will be slower, diffusion of gaseous species could be more rapid [9]. The second stage begins when temperatures decrease after the initial heat release from radioactive decay. Lower temperatures will allow bentonite resaturation, a process estimated to take 50 years in the case of a crystalline host rock and 5000 years in the case of a sedimentary host rock [9]. The third and final stage will begin when temperatures have equilibrated and bentonite has saturated, and will continue indefinitely [7].

Oxygen availability in a DGR is another factor that will change over time. Deep ground waters, where the DGR will be located, are anoxic, thus the only oxygen available in the DGR will be that trapped inside at the time of closure [9]. Initial models suggested that oxygen may persist within a DGR for several decades [17]. These models accounted for diffusion of oxygen into the surrounding host rock and chemical reactions consuming oxygen, but failed to consider the oxygen-consuming role of aerobic microorganisms potentially living within bentonite clay [17]. A more recent experiment simulating the implementation of a DGR in the Opalinus clay formation in Switzerland predicted that oxygen would be consumed within two to three months after closure [18].

Although UFCs will not come into direct contact with ground water, they will be adjacent to bentonite clay pore water, which will resaturate with ground water after temperatures cool within the DGR. Thus, after the initial high temperature stage, the contents of the ground water will play a substantial role in determining the corrosive conditions. Deep ground waters associated with crystalline and sedimentary host rocks in Canada are generally saline, with sodium concentrations between 0.1 and 0.5 M [9]. Sodium and calcium ions are the dominant cations in deep ground water, and both sulfate and bicarbonate are present at lower concentrations [9]. The anions of greatest interest in a DGR are sulfide (S^{2-}), which is ionized to bisulfide (HS^-) in aqueous conditions, and chloride (Cl^-), which may contribute to the corrosion of copper surrounding the UFCs [19]. Once all initially present O_2 has been consumed, UFC corrosion is expected to predominantly occur in the presence of sulfide [9].

Importantly, the ground waters in locations being considered for the placement of a DGR in Canada contain no detectable dissolved sulfide [9]. This means that the only possible source of sulfide in the DGR is through the metabolic reduction of sulfate to sulfide by sulfate-reducing bacteria (SRB) [9].

1.5 Importance of studying DGR microbiology

In general, DGRs are predicted to be inhospitable environments for microbial activity as a result of limited water availability, lack of space, increased mechanical force (due to the highly compacted nature of saturated bentonite clay), limited nutrient availability, high temperatures, and radiation surrounding the UFCs [20]. Nonetheless, early studies using cultivation techniques predicted that microorganisms are naturally found in environments deep underground [21, 22], thus necessitating the need to study their potential role in the long term safety of a DGR. Between 10^5 and 10^8 culturable bacteria/gram dry weight (gdw) were found in sandy aquifer sediments to depths of 265 m, and $<10^3$ culturable bacteria/gdw were estimated in clay-dominated layers of aquifer systems [21]. Microorganisms at this depth were primarily heterotrophic and physiologically flexible, and their community size was positively correlated with hydraulic conductivity, pore size, and water availability [21]. Another study examined Yucca Mountain volcanic rock, a proposed host rock for an American DGR, showing average total microscopic counts between $<10^4$ cells/gdw (the detection limit) and 10^5 cells/gdw, with orders of magnitude fewer cells estimated by cultivation on R2A agar [22].

1.6 Biogeochemical cycling relevant to a DGR

The construction of a DGR will change the natural deep subsurface environment and its naturally occurring microbial communities through the introduction of oxygen, water, space, nutrients, and exogenous microorganisms, which may initially favour growth of aerobes and facultative anaerobes [23]. Once oxygen and nutrients have been consumed, the DGR is expected to return to reducing conditions. In the absence of oxygen, light, and readily available organic matter, chemolithoautotrophic forms of primary production may be favoured. With respect to microbial metabolism, production of gases and sulfide are of

particular importance due to their implications in DGR longevity. The production of sufficient volumes of gases could lead to the formation of fissures in the clay or host rock, which would increase groundwater and ion transport to the UFCs [24]. Metabolic sulfide production is an important consideration because it can corrode metals, including the copper and steel of UFCs (equation 1) through a process called microbiologically influenced corrosion (MIC). Microbiologically influenced corrosion refers to occurrences of corrosion initiated or propagated by metabolic compounds produced by microorganisms. It is an issue that has been observed in a wide range of environments where metals are placed underground or underwater, including underwater steel bridge foundations [25], underground pipes [26], drilling and pumping pipes [27], underground [28] and subsea oil pipelines [29], concrete in sewer systems [30], and dental implants [31]. The majority of occurrences of MIC reported for engineered structures occur under biofilms [20], which are unlikely to form on the surface of the UFCs, particularly immediately after emplacement because of the harsh environmental conditions including high heat [32]. Due to the ubiquitous nature of sulfate (SO_4^{2-}), SRB tend to dominate occurrences of MIC in anoxic environments [33].

$$2Cu + HS^- + H^+ \rightarrow Cu_2S + H_2 \quad (1)$$

1.6.1 Primary Production in a DGR environment

Although HS^- does not naturally occur in the groundwater relevant to a Canadian DGR [9], and is expected to exist exclusively as a result of microbial metabolism, geogenic gases such as dihydrogen (H_2), methane (CH_4), and carbon dioxide (CO_2) do exist in proposed DGR environments as a result of abiotic processes. Of these geogenic gases, the one expected to be the most relevant to anoxic corrosion of UFCs is H_2 [34–36], which is present in subsurface environments from the radiolytic dissociation of water through the radioactive decay of elements such as uranium, thorium, and potassium [37]. The combined rate of production of H_2 in a DGR and rate of diffusion of H_2 from the host rock into the DGR is expected to exceed the rate at which it can diffuse out of the DGR [34]. Geogenic gases have been shown to drive primary production in DGR-relevant subsurface environments through a variety of

chemolithoautotrophic metabolisms. These types of metabolism, where a greater number of moles of gas are consumed than are produced, are beneficial to reducing the overall gas volume in a DGR. Specifically, H_2 is an important electron donor in methanogenesis (equation 2) [38–41], homoacetogenesis (equation 3) [39, 42], and the reduction of oxidized sulfur compounds such as sulfate (equation 4) or sulfite (equation 5) [24, 35, 47–49, 36–38, 40, 43–46], and metals such as iron (equation 6) [38, 40, 50–52].

$$4H_2 + CO_2 \rightarrow CH_4 + 2H_2O \quad (2)$$

$$4H_2 + 2CO_2 \rightarrow CH_3COOH + 2H_2O \quad (3)$$

$$4H_2 + SO_4^{2-} + H^+ \rightleftharpoons HS^- + 4H_2O \quad (4)$$

$$3H_2 + SO_3^{2-} + H^+ \rightleftharpoons HS^- + 3H_2O \quad (5)$$

$$H_2 + 2Fe^{3+} \rightleftharpoons 2H^+ + 2Fe^{2+} \quad (6)$$

Methane, present both as a geogenic gas and as a result of microbial methanogenesis (equation 2), can be used by methanotrophs. Anaerobic methanotrophic (ANME) archaea have been shown to couple the anaerobic oxidation of methane (AOM) to the reduction of SO_4^{2-} (equation 7) [53, 54], nitrate (NO_3^-; equation 8) [55], iron(III) (Fe^{3+}; equation 9) [38, 50–52], manganese (equation 10) [50] , or to acetogenesis (equation 11) [47, 56], either independently or with a microbial symbiont. Results from experiments in Olkiluoto, the site of Finland's DGR, show potential evidence of sulfate reduction coupled to methane oxidation [47, 57], although this was not supported by all studies from this site [45].

$$CH_4 + SO_4^{2-} \rightarrow HCO_3^- + HS^- + H_2O \quad (7)$$

$$CH_4 + 4NO_3^- \rightarrow CO_2 + 4NO_2^- + 2H_2O \quad (8)$$

$$CH_4 + 8Fe(OH)_3 + 15H^+ \rightarrow HCO_3^- + 8Fe^{2+} + 21H_2O \quad (9)$$

$$CH_4 + 4MnO_2 + 7H^+ \rightarrow HCO_3^- + 4Mn^{2+} + 5H_2O \quad (10)$$

$$2CH_4 + 2H_2O \rightarrow CH_3COOH + 4H_2 \quad (11)$$

Other chemolithoautotrophic microorganisms can grow without geogenic gases as electron sources. For example, several SRBs are capable of the disproportionation of sulfur species of intermediate oxidation state such as thiosulfate ($S_2O_3^{2-}$; equation 12). This is most common for deltaproteobacterial SRBs [58], and metagenome assembled genomes (MAGs) corresponding to the deltaproteobacterial genera *Desulfomicrobium*, *Desulfarculus*, and *Pseudodesulfovibrio* possessing the genes necessary for $S_2O_3^{2-}$ disproportionation were identified in a groundwater metagenomics study from Olkiluoto [45].

$$S_2O_3^{2-} + H_2O \rightarrow SO_4^{2-} + HS^- + H^+ \quad (12)$$

Several carbon fixation pathways have been identified in members of DGR-relevant communities. A metagenomic study of groundwater in Olkiluoto showed the presence of the reductive acetyl-coenzyme A (acetyl-coA) pathway (also known as the Wood-Ljungdahl pathway) genes in all deltaproteobacterial MAGs, and the additional presence of the genes for the reductive pentose phosphate pathway and the reductive tricarboxylic acid (TCA) pathway in MAGs represented by sulfide-oxidizers [49]. In another study examining sediments at the Horonobe Underground Research Laboratory (Hakkaido, Japan), carbon fixation genes belonging to the reductive acetyl-coA pathway and the TCA pathway were identified in approximately one quarter of the genome bins [38]. A genomic study on borehole fluid from the Opalinus clay formation (Switzerland) also identified microorganisms with the genomic potential for carbon fixation via the Calvin cycle [35].

1.6.2 Chemoorganoheterotrophic metabolisms

Even in carbon-limited environments with diverse forms of chemolithoautotrophic growth, chemoorganoheterotrophic fermenters contribute to subsurface biogeochemical cycling. Some heterotrophic growth may be possible using recalcitrant natural organic matter or ancient organic carbon derived from the bedrock as a carbon source, but these microorganisms are likely reliant instead on the primary producers in the ecosystem through the use of microbial necromass or the compounds produced through the metabolism of

primary producers [35, 45, 59, 60]. An *in situ* experiment in the Mont Terri Underground Rock Laboratory (Switzerland) identified a fermenting bacterium belonging to the genus *Hyphomonas* capable of oxidizing organic macromolecules to acetate [35].

Whereas some SRB can grow autotrophically, others couple the reduction of sulfate to the oxidation of small organic compounds such as formate, acetate (equation 13), ethanol, and lactate, either naturally occurring in the environment or from microbial necromass [35, 45]. Other microorganisms, such as *Desulfuromonas acetoxidans*, have similar metabolisms but can instead use partially oxidized sulfur species such as elemental sulfur (S^0) as an electron acceptor in place of SO_4^{2-} (equation 14).

$$CH_3COO^- + SO_4^{2-} + 2H^+ \rightleftharpoons 2CO_2 + HS^- + 2H_2O \quad (13)$$

$$CH_3COO^- + 4S^0 + 2H_2O \rightleftharpoons 2CO_2 + 4HS^- + 3H^+ \quad (14)$$

1.6.3 Sulfide sequestration

Several studies have shown that SRB dominate anoxic environments where SO_4^{2-} is available [24, 35, 44, 45, 49, 59] and can even proliferate within SO_4^{2-}-limited systems [38, 60, 61]. Additionally, SRB have been reported in commercially available bentonites proposed for use in a DGR [62]. Thus, there is potential for HS^- production in or around a poorly designed DGR, making the potential for HS^- sequestration an important consideration for DGR safety and longevity.

If Fe^{3+} is present in large enough quantities, UFC corrosion by HS^- can be diverted through the immobilization of HS^- via the partial reduction of Fe^{3+} to Iron(II) (Fe^{2+}) and S^0 (equation 15), and the Fe^{2+} produced can react with additional HS^- to produce an iron sulfide precipitate (FeS; equation 16) [24]. The reduction of naturally occurring Fe^{3+} in bentonite clay by SRB-derived HS^- has been experimentally demonstrated [63], although this reaction could not be demonstrated in a second experiment using artificial porewater inoculated with Opalinus clay and its associated porewater [24]. Instead, a reaction between HS^- and Fe^{2+},

derived either from celestite dissolution [24] or microbially mediated Fe^{3+} reduction [49], to produce the ferrous sulfide (FeS) precipitate (equation 16) was observed. Both the reduction of Fe^{3+} from bentonite clay and the production of FeS have been shown to destabilize dioctahedral smectites such as montmorillonite [64–66], thus leading to decreased swelling and an increased potential for microbial growth in a DGR.

$$HS^- + 2Fe^{3+} \rightleftharpoons 2Fe^{2+} + S^0 + H^+ \quad (15)$$

$$HS^- + Fe^{2+} \rightleftharpoons FeS + H^+ \quad (16)$$

Biologically mediated HS^- sequestration is also possible by the metabolism of microorganisms capable of HS^- oxidation. Under anoxic conditions, HS^- oxidation can be coupled to dissimilatory NO_3^- reduction to ammonium (NH_4), in microorganisms such *Desulfurivibrio alkaliphilus*, and to dinitrogen (N_2) gas or nitrite (NO_2^-) by other microorganisms [49]. The genomic potential for this process has been identified in groundwater from Olkiluoto [45, 67]. Metatranscriptomic and metaproteomic analyses confirmed the activity of sulfide-oxidizing denitrifying bacteria at this site [49], and revealed a community of active sulfur compound oxidizing denitrifying bacteria in the Witwatersrand Basin in South Africa [68] (equation 17 and 18). Nitrate (equation 17) or nitrite (equation 18) reduction to N_2 gas coupled to sulfide oxidation was additionally demonstrated in groundwater amended with sulfide and nitrite or nitrate [49].

$$2NO_3^- + 5HS^- + 7H^+ \rightarrow N_2 + 5S^0 + 6H_2O \quad (17)$$

$$2NO_2^- + 3HS^- + 5H^+ \rightarrow N_2 + 3S^0 + 4H_2O \quad (18)$$

Most microorganisms identified in DGR-relevant systems with the genomic potential for sulfur oxidation belong to the former class *Betaproteobacteria* (now part of the *Gammaproteobacteria*) [38, 45], although a species of *Sulfurimonas* from the former class *Epsilonproteobacteria* (now part of the *Campylobacteria*) and a species of *Hoeflea* from the class *Alphaproteobacteria* with this ability have also been identified [45].

1.7 Preventing microbial growth in a DGR

Although several microbial metabolisms are expected to have little impact on the safety of a DGR, others result in the production of HS^- and gases, and the potential reduction of bentonite-associated Fe^{3+}, which all might negatively impact the longevity of a DGR. Even though there are additional microbial metabolisms that result in the removal of HS^- and gases, it may be difficult to ensure that only those metabolic reactions occur in a DGR. Instead, an ideal solution for ensuring that HS^- and gases are not produced is to suppress the growth of all microorganisms in the area surrounding the UFCs.

Several studies have tested the conditions necessary to suppress microbial growth in bentonite clay under DGR-relevant conditions. Apart from nutrient availability, the factors that impact microbial growth in bentonite clay are water activity, dry density, and swelling pressure [7, 22, 69, 70]. A study examing dry densities of compacted bentonite clay showed that bacterial culture counts did not increase for saturated bentonite clays with dry densities of 1.6 g/cm^3 or higher [7]. This dry density threshold corresponds to a water activity <0.96 and swelling pressure >2 MPa. A water activity of less than 0.96 in compacted bentonite clay was also shown to be achieved with a porewater salinity of greater than 100 g/L [7].

Phospholipid fatty acid (PLFA) analysis of compacted bentonite clay predicted a similar number of bacterial cells regardless of porewater salinity, suggesting that under these high pressure and low water activity conditions, bacteria can potentially survive as dormant cells, inactive endospores, or background relic PLFA molecules [7]. In another study, commercial Wyoming MX-80 bentonite clay was saturated with sterile water in a pressure vessel that was compacted with bentonite clay at a dry density of 1.7 g/cm^3. These conditions were maintained for 2811 days at room temperature, and heterotrophic aerobes and anaerobes, as well as nitrate-reducing bacteria, were successfully cultivated from the bentonite at the end of the incubation period. A similar number of microorganisms were cultivated from the inner layer of the clay after incubation and the dry clay before incubation [71]. This demonstrates that the DGR-relevant conditions suppressed microbial growth in the clay but did not have a

lethal effect on the microorganisms. Thus, it is important to ensure that growth-suppressing conditions are maintained for the planned lifetime of the DGR because microorganisms present as inactive cells or spores might otherwise take advantage of suitable growth conditions if they occur.

1.8 Methods for characterizing the microbiology of bentonite clay

Early microbiology research of bentonite clay used cultivation methods to identify and quantify the microorganisms present in bentonite clay samples [7, 22, 69, 70, 72–75]. Some studies only considered the cultivability of SRB due to their relevance to DGR safety [70], whereas others also considered aerobic and anaerobic heterotrophs [7, 72–75]. In some studies, changes in cultivability of the various groups of microorganisms were measured after incubation of bentonite clay in pressure cells, wherein exposure to low water activity and high swelling pressure occurred [7, 70]. In others, surveys of the microbial community of undisturbed bentonite were performed [72–75]. Although these methods can give insight into the conditions that suppress microbial growth, only microorganisms that can grow in the given cultivation conditions are considered. Depending on the cultivation conditions applied, this could mean that only rare microorganisms, or microorganisms with less relevant metabolisms to the safety of the DGR, are targeted. Nonetheless, cultivation methods do have the benefit of only accounting for viable microorganisms.

More recent studies on the microbiology of bentonite clay have made use of DNA sequencing methods to overcome some of the limitations of cultivation approaches. The main obstacle faced when using DNA-based methods for the microbial characterization of clay is the difficulty extracting sufficient DNA for detection due to the low biomass nature of clay combined with its adsorptive and swelling properties. Attempts have been made to extract DNA from Opalinus clay [24, 74, 76] and from Toarcian argillite (Tournemire, France) [72] with no success. Some studies have overcome this difficulty by extracting DNA from filter-concentrated borehole water or porewater associated with clays of interest, instead of extracting DNA directly from the clay. Metagenomic [35, 38, 45, 47, 49, 57, 77] and

amplicon sequencing [24, 60] studies from these types of DNA extracts have contributed important information about the potential types of microbial metabolism possible under DGR-relevant conditions. Other studies employed cultivation techniques and then sequenced DNA from culture extracts [73, 74]. Although this approach provides more information than cultivation alone, it faces the same limitation as other cultivation approaches because it selects for specific microorganisms that grow under laboratory culture conditions.

The use of DNA extraction and subsequent sequencing for clay has only been successfully reported in a few cases [78–81]. In one study, DNA was extracted from five bentonite clay samples in Almeria (Spain) and the V5-V6 hypervariable regions of the 16S ribosomal RNA (rRNA) gene was amplified and sequenced [79]. This study revealed 174 unique operational taxonomic units (OTUs) belonging to 13 different phyla [79], as compared to the 16 bacterial strains that were previously identified in samples from the same site using cultivation approaches [73]. These contrasting numbers highlight how much of the bacterial community could be missed with standard cultivation approaches alone.

1.9 Objectives

Although several studies have explored bentonite clay microbiology under DGR-relevant microcosm experiments, very few studies have looked at the microbiology of naturally occurring ancient clays and rocks that may serve directly as analogues for future DGR barrier components. Even fewer studies have employed sequencing techniques to analyze these DGR barrier component analogues using a combination of cultivation and sequencing techniques for the same samples [73, 79].

The primary purpose of this research was to analyze the microbiology of ancient, natural analogues of DGR barrier components using a combination of cultivation and DNA-based approaches. Specifically, the goals of this research were to estimate the number of microorganisms present and to assess the viability of microbial groups using cultivation techniques, to quantify DNA templates (from cells and relic DNA) using quantitative

polymerase chain reaction (qPCR), and to generate microbial profiles using 16S rRNA genes to assess *in situ* nucleic acids from these analogue samples. Combining the results of more than one technique will help overcome the limitations of any single technique.

1.9.1 Sample sites

Three different ancient natural barrier component analogues were selected for microbiological analysis. The first is the Tsukinuno deposit, which hosts the largest underground bentonite mine in Japan, consisting of 35 layers of bentonite within the mining area [82]. This bentonite deposit was formed in the middle Miocene (16-11.7 million years ago) and is composed primarily of sodium smectite with smaller amounts of quartz, feldspar, illite, calcite, and zeolite [82]. Ten ancient bentonite samples from this site were studied.

The second study site is the Opalinus clay formation, which is the only host rock currently being considered for the placement of Switzerland's DGR. Opalinus clay is a Mesozoic shale formation that was formed about 174 million years ago in the Jura Mountains in northwestern Switzerland [83]. Opalinus clay consists of approximately 65% clay minerals, namely illite, smectite, kaolinite, and chlorite, of which 10% are swelling [74, 84]. Additionally, it contains minerals such as quartz, calcite, siderite, pyrite, and feldspar [84]. It contains less than 1.5% organic matter, and has a moisture content between 3 and 8% (w/w) [74]. An average pore size of less than 0.02 μm in diameter has been reported, and pores are generally water-saturated, making up a total porosity of 7 to 18% [74]. One Opalinus clay core was studied in these experiments.

The final sample site is in Northern Ontario (Canada), and is among several locations being considered for the placement of a Canadian DGR. The sample site is situated in the Superior province of the Canadian shield, large portions of which have been stable for the last 2.5 billion years. Despite multiple glaciation events in the last million years, the deep crystalline formations of the Canadian shield have been largely unaffected. Three rock core samples from varying depths were studied.

Chapter 2
Materials and Methods

2.1 Sampling and storage

Bentonite clay was sampled from ten locations along a mining tunnel wall in the Tsukinuno mine in Japan. The samples were packaged in plastic wrap and aluminum foil before shipping to the University of Waterloo (Ontario, Canada). Samples were stored at 4°C upon arrival at the University of Waterloo. After subsamples were taken for analyses, the remaining bentonite was stored at -20°C.

A 10 cm core of Opalinus clay (O1) was drilled in 2017 using non-sterile pressurized air. The core was placed in sterile bags and air was evacuated. The core was stored on dry ice until arrival at the University of Waterloo, at which point it was stored at -80°C until processing.

For the Northern Ontario crystalline rock (NOCR) samples, a borehole was drilled in 2017 and cores were recovered. Sample N2 came from a depth of 99.0-99.3 m, sample N4 came from a depth of 219.7-219.9 m, and sample N6 came from a depth of 513.4-513.7 m belowground. The outer layer of each core was sampled using sterile swabs; both swabs and rock samples were stored at -20°C until processing.

2.2 Sample preparation for DNA extraction, cultivation, water activity, and moisture content

All samples were processed for DNA extraction, amplicon sequencing, and qPCR. Cultivation methods were additionally applied to the ten Tsukinuno bentonite samples, and moisture content and water activity of these samples were measured. These additional assessments were not possible for the Opalinus clay and NOCR samples because these samples were incubated at -80°C for two years before being processed.

2.2.1 Tsukinuno bentonite and Opalinus clay samples

The outer layers of bentonite and Opalinus clay samples were removed using a sterile scalpel to eliminate possible contaminants introduced during the sampling process. The inner layers of the Tsukinuno bentonite samples were crushed using a mortar and pestle to achieve a homogeneous mixture of the clay. The inner layer of the Opalinus clay was crushed in a 50 mL stainless steel grinding jar (Retsch) in a mixer mill MM 400 (Retsch). The mortars, pestles, and grinding jars were rinsed with bleach followed by Milli-Q water before usage and were swabbed to identify any contaminants introduced during the sample crushing process.

2.2.2 Northern Ontario crystalline rock samples

The crushing of the NOCR cores took place at McMaster University. The three cores were cut into slices and the outer layer was removed using a solvent-rinsed hammer and chisel. The inner samples were crushed using a stainless-steel mortar and pestle, and then ground to a 1 mm grain size using a puck mill. Crushed inner layer samples and outer layer swabs were sent to the University of Waterloo where they were stored at -80°C until further processing.

2.3 Water activity and moisture content

A WP4C Water Potential Meter (Decagon) was used to measure the water activity of the Tsukinuno bentonite clay samples using the fast mode of the instrument. From a separate aliquot of each sample, sample weights were recorded before oven baking at 110°C for 48 hours. The difference in weight before and after baking was used to determine the moisture content of the sample. These values were used to report measurements of 16S rRNA gene copy numbers, most probable number (MPN), and colony forming unit (CFU) on a per gram dry weight basis.

2.4 Cultivation

Two grams of the crushed Tsukinuno bentonite clay samples were suspended in 18 mL of phosphate buffered saline (PBS) solution (dilution A) and vortexed at low speed for 30

minutes. Two 10-fold serial dilutions were made from the original clay suspension (dilutions B and C) and these were used to inoculate aerobic and anaerobic heterotroph and SRB cultures as described below.

2.4.1 Aerobic and anaerobic heterotrophs

Dilution A (100 µL) was added to six Reasoner's 2A (R2A; M1687, HiMedia Laboratories, PA, USA) agar plates and dilution B (100 µL) was added to three R2A agar plates. The liquid was spread onto the surface of the agar with a flame sterilized glass spreader until the surface of the agar was dry. Three of the dilution A plates and all of the dilution B plates were incubated under oxic conditions in a 30°C incubator for seven days. The remaining three dilution A plates were placed in an anaerobic chamber (Best Value Vacs, three gallon stainless steel vacuum chamber) containing a GasPak EZ anaerobe sachet (BD), which was evacuated and flushed three times with a 90% N_2 and 10% CO_2 gas mixture to create an anoxic environment. The chamber was placed in a 30°C incubator for 28 days. After incubation, colonies were counted on each of the plates, and the number of CFU per gram of clay was calculated.

2.4.2 Sulfate reducing bacteria

One mL of dilution A, B, and C were added to five test tubes, each containing nine mL of a SRB enrichment medium (M803, HiMedia Laboratories, PA, USA), and tubes were placed in an anaerobic chamber (Best Value Vacs, 3 gallon stainless steel vacuum chamber) that was evacuated and flushed as described above. The chamber was placed in a 30°C incubator for 28 days. After incubation, tubes positive for SRB activity were identified by the formation of a black iron sulfide precipitate. The MPN method was used to estimate the number of SRB present in one gram of the original clay sample.

2.5 DNA extraction

Total genomic DNA was extracted from the Tsukinuno bentonite clay, Opalinus clay, and NOCR samples, from the aerobic heterotroph, anaerobic heterotroph, and SRB cultures, and from the mortar and pestle controls. A kit control containing no sample was included for each

batch of extractions. The DNA extraction method used for clay and rock samples was validated previously [81].

2.5.1 Clay and rock samples

Total genomic DNA was extracted from duplicate 5-g aliquots of the crushed inner layer of each clay sample and 10-g aliquots of the crushed inner layer of each rock sample using the DNeasy PowerMax Kit (Qiagen). After addition of lysis solution, PowerBead tubes were incubated at 65°C for 30 minutes, followed by bead beating at 30 Hz for 10 minutes using an mixer mill MM 400 (Retsch). The remainder of the extraction was carried out following the manufacturer's instructions. Extracted DNA was eluted in 2 mL of elution buffer and stored in aliquots at -20°C until further analysis.

2.5.2 Cultures

A pipette tip was used to collect approximately equal amounts of microbial biomass from each colony type on the surface of the R2A agar plates, and the biomass was added to a separate microcentrifuge tube containing 20 μL of PCR water for anaerobic heterotrophs and aerobic heterotrophs of each of the ten Tsukinuno bentonite clay samples. A 1-mL aliquot of the positive SRB culture was centrifuged for 2 min at 10,000 × g to form a cell pellet and the supernatant was decanted. Total genomic DNA was extracted from the cells of each culture type for each sample using the DNeasy UltraClean Microbial Kit (Qiagen). After addition of lysis solution, the PowerBead tubes were incubated at 65°C for 10 min, followed by bead beating using a FastPrep instrument (MP Biomedicals, OH, USA) at 5.5 m/s for 45 s. The remainder of the extraction was carried out following the manufacturer's instructions. Extracted DNA was eluted in 50 μL of elution buffer and stored in aliquots at -20°C until PCR analysis.

2.5.3 Swabs

Total genomic DNA from foam swabs used to test for background DNA on the mortars and pestles used to crush the Tsukinuno bentonite samples and to collect biomass from the outer layer of the NOCR cores was extracted using the DNeasy PowerSoil Kit (Qiagen). The swab

tips were cut with flame-sterilized scalpels into the PowerBead tubes. After addition of lysis solution, the PowerBead tubes were incubated at 65°C for 30 min, followed by bead beating using a FastPrep instrument (MP Biomedicals, OH, USA) at 5.5 m/s for 45 s. The remainder of the extraction was carried out following the manufacturer's instructions. Extracted DNA was eluted into 60 µL of elution buffer and stored in aliquots at −20°C until PCR analysis.

2.6 DNA quantification

Extracted total genomic DNA was quantified using the Qubit dsDNA High Sensitivity Assay kit (Invitrogen, CA, USA, cat. No. Q32854). Ten µL of DNA extract was added to 190 µL of Qubit dsDNA HS reagent diluted 200-fold in buffer. The mixture was vortexed, and fluorescence was measured using a Qubit 4.0 fluorometer (Life Technologies, CA, USA) after three minutes of incubation.

2.7 Quantitative PCR

The 16S rRNA genes in the Tsukinuno bentonite clay, Opalinus clay, and NOCR core DNA extracts were quantified using qPCR with primers 341F and 518R (Muyzer *et al.*, 1993). The 15 µL PCR mix contained 1× SsoAdvanced Universal SYBR Green Supermix (Bio-Rad), 0.3 µM final concentration of each primer, 7.5 µg of bovine serum albumin (BSA), and 4 µL of template DNA (between 0 and 1 ng; see concentrations of DNA from Tsukinuno bentonite clay samples included in Table 3.1). The PCR was performed on a CFX96 Real-Time PCR Detection System (Bio-Rad) as follows: 98°C for three minutes followed by 40 cycles of 98°C for 15 seconds and 55°C for 30 seconds.

The V3 to V5 region of the *Thermus thermophilus* 16S rRNA gene was previously cloned into the pUC57-Kan plasmid, flanked by M13F/R primers. Both primers were used to amplify the 16S rRNA gene fragment, which was then purified and used as a template for the

standard curve. Bacterial 16S rRNA gene copy numbers were calculated from the linear regression equation of the standard curve.

2.8 Amplification and sequencing of 16S rRNA genes

For all samples from which DNA was extracted, the V4-V5 region of the 16S rRNA genes were amplified in triplicate using primers 515F-Y [87] and 926R [88], modified to contain a unique 6 base index sequence and flow cell binding and sequencing sites [89]. The PCR was set up in a workstation with ISO 5 HEPA-filtered air and surfaces treated with UV light (AirClean Systems, ON, Canada). The tubes, PCR water, and bovine serum albumin (BSA) were UV-treated for 20 minutes with 302 nm wavelength light on a transilluminator (ProteinSimple, CA, USA). The 25 µL PCR mix contained 1× ThermoPol Buffer, 0.2 µM final concentrations of forward and reverse primer, 200 µM final concentration of dNTPs, 15 µg BSA, 0.625 units hot start *Taq* DNA polymerase (New England Biolabs, MA, USA), and 1 µL of template DNA (between 0 and 0.3 ng). The PCR was performed as follows: 95°C initial denaturation for three minutes, followed by 40, 45, or 50 cycles of 95°C denaturation for 30 sec, 55°C annealing for 30 sec, 68°C extension for 1 min, and a final extension of 68°C for 7 min. Clay and rock samples were amplified for 40, 45, and 50 cycles to identify the impact of cycle number on amplification product and subsequent sequence data. Extracted DNA from cultures was amplified for 35 cycles. Negative PCR controls containing no template DNA were included in the 96-well plates to test for cross-contamination effects and were also prepared in single tubes to test for background amplification from the PCR mixture. Triplicate, uniquely indexed PCR products were pooled and quantified on a 1% agarose gel containing GelRed (Biotium, CA, USA), and equimolar quantities of each amplicon were pooled into a single tube. Negative PCR controls, and PCR-amplified DNA extraction kit controls and swab controls were included in the Illumina sequencing pool (5 µL each), even if amplification was not detected on the gel. The pooled 16S rRNA gene amplicons were run on a 1.5% agarose gel and were then excised and purified using the Wizard SV Gel and PCR Clean-Up System (Promega, WI, USA). The library was denatured and diluted following Illumina guidelines (Document no. 15039740 v01). An 8-pM library

containing 15% PhiX control v3 (Illumina Canada Inc, NB, Canada) was sequenced on a MiSeq instrument (Illumina Inc, CA, USA) using a 2 × 250 cycle MiSeq Reagent Kit v2 (Illumina Canada Inc).

The 16S rRNA gene amplicons from all Tsukinuno bentonite clay, Opalinus clay, NOCR, and SRB and anaerobic heterotroph cultures were sequenced in a single run with a cluster density of 799 +/- 65, and 89% of clusters passing the quality filter. The extracted DNA from the aerobic heterotroph cultures was sequenced in a second Illumina run with a cluster density of 775 +/- 78 and 90% passing filter.

2.9 Sequence analysis

Sequence reads were demultiplexed using MiSeq Reporter software version 2.5.0.5 (Illumina) and analyzed using Quantitative Insights Into Microbial Ecology 2 (QIIME2, release 2019-10) [90]. Paired end reads were imported into QIIME2 using *qiime tools import*. DADA2 (*dada2 denoise-paired*) [91] was used to remove primer sequences and to trim low quality sequence bases after 250 bases for forward and reverse reads. Furthermore, DADA2 was used to denoise and dereplicate paired-end merging and amplicon sequence variants (ASVs) table construction. Taxonomy was assigned to ASVs using a naive Bayes classifier (*feature-classifier classify-sklearn*) pre-trained with SILVA database release 132 [92].

Contaminant ASVs were identified using the Decontam R package [93] with a threshold value of 0.5. The threshold value was selected by analyzing histograms of score statistic distribution across all samples (Appendix Figure S1), and bubble plots showing the identity of putative contaminant ASVs at all possible threshold values. Due to the expected different levels of contamination between samples PCR-amplified for different numbers of cycles, the clay and rock samples amplified with 40, 45, and 50 cycles of PCR were all processed with Decontam separately. After contaminant identification, contaminant ASVs were removed from the ASV table (Appendix Figure S2-S4). This ASV table was used for all subsequent analyses.

All sequences generated in this study were deposited in the European Nucleotide Archive with project accession number PRJEB39438.

Chapter 3
Results and discussion

3.1 Description of samples

The Tsukinuno bentonite samples had a variety of appearances and textures ranging from thick mud to rock (Table 3.1, Figure 3.1). Shipping delays resulted in approximately four weeks between sample extraction from the mine and arrival at the University of Waterloo. During this time, the samples were exposed to temperatures between -7°C and 27°C (Figure 3.2), as measured by a temperature tracker in the sample package (Lascar EL-USB-LITE). The ten Tsukinuno bentonite samples had moisture contents between 7.6% (T3) and 33.3% (T2) and water activities between 0.623 (T3) and 0.997 (T2; Figure 3.3). There was a strong positive correlation between moisture content and water activity for these ten samples (r_s=0.92).

Qualitatively, the Opalinus clay core (Figure 3.4) was similar in hardness to samples T1 and T10. The NOCR cores all had similar appearances to each other (Figure 3.4). Moisture content and water activity of the Opalinus clay and NOCR samples were not measured. A maximum DNA concentration of 2.6 x 10^2 pg/μL (5.2 x 10^2 ng of DNA from 5 g of clay) was measured in the Tsukinuno bentonite samples, and six of the samples had DNA concentrations below the detection limit of the Qubit fluorometer with 10 μL of DNA input (Table 3.1). The Opalinus clay sample and all NOCR samples also had DNA concentrations below this detection limit.

Table 3.1 List of Tsukinuno bentonite samples and site characteristics. Values of BDL indicate DNA concentrations below the detection limit of the Qubit fluorometer with 10 μL of sample input.

Sample	Appearance	Description	Sampling site	Clay bed	Average DNA yield per gram of clay (ng)
T1	Rock	Hand specimen taken from the bentonite exposed at the tunnel wall. Sample location 26-27cm up from the lower bentonite-shale contact.	1	19	BDL
T2	Soft	Sample taken from a very wet tunnel wall S side of the tunnel, pH around 6-7.	1	17	104
T3	Stones	Samples taken from tunnel wall, very dry bentonite. No drilling at this site.	2	2	BDL
T4	Soft	Samples taken from cleaned tunnel wall (15 cm from original surface).	1	20	44
T5	Rock and soft	Yellow bentonite, at lower contact of bed #19.	1	19	BDL
T6	Rock and soft	Gray bentonite, 20 cm from lower contact.	1	19	BDL
T7	Rock and soft	Brownish bentonite, 50 cm from lower contact.	1	19	BDL
T8	Rock and soft	Orange bentonite, 65 cm from lower contact.	1	19	16
T9	Rock and soft	Yellow bentonite, upper contact of bed #19.	1	19	8
T10	Rock	Massive dry bentonite from upper contact of bed #29.	3	29	BDL

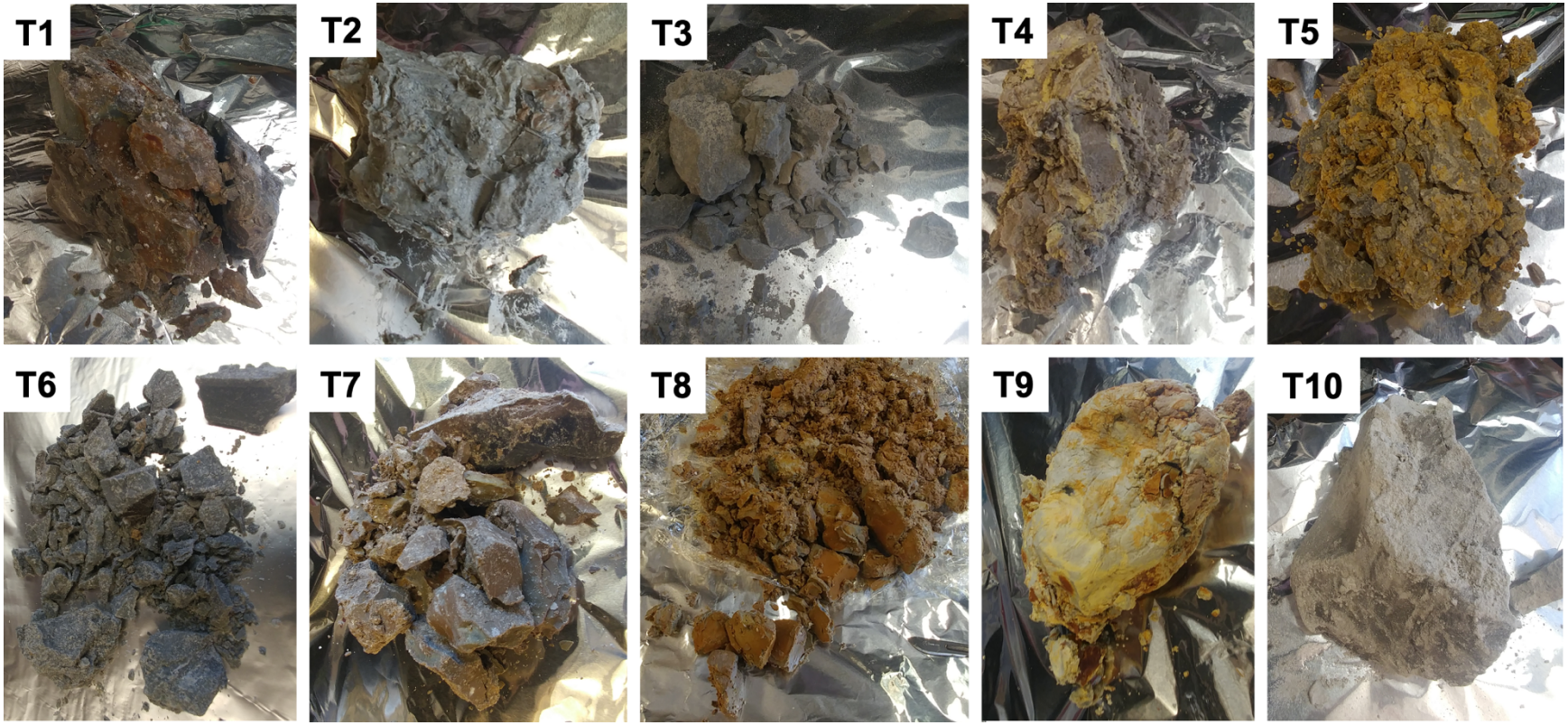

Figure 3.1 Images of the ten Tsukinuno bentonite samples immediately after arrival at the University of Waterloo. See Table 3.1 for additional sample information.

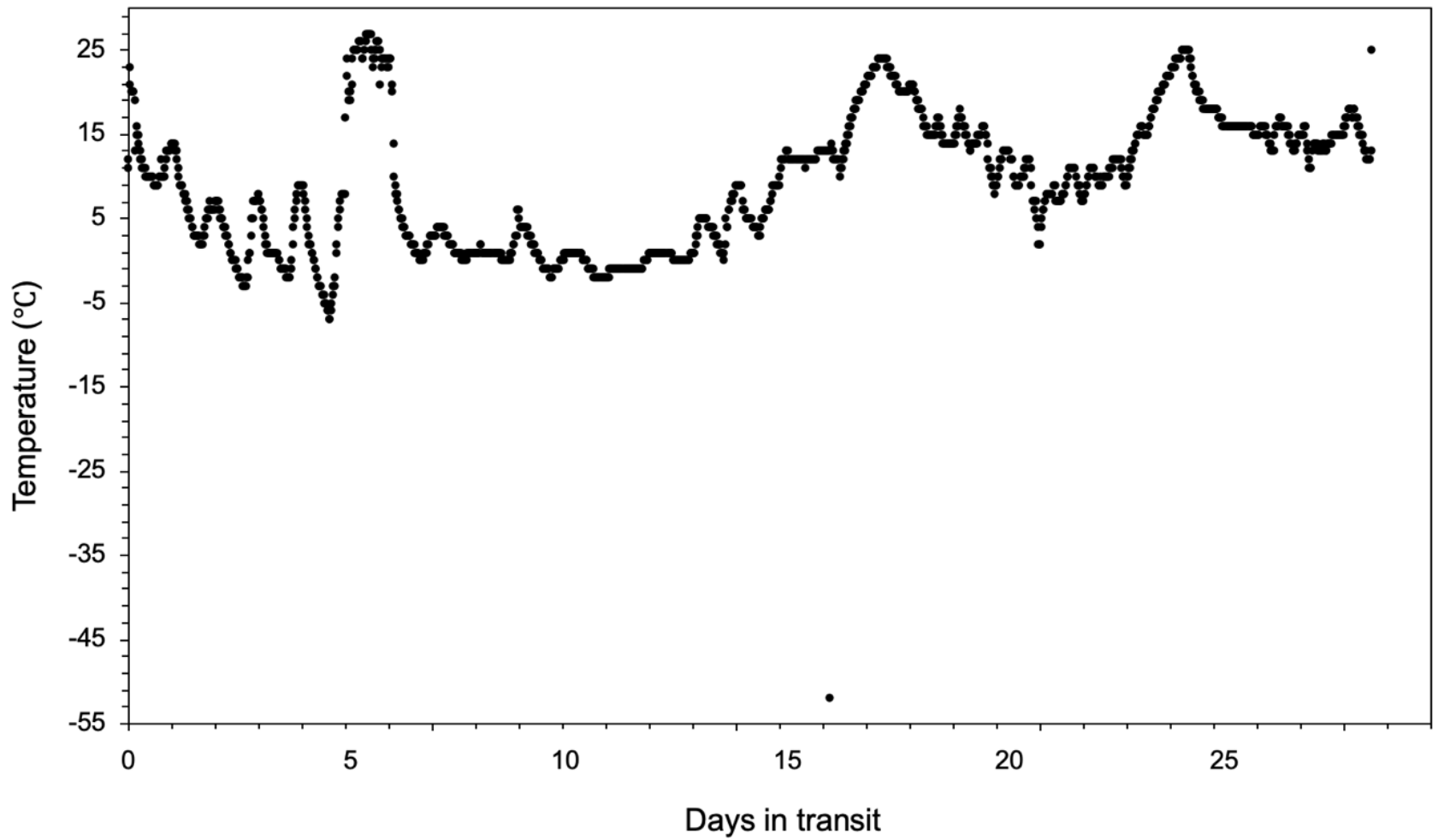

Figure 3.2 Temperature inside the package containing the Tsukinuno bentonite samples between the time of sampling and arrival at the University of Waterloo. The point at -52°C is likely an erroneous temperature recording.

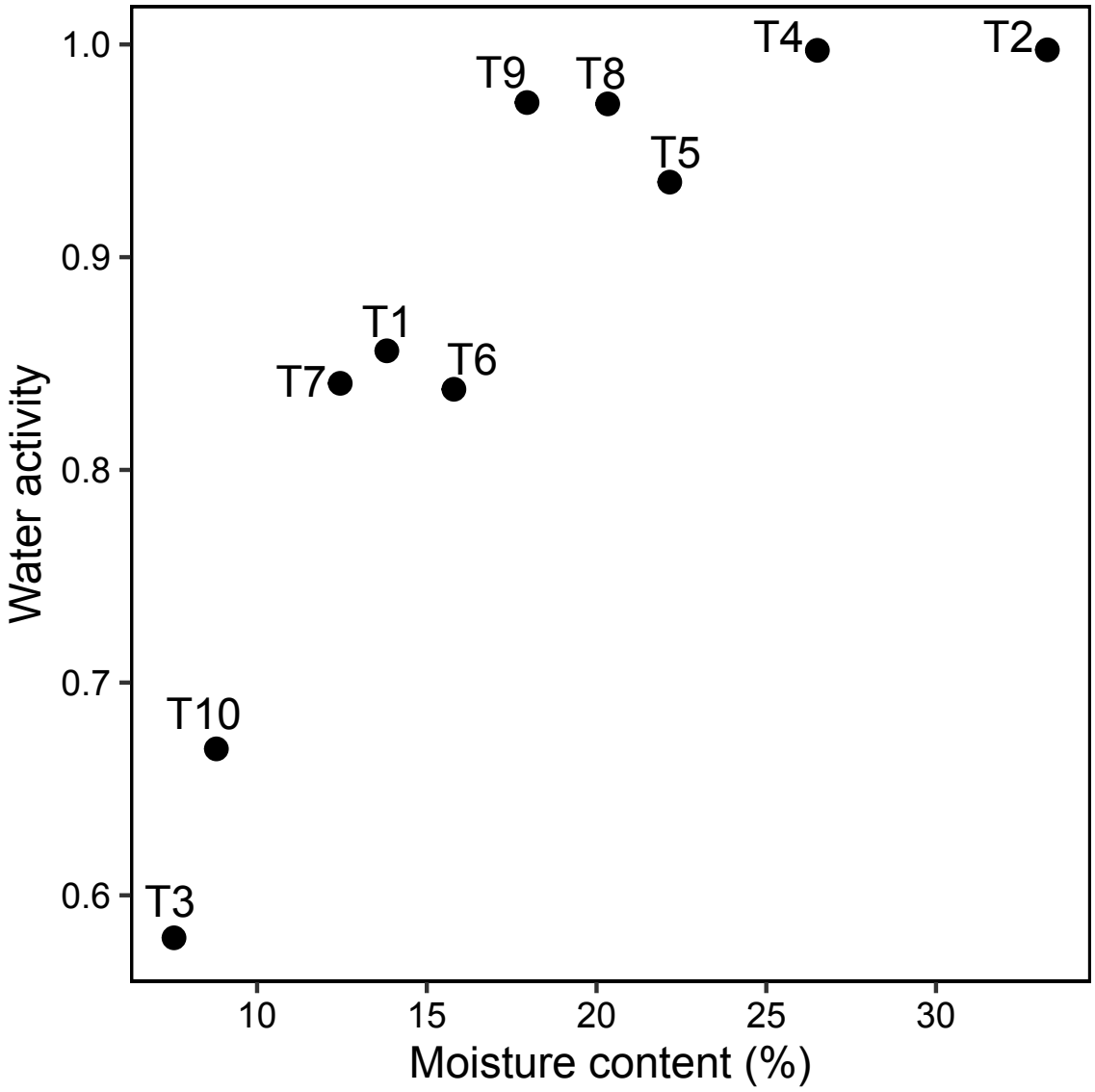

Figure 3.3 Water activity and moisture content of the Tsukinuno bentonite samples. The Spearman correlation coefficient for all water activity and moisture content values was 0.92. See Table 3.1 for additional sample information.

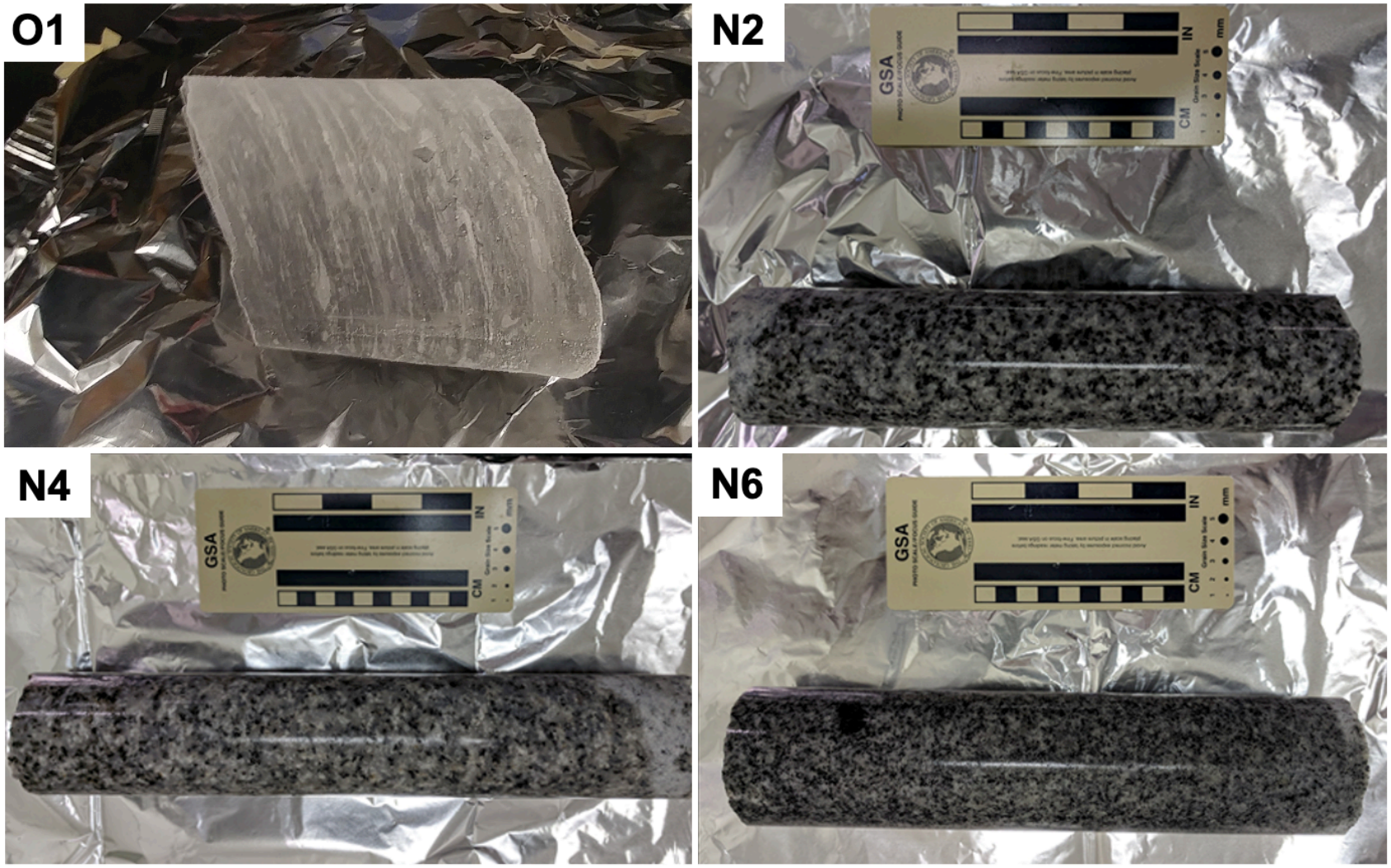

Figure 3.4 Opalinus clay core (O1), and NOCR cores N2 (99.0-99.3 m belowground), N4 (219.7-219.9 m belowground), and N6 (513.4-513.7 m belowground).

3.2 Microbial abundance

An important objective of this research was to characterize microorganisms in ancient natural barrier component analogues: Tsukinuno bentonite clay, Opalinus clay, and NOCR cores. Abundances of 16S rRNA genes, aerobic heterotrophs, anaerobic heterotrophs, and SRB per gram of dry bentonite were assessed for each of the Tsukinuno bentonite samples (Figure 3.5). The Tsukinuno bentonite samples had between 3.2×10^1 (T6) and 7.2×10^7 (T2) 16S rRNA gene copies/gdw with an average of 5.7×10^6 16S rRNA gene copies/gdw. The average number of 16S rRNA gene copies/gdw across the ten Tsukinuno bentonite samples was higher than the estimated average number of aerobic or anaerobic heterotrophs (Wilcoxon signed-rank test; $p<0.05$). The number of 16S rRNA gene copies detected is an overestimate of the number of cells present, because most bacterial cells have multiple copies of the 16S rRNA gene, and qPCR will also amplify environmental DNA (eDNA) in addition to DNA from living cells [94].

Aerobic heterotrophs were cultivated from all Tsukinuno bentonite samples with estimates of CFU/gdw between 4.1×10^1 (T9) and 1.1×10^4 (T2) (Figure 3.6). The average number of aerobic heterotrophs detected across the ten Tsukinuno bentonite samples was higher than the average number of anaerobic heterotrophs detected (Wilcoxon signed-rank test; $p<0.05$). The Tsukinuno bentonite samples were taken from a tunnel wall, and thus were all exposed to oxic conditions. As such, aerobes were expected to be in higher abundance than anaerobes. Anaerobic heterotrophs were only cultivated from five samples, and SRB were only detected in one sample. Measures of CFU/gdw of anaerobic heterotrophs were between 4.5×10^1 (T4) and 9.9×10^2 (T7), with an average of 3.10×10^2 CFU/gdw across the five samples from where they were detected. Sample T2, the only sample where SRB were detected using the cultivation approach, had an MPN estimate of 5 SRB/gdw.

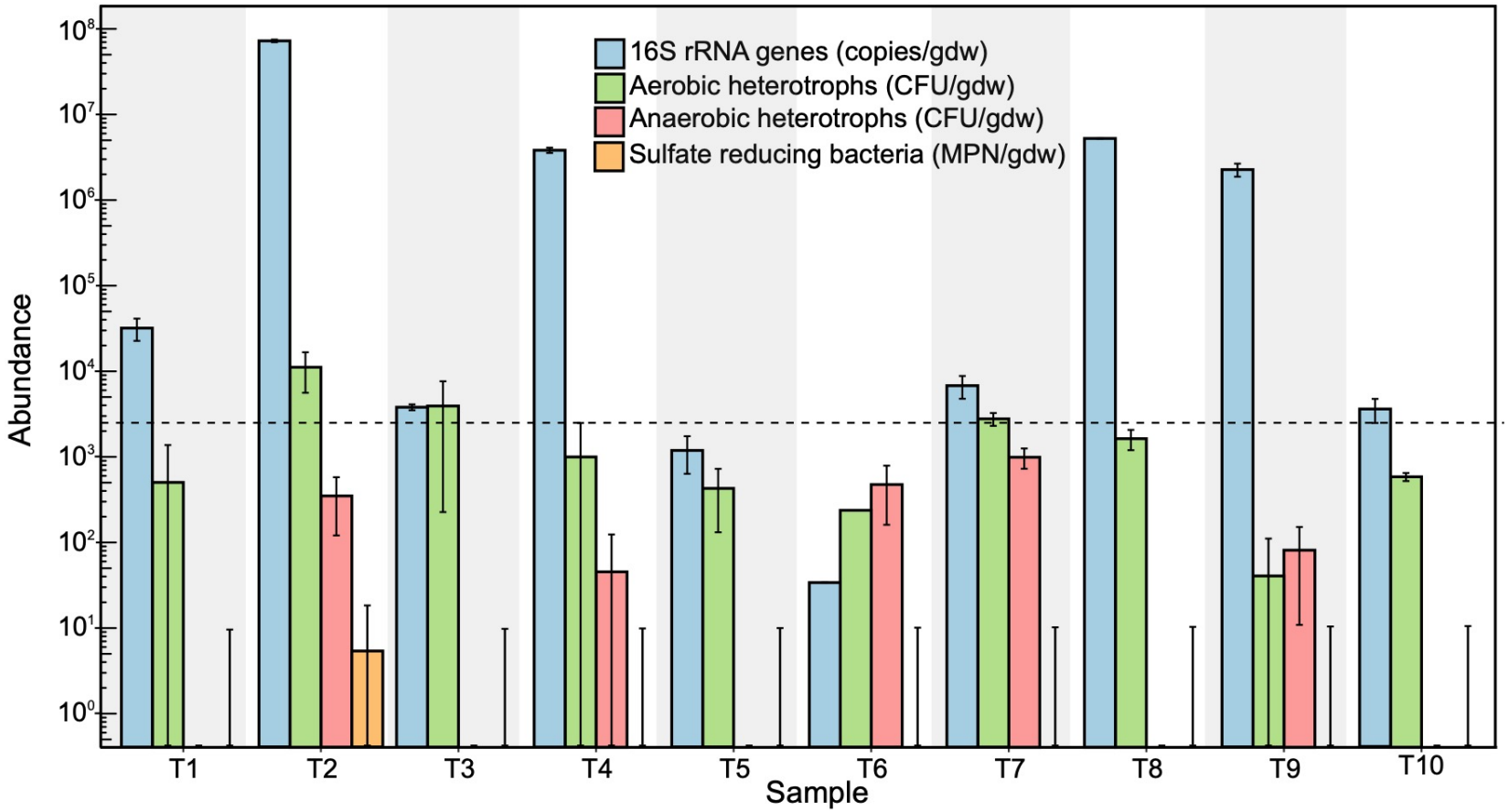

Figure 3.5 Abundance of 16S rRNA gene copies, cultivatable aerobic heterotrophs, anaerobic heterotrophs, and SRB in the Tsukinuno bentonite samples from Japan. The dotted line indicates the lower limit of quantification for abundance estimates of CFU/g. The error bars represent standard deviation of technical duplicates for measures of 16S rRNA gene copies/gdw, standard deviation between calculated CFU/gdw on triplicate R2A agar plates for measures of CFU/gdw, and confidence intervals specified by the MPN table for measures of MPN/gdw. See Table 3.1 for additional sample information.

The Tsukinuno bentonite samples had a higher average number of 16S rRNA gene copies/gdw than the NOCR samples (Mann-Whitney U test; $p<0.05$; Figure 3.6). Compared to the average measured 16S rRNA gene copies/gdw of 5.7×10^6 for the ten Tsukinuno bentonite samples, the three NOCR samples had an average of 1.1×10^3 16S rRNA gene copies/g, and the Opalinus clay sample had 1.2×10^3 16S rRNA genes copies/g.

In previous research quantifying the 16S rRNA gene copies in compacted and dry MX-80 bentonite clay, medians of 4.1×10^4 copies/g [95] and 1.7×10^7 copies/gdw [81] were detected, respectively. Four of the ten Tsukinuno bentonite sample had 16S rRNA gene copies/gdw within the range of 10^4 and 10^7, one of the samples was slightly higher than this range, and the remaining four were lower. The wide range of 16S rRNA gene copies/gdw measured in the Tsukinuno bentonite samples may be explained, at least in part, due to the broad range of water activities and moisture contents measured in these samples. The 16S rRNA gene copy number and moisture content of the Tsukinuno bentonite samples were strongly correlated (r=0.72), as was 16S rRNA gene copy number and water activity (r_s=0.77; Figure 3.7). The four samples with the highest 16S rRNA gene copy number were also the four samples with the highest water activities, and the only samples with water activities greater than 0.96. Microbial activity has been shown to be suppressed in bentonite clay with a water activity less than 0.96 [7].

The 16S rRNA gene copy numbers of the Opalinus clay and NOCR samples were all lower than the range of previously measured 16S rRNA gene copy numbers in MX-80 bentonite [81, 95]. The number of 16S rRNA gene copies detected in the NOCR samples are more similar to the estimated microbial abundances of clay-dominated aquifer layers of 10^3 cells/gdw [21]. The estimated microbial abundance of both the NOCR and Opalinus clay samples was orders of magnitude lower than the estimate of microbial abundance made for volcanic rock from Yucca mountain, a proposed host rock for the American DGR, of between 3.2×10^4 and 3.2×10^5 cells/gdw [22].

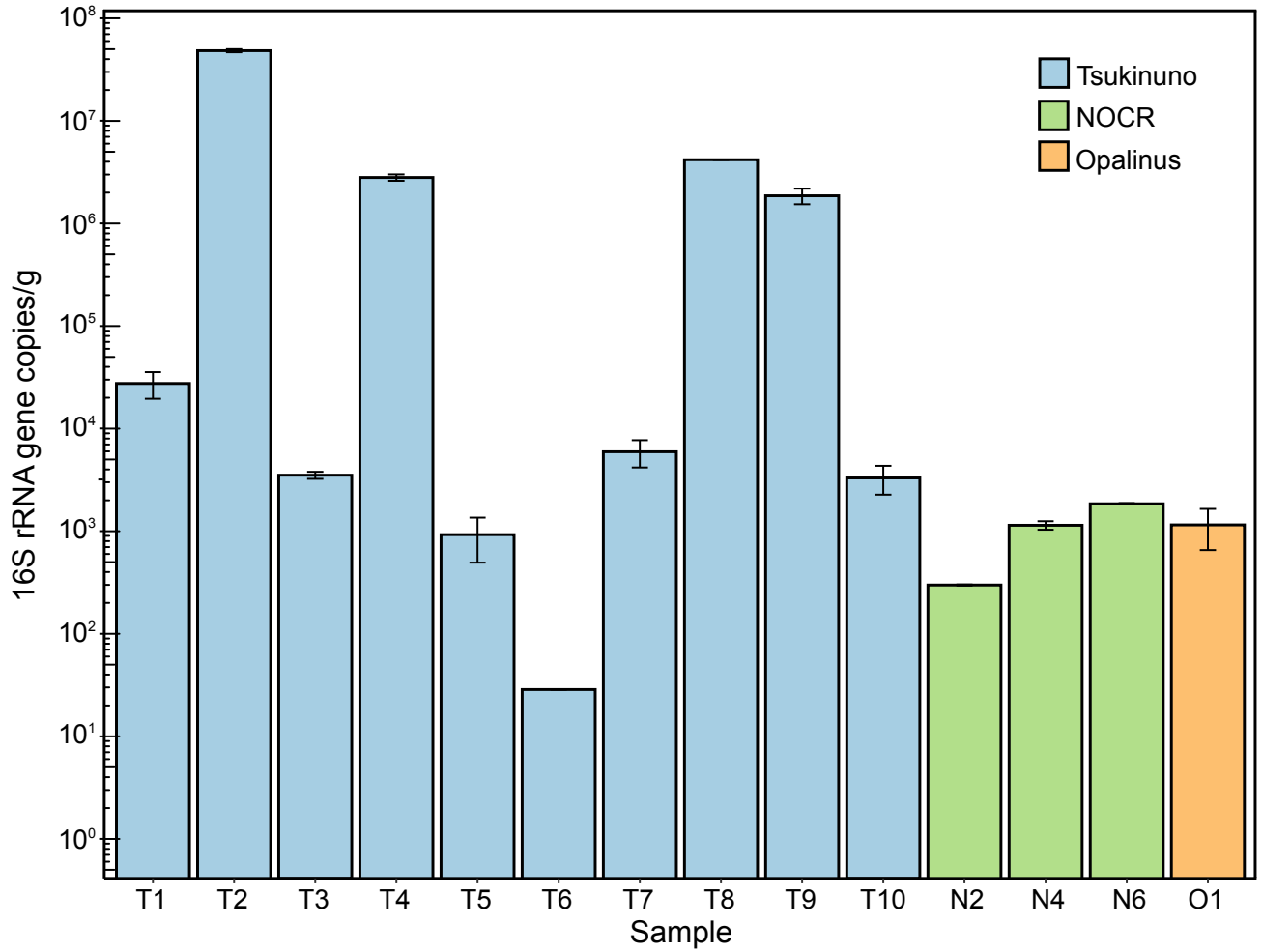

Figure 3.6 Number of 16S rRNA gene copies per gram of clay in the Tsukinuno bentonite samples from Japan, the NOCR samples, and the Opalinus clay sample. Error bars represent the standard deviation between technical duplicate samples. See Table 3.1 for additional sample information.

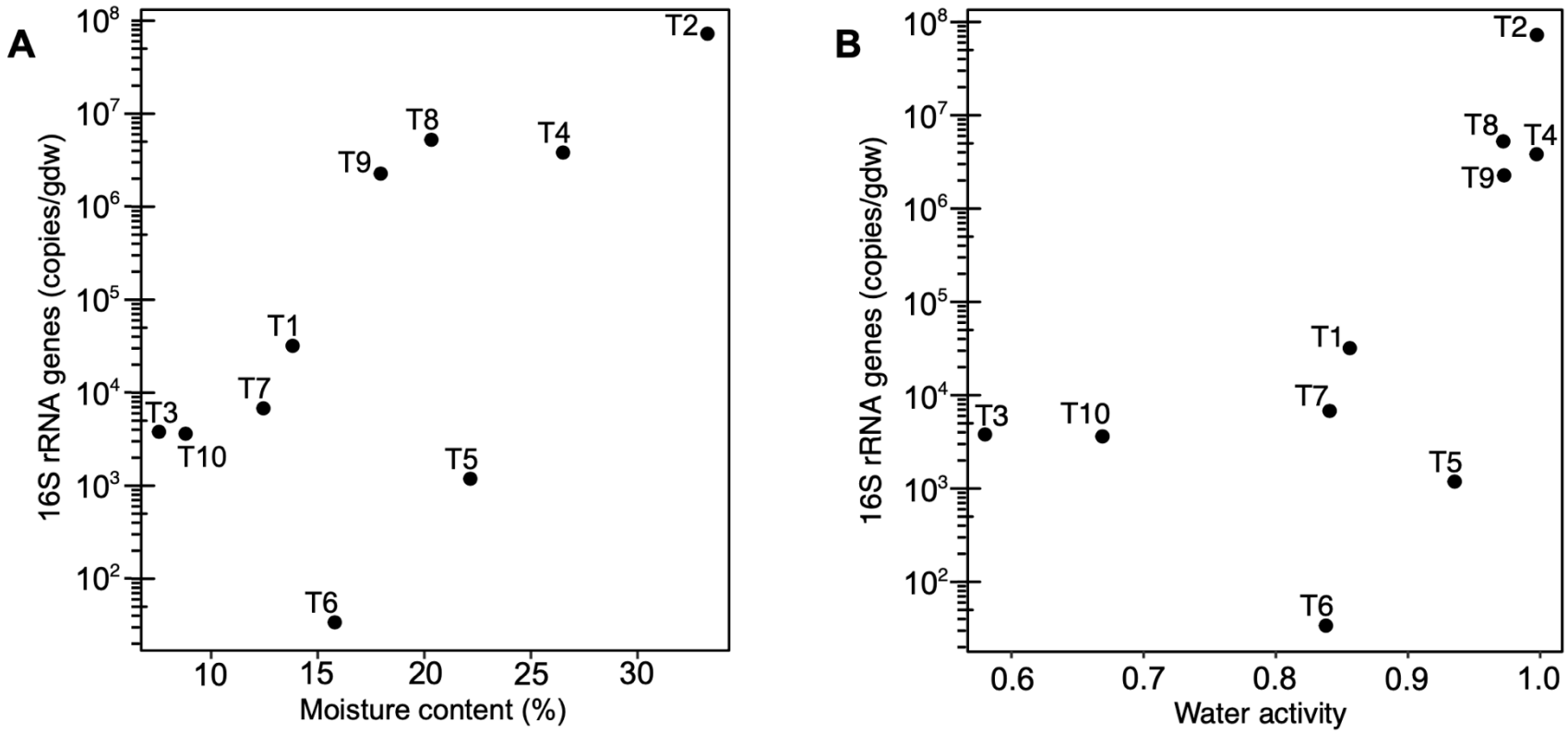

Figure 3.7 Scatterplots showing the relationship between the number of 16S rRNA gene copies/gdw and the moisture content (A) or water activity (B) of the Tsukinuno bentonite samples. The number of 16S rRNA gene copies/gdw was correlated to moisture content and water activity with Pearson correlation of 0.72 and Spearman correlation of 0.77, respectively.

3.3 Microbial viability

The DNA-based methods used to analyze the clay and rock samples can provide insight into the abundance and composition of microbial communities, however the microorganisms detected through such methods are not necessarily living or viable. Microorganisms can exist in a living but metabolically inactive state during exposure to unfavourable conditions [96], other bacteria can form spores when conditions are not favourable [97], and bacterial DNA can be preserved in environments for thousands of years after an organism has died [98]. Conversely, cultivation approaches can test the viability of the microorganisms present in a sample. The detection of cultivatable microorganisms from all Tsukinuno bentonite samples demonstrates that at least a portion of the total microorganisms detected in the clay are living cells, either active or inactive; however, this does not mean that all detected microorganisms are living or viable. Because cultivation approaches were not possible for the Opalinus clay and NOCR samples, it is not known whether any of the microorganisms quantified in these samples were viable or even extant. There are cultivation-independent techniques that could be applied to differentiate living cells from dead cells or relic biomarkers. For example, the adenosine triphosphate (ATP) assay, which makes use of the short-lived nature of ATP outside of a living cell, and DNA extraction modified to include a propidium monoazide incubation step, which excludes DNA not protected by an intact cell membrane from downstream analyses, have been used to study the living cells in other environments [99], and could be optimized for use in DGR relevant environments.

The potential for the growth of SRB in DGR-relevant bentonite clays is of particular interest due to their potential contributions to MIC. Sulfate reducing bacteria were only detected in one sample, T2, using cultivation approaches. It is important to note that the abundance of cultivatable SRB is likely lower in these clay samples than it would be in similar samples exposed to anoxic conditions, because, although previous studies have shown their ability to survive oxygen exposure for a limited period of time, SRB are strict anaerobes [100, 101].

3.4 Comparison of clay and rock reads to control reads

When amplifying and sequencing DNA, especially from low biomass samples, it is important to examine negative controls to ensure that the DNA detected in the samples is from the actual samples and was not introduced during the sample preparation, DNA extraction, or PCR steps. No DNA was detected in the DNA extraction kit controls and no template controls on a 1% agarose gel stained with gel red after PCR amplification for 40 cycles; however, some amplification was detected in these controls after 45 or 50 cycles of PCR (data not shown). The number of reads obtained by sequencing increased for samples and controls with increasing cycle number (Figure 3.8). The average number of reads for Tsukinuno bentonite samples amplified for 40 cycles of PCR was two orders of magnitude greater than the average number of reads in controls amplified with the same number of PCR cycles, although there was some overlap in read counts for these two groups of samples. For the same samples amplified with 45 cycles of PCR, there was only a difference of one order of magnitude between average reads of Tsukinuno bentonite samples and their controls, and samples amplified with 50 cycles of PCR had averages in the same order of magnitude for these two groups. For all PCR cycle numbers, the number of reads sequenced for Opalinus clay samples was similar to the average read count for controls. All sequenced NOCR samples were amplified for 50 cycles of PCR, and the average number of reads for these samples was in the same order of magnitude as the average number of reads for controls. The similarity in read number for Opalinus clay samples, NOCR samples, and the lower biomass Tsukinuno bentonite samples compared to the controls suggests that the sequenced reads of these samples may be comprised largely of contaminant sequences as opposed to reflecting the true clay and rock microbiomes.

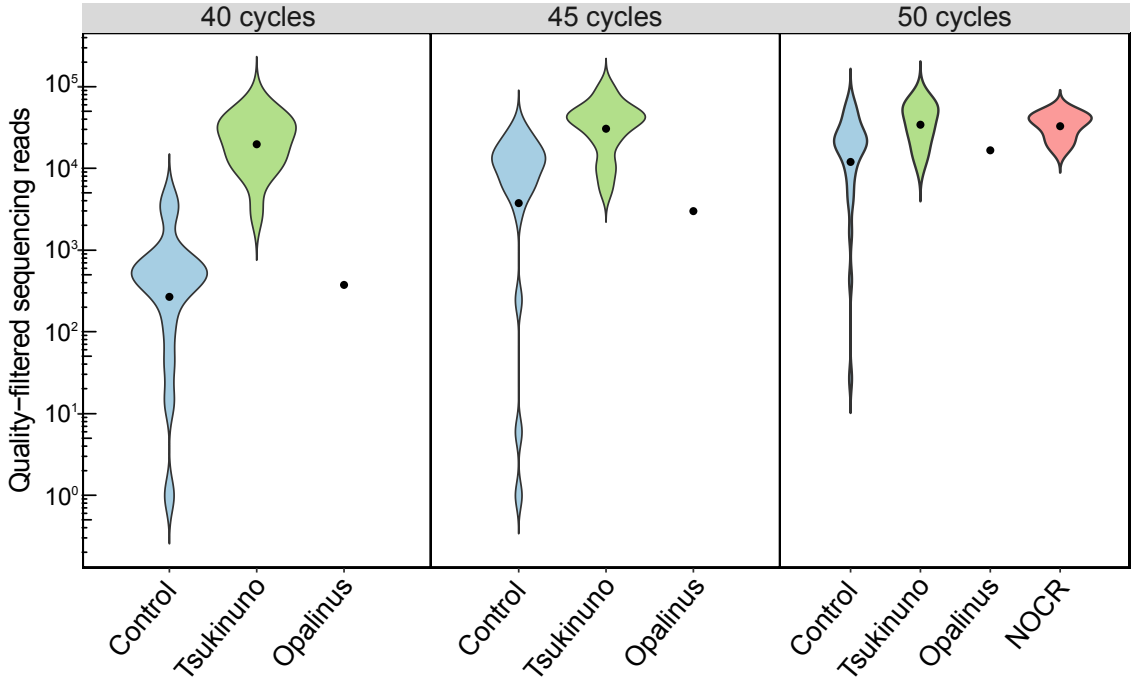

Figure 3.8 Violin plots of the distribution of sequenced reads for the Tsukinuno bentonite, Opalinus clay, and NOCR samples and their corresponding controls. Controls include DNA extraction kit controls and negative PCR controls, both those included in the 96-well plate with the samples and those amplified in individual tubes. The black dots indicate the mean number of reads for each group.

3.5 Comparison of Tsukinuno bentonite samples

With all tested distance metrics, the replicates of all Tsukinuno bentonite samples grouped with each other, regardless of cycle number (Figure 3.9). With weighted distance metrics, where abundant ASVs carry a higher weight than less abundant ASVs, replicates of samples grouped closer to each other than to replicates of other samples when phylogeny was not additionally taken into accounted (Figure 3.9, panel A). When phylogeny was considered in a distance metric, sample T4 was the only sample whose replicates grouped together and separately from the remainder of samples (Figure 3.9, panel C). This suggests that the dominant ASVs of sample T4 were phylogenetically more dissimilar to the dominant ASVs of the remaining samples, which had dominant ASVs that are likely more phylogenetically similar to each other.

With unweighted distance metrics (Figure 3.9, panels B and D), where abundant and rare ASVs carry equal weights, samples T2, T4, T8, and T9 were the only samples that grouped separately from other samples regardless of whether phylogeny was additionally taken into account (Figure 3.9, panel D) or not (Figure 3.9, panel B). This suggests that these four samples have overall different microbial compositions to the remaining samples, with samples T4, T8, an T9, that were taken from adjacent locations in the mine, having more similar microbial compositions to each other than to sample T2, which was taken from a different site in the mine. Samples T1 and T7 originated from the same clay bed and also grouped together in ordination space with all tested dissimilarity matrices; however, they did not group with the remaining samples from the same bed, T5, T6, T8, and T9.

A total of nine phyla were identified across all Tsukinuno bentonite samples at a relative abundance equal to or greater than 5% (*Actinobacteria*, *Bacteroidetes*, *Chloroflexi*, *Cyanobacteria*, *Euryarchaeota*, *Firmicutes*, *Nitrospirae*, *Proteobacteria*, and *Tenericutes*), with *Euryarchaeota* associated with sample T4 in particular (Figure 3.10). This was the only archaeal phylum detected with this relative abundance threshold, and its close grouping with sample T4 supports the observed dissimilarity of this sample compared to the other samples (Figure 3.9). With a goodness of fit statistic (R^2) threshold of 0.2, water activity, DNA concentration, and moisture content correlated with samples within ordination space, with moisture content having the highest correlation (Figure 3.10). This indicates that these three factors are all associated with differences in microbial communities among samples.

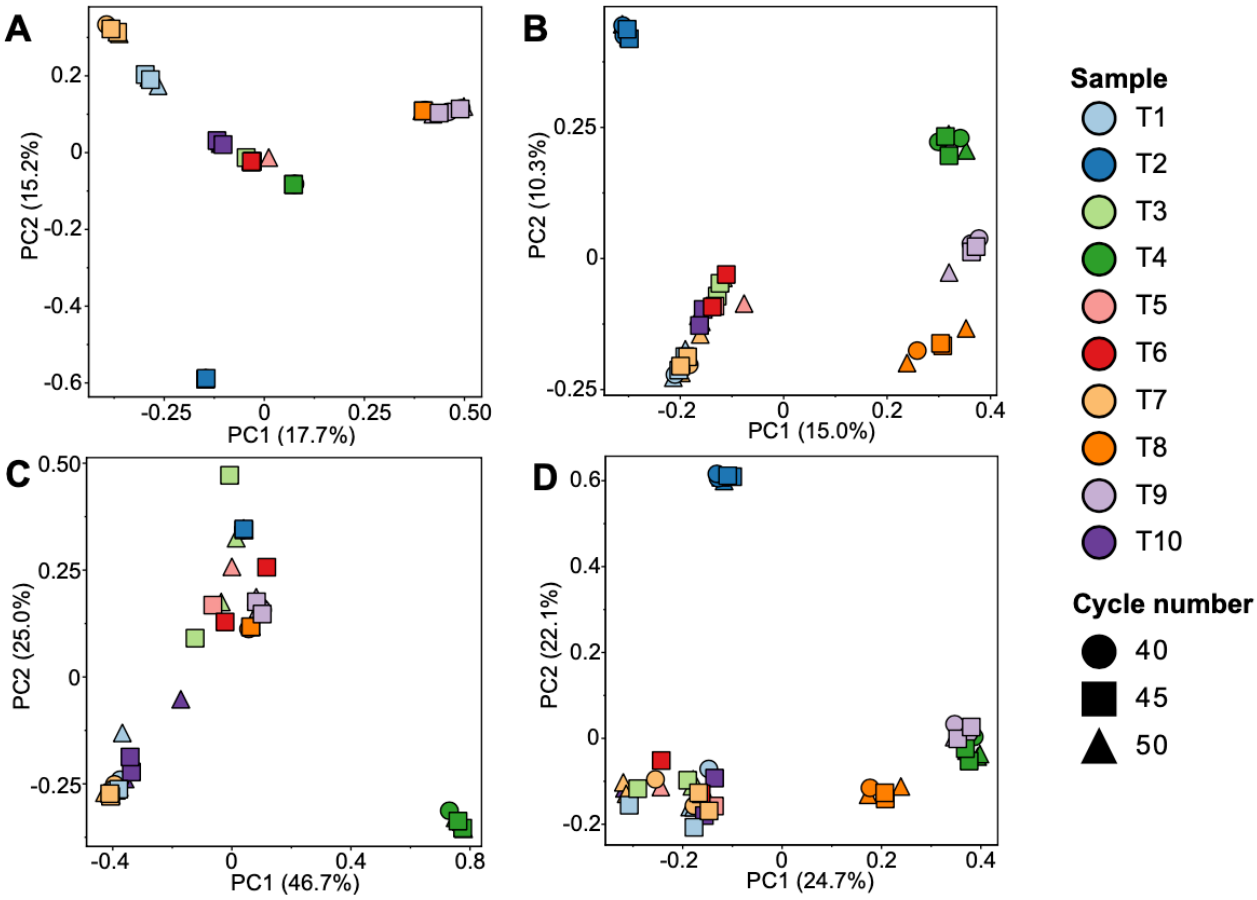

Figure 3.9 Principal coordinate analysis (PCoA) plots of Bray Curtis distances (A), Jaccard distances (B), weighted UniFrac distances (C), and unweighted UniFrac distances (D) of the Tsukinuno bentonite samples. Each sample (T1-T10) has two technical replicates from PCR amplification for each of 40, 45, and 50 cycles. When only one replicate of a sample is visible, the remaining replicates are hidden beneath. Samples were rarefied to 5100 reads. See Table 3.1 for additional sample information.

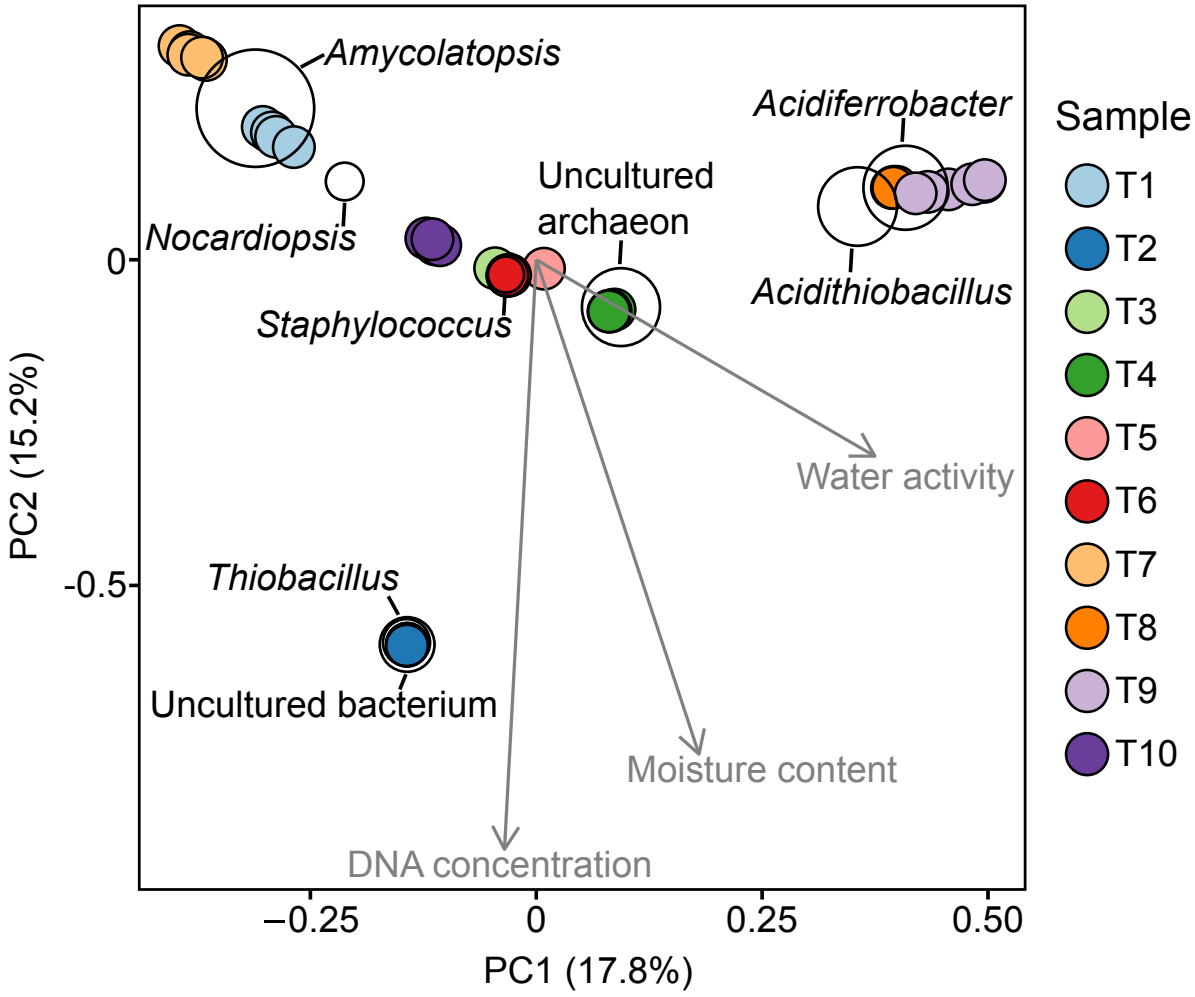

Figure 3.10 PCoA triplot based on Bray Curtis distances of the Tsukinuno bentonite samples. Genera greater than or equal to 5% relative abundance were displayed as clear circles. Environmental variables were displayed if they passed the goodness of fit statistic (R^2) threshold of 0.2. Water activity, moisture content, and DNA concentration had R^2 values of 0.2, 0.7, and 0.8 respectively. Samples were rarefied to 5100 reads. See Table 3.1 for additional sample information.

3.6 Diversity of clay and rock samples

Clay and rock samples had Shannon index values of 0.5 (T8) to 4.6 (T2; average of 2.3), Faith's phylogenetic diversities of 3.3 (T10) to 26.7 (T2; average of 7.9), and Pielou's evenness index values of 0.1 (T8) to 0.8 (T6; average 0.5; Figure 3.11). Faith's phylogenetic diversity values and Shannon index values had weakly positive correlations, whereas Pielou's evenness index values were strongly and positively correlated with Shannon index values (Figure 3.11). Sample T2 replicates had higher overall diversity (Shannon index) and richness (Faith's phylogenetic diversity) than any other samples and appear to have diversities driven more so by richness than by evenness (Figure 11). The remaining clay and rock sample diversities are driven primarily by evenness and not richness.

The Tsukinuno bentonite samples had a larger range of diversities than the Opalinus clay sample or the NOCR samples (Figure 3.12). NOCR and Tsukinuno bentonite samples had greater average Shannon index values than the average Shannon index of cultures (Mann-Whitney U test; $p<0.05$). There was no significant difference in diversity between the Tsukinuno bentonite, Opalinus clay, and NOCR samples, or between the aerobic heterotrophs, anaerobic heterotrophs, and SRB cultures (Mann-Whitney U test; $p<0.05$)

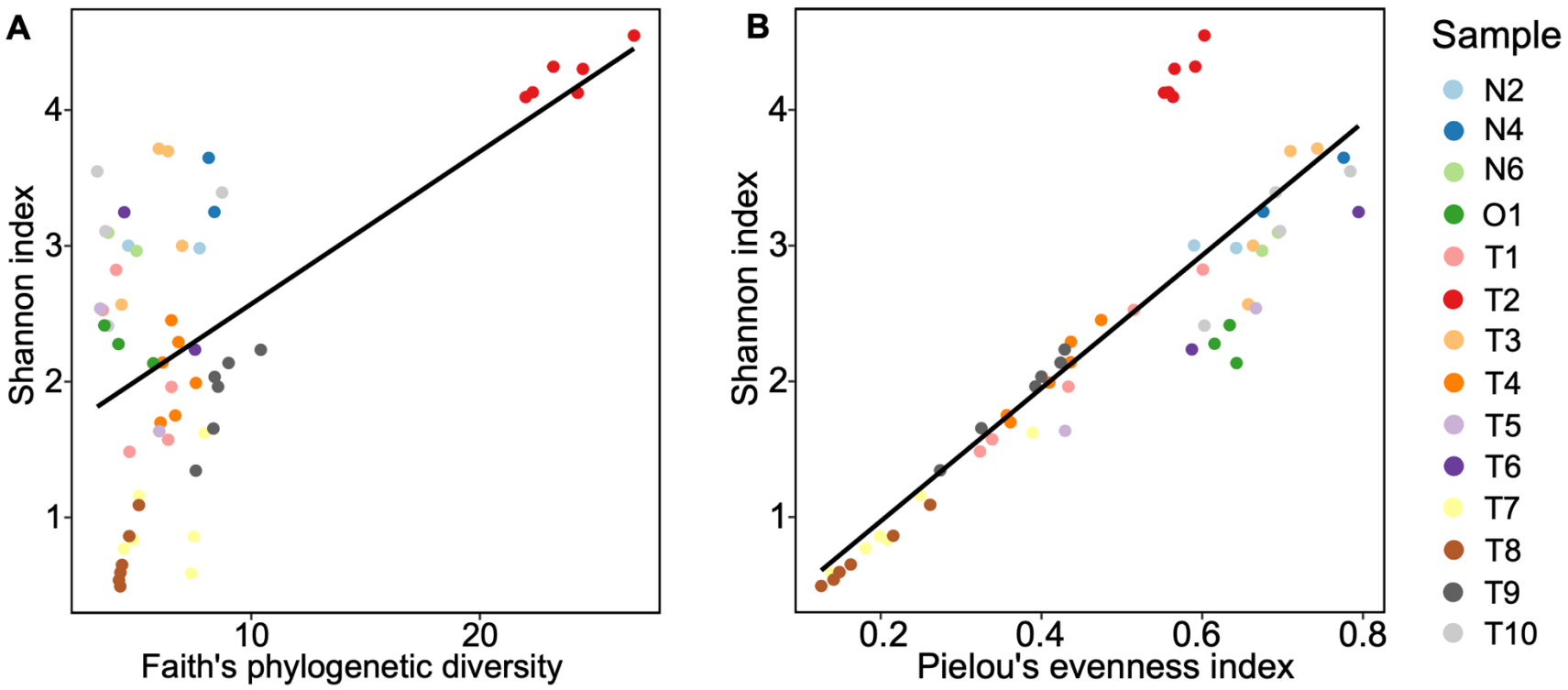

Figure 3.11 A measure of total diversity (Shannon index) compared to richness (Faith's phylogenetic diversity; A) and to evenness (Pielou's evenness, B) in the Tsukinuno bentonite, Opalinus clay, and NOCR samples. Samples were rarefied to 5100 reads. Shannon index and Faith's phylogenetic diversity (A) were weakly correlated with a Pearson correlation of 0.59 for these samples, and Shannon index and Pielou's evenness index were strongly correlated with a Pearson correlation of 0.86. See Table 3.1 for additional sample information.

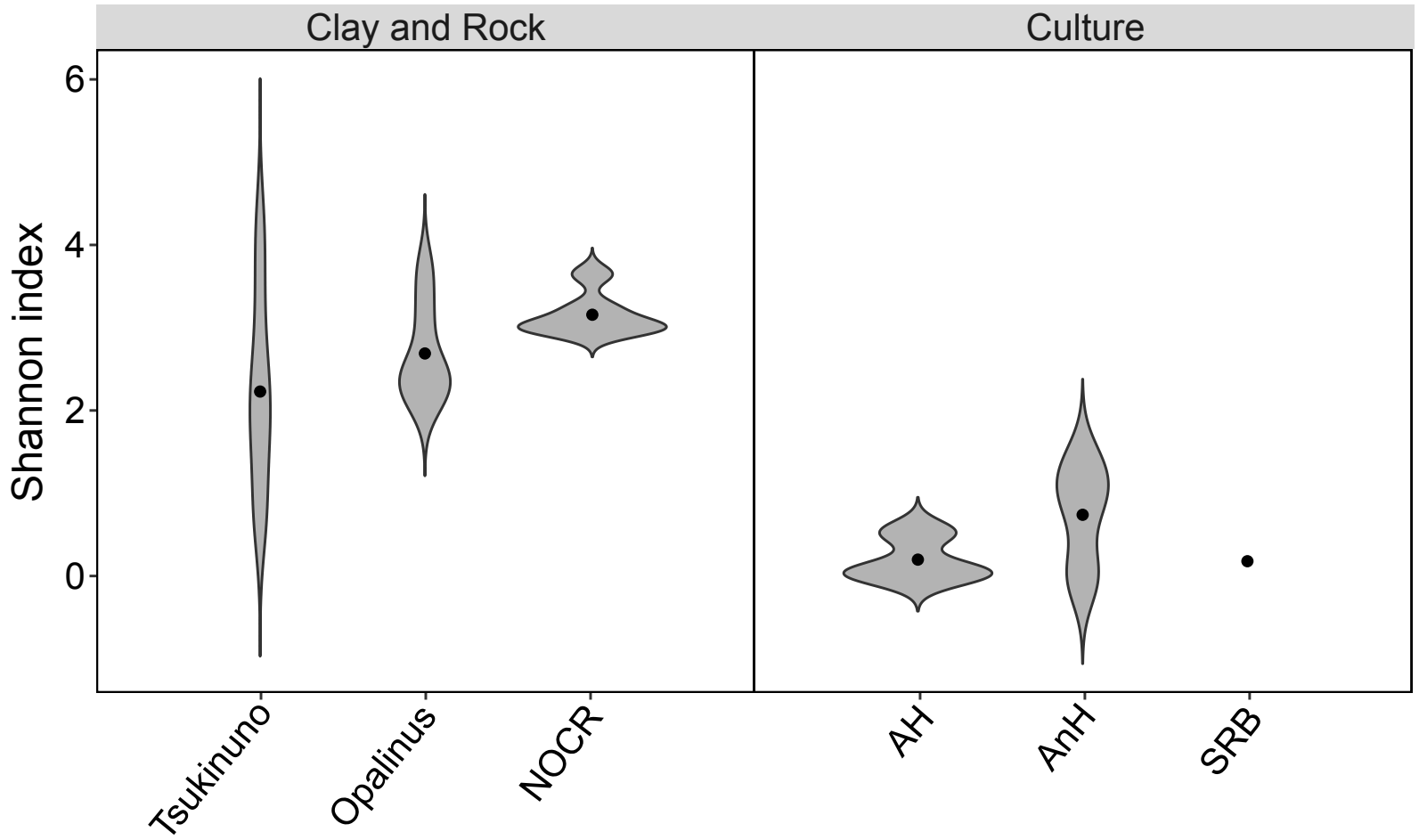

Figure 3.12 Violin plots showing the Shannon diversity of the aerobic heterotrophs (AH), anaerobic heterotrophs (AnH), and sulfate reducing bacteria (SRB), as well as the Tsukinuno bentonite samples, the Opalinus clay sample, and the NOCR samples. Samples were rarefied to 5100 reads. The average Shannon index is indicated by the black dot.

3.7 Microbial characterization of clay and rock samples

3.7.1 Tsukinuno bentonite samples

Tsukinuno bentonite samples T1, T2, T4, T7, T8, and T9 each had replicates with consistent 16S rRNA gene profiles (Figure 3.13). For each of these samples, the 16S rRNA gene profiles were dominated by one to three ASVs. None of these dominant ASVs occurred in more than one sample. However, similar to the ordinations, the 16S rRNA gene profiles show that samples taken from adjacent locations in the same bed had taxonomically similar dominant ASVs when the samples had similar appearance, water activity, and moisture content. Although samples T3, T5, T6, and T10 had several shared ASVs among replicates, the profiles show a higher degree of variation in 16S rRNA gene profiles. Overall, bed two (T3) had ASV representation from seven of the nine phyla detected across all samples at or above 5% abundance, bed 17 (T2) was dominated by *Proteobacteria*, bed 19 (T1; T5-T9) by *Actinobacteria* and *Proteobacteria*, bed 20 (T4) by *Euryarchaeota*, and bed 29 (T10) by *Actinobacteria*.

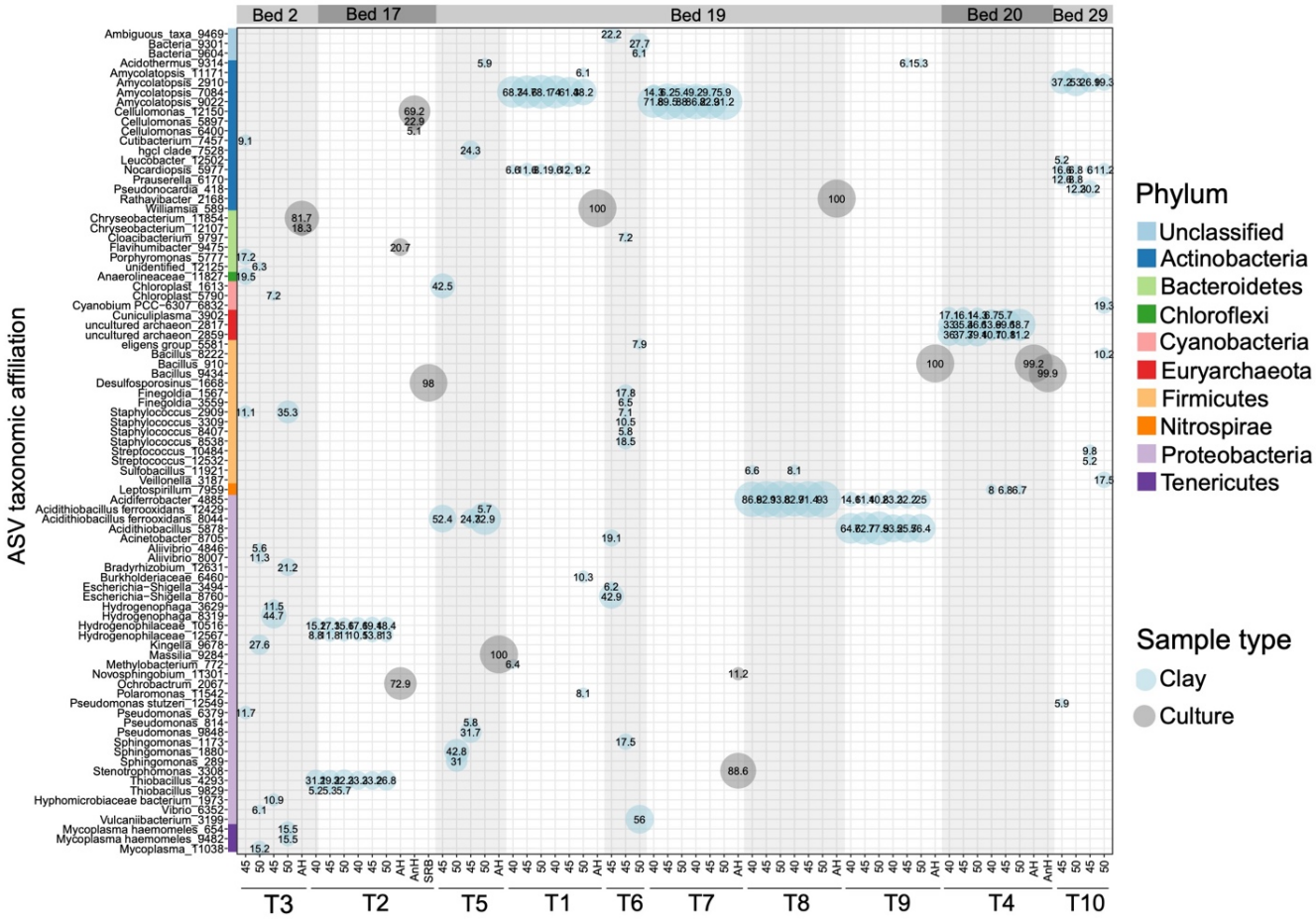

Figure 3.13 Bubble plot showing the 16S rRNA gene profiles of the Tsukinuno bentonite clay samples (blue) and the corresponding aerobic heterotroph (AH), anaerobic heterotroph (AnH), and SRB cultures (grey). Only ASVs at or above 5% relative abundance in a sample are included. Up to six replicates were analyzed for each of the ten bentonite samples, comprising of duplicate extractions which were amplified at 40, 45, and 50 cycles. Samples that showed no visible amplicon in an agarose gel after PCR were not included in the sequencing analysis and thus are not included in this plot. Bed number indicates which bed of the clay deposit each sample was taken from. See Table 3.1 for additional sample information.

Samples T3 and T6 had the least consistent 16S rRNA gene profiles between replicates. The only ASV that was detected in more than one replicate of sample T3 at or above 5% abundance was one assigned to *Staphylococcus*, a member of the phylum *Firmicutes*, which occurred in two replicates of the sample. Although *Staphylococcus* is generally a mammalian skin-associated genus of bacteria, it has been cultivated from bentonite clay in Spanish bentonite formations [73], and from the Boom clay formation in two separate studies [77, 78]; however, it was suggested in both to be a potential contaminant. With no relative abundance threshold, there was one additional ASV, assigned to *Cutibacterium*, that was found in two replicates of this sample. The five species belonging to this genus are often reported on human skin [102].

The only ASV present in the 16S rRNA gene profile of more than one replicate of sample T6 was assigned to the genus *Afipia*, which contains six species of human pathogens [103], some of which have more recently been shown to be methylotrophs growing in non-human associated environments [104, 105]. With the exception of sample T2, the same ASV assigned to the genus *Afipia* was found in all Tsukinuno bentonite samples at relative abundances up to 2.8%. This same ASV was detected in a several negative controls, where it was sometimes a dominant member of the control microbial community. The combined lack of consistency between replicate 16S rRNA gene profiles and the classification of the most prevalent ASVs in these samples as human-association microorganisms suggests that the 16S rRNA gene profiles of samples T3 and T6 likely do not represent the true clay microbial community.

The two samples taken from locations adjacent to sample T6, samples T1 and T7, both had 16S rRNA gene profiles dominated by ASVs assigned to the genus *Amycolatopsis*, a member of the phylum *Actinobacteria*, which contains over 30 species that grow by fermentation [106] or aerobic heterotrophy [107] (Figure 3.13). The genus is comprised of species with a variety of different metabolic functions. For example, *Amycolatopsis tucumanensis* has implications in the bioremediation of copper-polluted environments [108, 109], the polyester degradation ability of many strains of *Amycolatopsis* has been shown [110–112], and many

fermentative species of *Amycolaptopsis* are responsible for the production of antibiotics such as rifamycin B [106], epoxyquinomicin [113], vancomycin [114], and ristocetin [115].

At lower relative abundances, all six replicates of sample T1, and five of six replicates of sample T7 had 16S rRNA gene profiles with an ASV belonging to the genus *Nocardiopsis*. Like *Amycolatopsis*, the genus *Nocardiopsis* is comprised of many aerobic heterotrophs that are together both ecologically versatile and biotechnologically important. Most *Nocardiopsis* species are soil-associated, and can thrive in saline and hypersaline [116–118], desert [119], and alkaline [120] soils. Members of the genus produce the anti-cancer compounds apoptolidin [121], the antibiotic and anti-cancer naphthospirononones compounds [122], the antibiotics pyranonaphthoquinone and thiopeptide [123, 124], and biosurfactants [125].

Among rare ASVs, the 16S rRNA gene profiles of most sample T1 replicates additionally had ASVs assigned to the genera of aerobic bacteria *Pseudonocardia* and *Frankia*, and *Pseudonocardia* was also prevalent in sample T7 replicates. Some species of *Pseudonocardia* are heterotrophic, most notably using cyclic organic molecules such as tetrachlorobenzene [126], 1,4-dioxane [127], and tetrahydrofuran [128] as carbon and energy sources. Other species of this genus can oxidize sulfur-compounds to sulfate [129]. Species in the genus *Frankia* are characterized by their ability to induce N_2-fixing root nodules on non-leguminous plants [130], and can fix nitrogen in both free-living and symbiotic states [131]. The only metabolic predictions made by FAPROTAX [132] for all replicates of sample T1 and T6 is chemoheterotrophy, though predictions could not be made for a large proportion of the ASVs (Figure 3.14). The similarity in microbial composition of samples T1 and T7 was supported by their grouping in ordination space (Figure 3.9).

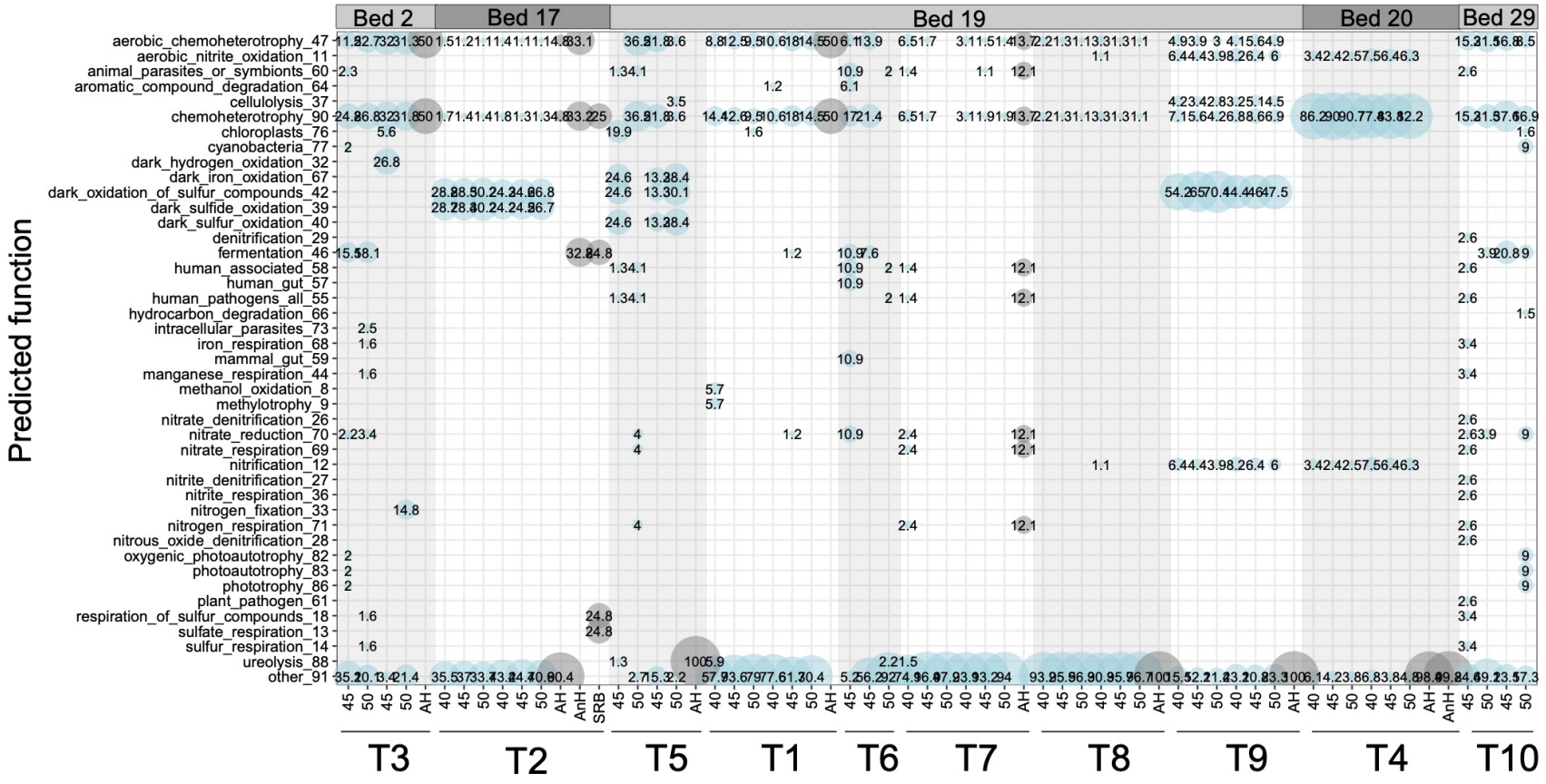

Figure 3.14 Bubble plot showing the relative abundance of ASVs predicted to have the listed functions in the Tsukinuno bentonite samples and the corresponding aerobic heterotroph (AH), anaerobic heterotroph (AnH) and SRB cultures. Functions that occurred at less than 1% relative abundance in a sample were not included. Predicted functions were made by FAPROTAX [132] and were based on the sequenced V4-V5 region of the 16S rRNA gene. Bed number indicates which bed of the clay deposit each sample was taken from. See Table 3.1 for additional sample information.

Like samples T1 and T7, the 16S rRNA gene profile of sample T10 was also dominated by biotechnologically important genera of aerobic heterotrophs and fermenting bacteria, specifically *Amycolatopsis* and *Nocardiopsis*, which were both detected in samples T1 and T7 (Figure 3.13). The 16S rRNA gene profile of sample T10 had no rare ASVs present in the majority of replicates. The only metabolic activity predicted by FAPROTAX to exist in all replicates of sample T1, T7, and T10 was chemoheterotrophy, which is consistent with the classification of ASVs prevalent across replicates (Figure 3.14).

The remaining Tsukinuno bentonite samples, T2, T5, T8, T9, and T4, had 16S rRNA gene profiles that suggested that these samples supported primarily chemolithoautotrophic and often acidophilic microorganisms. Sample T2 had predicted metabolisms suggesting a community comprised primarily of sulfur-compound oxidizers, with the rarer members living chemoheterotrophically (Figure 3.14). The 16S rRNA gene profile of sample T2, at or above 5% abundance, consisted of two ASVs belonging to the family *Hydrogenophilaceae* and one belonging to the genus *Thiobacillus*, one of three genera in the family *Hydrogenophilaceae*, in all six replicates (Figure 3.13). There are two species of *Thiobacillus*: *Thiobacillus denitrificans* and *Thiobacillus thioparus*, both of which are obligate chemolithoautotrophs capable of sulfur-compound oxidation [133]. *Thiobacillus denitrificans* is best known for its ability to couple sulfur-compound oxidation to denitrification [133–136], however it has also been shown to be capable of coupling nitrate reduction to the oxidation of metals such as iron [137, 138] and uranium [139]. In contrast, the less studied *Thiobacillus thioparus* is only capable of aerobic growth using dioxygen (O_2) gas as a terminal electron acceptor [140]. The 16S rRNA gene profile of sample T2 had an additional 76 ASVs that were present, mostly at less than 1% relative abundance, in more than half of the six replicates. Of these 76 ASVs, 58 were present in all six replicates. The large number of prevalent ASVs across replicates of sample T2 is consistent with the high calculated diversity (Figure 3.11). This was also the sample with the highest water activity and moisture content (Figure 3.3), with the highest overall microbial abundance (Figure 3.5), and the only sample from which SRB were cultivated (Figure 3.5). This sample highlights the importance of maintaining DGR

conditions that will prevent the growth of microorganisms; it contains a high diversity of potentially living, metabolically versatile microorganisms, including SRB, ready to grow should environmental conditions allow.

The replicate 16S rRNA gene profiles of sample T5 were more dissimilar that those of the other chemolithoautotroph-dominated samples. That said, three of the four replicates of sample T5 had 16S rRNA gene profiles dominated by the same ASV classified as the acidophilic chemolithoautotroph *Acidithiobacillus ferooxidans* (Figure 3.13). This species of bacteria is known for its role in bioleaching in acidified mine drainages [141]. It is capable of the aerobic oxidation of Fe^{2+}, sulfur-compounds [142], hydrogen [143], and formate [144]. Under anoxic conditions, it can respire Fe^{3+} [145] or S^0 [146]. The species *Acidithiobacillus ferooxidans* has been identified as a primary producer in the environments in which it is found due to its ability to fix nitrogen and carbon from N_2 [147] and CO_2 respectively [148]. The potential for sulfur and iron oxidation by the microbial community in sample T5 was supported by the FAPROTAX predictions (Figure 3.14).

Samples T8 and T9, which were taken from the same clay bed as sample T5, had 16S rRNA gene profiles dominated by the gammaproteobacterial genus *Acidiferrobacter*, and additionally *Acidithiobacillus* in sample T9. The genus *Acidiferrobacter* is made up of a single named species, *Acidiferrobacter thiooxydans*. This obligately autotrophic, facultatively anaerobic, acidophilic species is capable of oxidizing S^0 or Fe^{2+} coupled to the reduction of either O_2 or Fe^{3+} [149]. The four named species of *Acidithiobacillus*, *Acidithiobacillus ferrooxidans* (present in sample T5 and described previously), *Acidithiobacillus caldus*, *Acidithiobacillus ferrivorans*, and *Acidithiobacillus thiooxidans,* are acidophilic, carbon-fixing, chemolithoautotrophs that oxidize sulfur-compounds to sulfuric acid [142, 150–152]. The species *Acidithiobacillus ferrooxidans* and *Acidithiobacillus ferrivorans* are additionally diazotrophs capable of Fe^{2+} and hydrogen oxidation, and can respire Fe^{3+} or S^0 in the absence of O_2 [145, 146, 151].

In addition to the dominant species, the 16S rRNA gene profiles of samples T8 and T9 had seven ASVs present in most or all replicates of both samples at relative abundances lower than 5%, and often less than 1%. All seven genera, *Acidibacter*, *Acidiphilium*, *Acidothermus*, *Alicyclobacillus*, *Ferrithrix*, *Leptospirillum*, and *Sulfobacillus*, consist of acidophilic species of bacteria, most of which have implications in acid mine drainage and bioleaching (Falagán and Johnson, 2014; Wichlacz *et al.*, 1986; Mohagheghi *et al.*, 1986; Goto *et al.*, 2007; Johnson *et al.*, 2009; Coram and Rawlings, 2002; Bogdanova *et al.*, 2006). Species of *Acidiphilium*, *Acidothermus*, and *Alicyclobacillus* are aerobic heterotrophs, and the latter two are thermophiles [154–156]. Species of *Acidibacter* are anaerobic heterotrophs that respire Fe^{3+} [153]. The genus *Sulfobacillus* is comprised of aerobic, thermotolerant, endospore-forming, heterotrophic species that oxidize Fe^{2+} and sulfur-compounds [159]. The only species in the genus *Ferrithrix*, *Ferrithrix thermotolerans*, is a moderate thermopile and obligate heterotroph that can oxidize Fe^{2+} with O_2 as an electron acceptor, or can respire Fe^{3+} with glycerol as an electron source in the absence of O_2 [157]. Bacteria belonging to the genus *Leptospirillum* are aerobic, obligate Fe^{2+} oxidizing bacteria [158]. Sample T9 had an additional low-abundance ASV classified as *Thiomonas* in all replicates. Bacteria within this genus are facultative chemolithoautotrophs that can oxidize sulfur compounds and Fe^{2+}, but can also use organic carbon as an energy source when present [160]. The FAPROTAX predictions for sample T9 suggest a community dominated by sulfur-compound oxidation (Figure 3.14), which is consistent with the abundance of *Acidithiobacillus* in this sample (Figure 3.13). The majority of the sample T8 ASVs, including *Acidiferrobacter*, were not classified by FAPROTAX.

The 16S rRNA gene profile of sample T4 was dominated by two ASVs of archaea in the family *Thermoplasmataceae*, and a third more well classified ASV belonging to the *Cuniculiplasma* genus of the family *Thermoplasmataceae*. These dominant taxa are phylogenetically dissimilar to all other dominant taxa in the Tsukinuno bentonite clay samples, which is supported by the position of sample T4 in ordination space (Figure 3.9). All species within the family *Thermoplasmataceae* are acidophiles, some having the lowest

known pH optima of any species [161]. Members of the family are facultatively anaerobic and can respire S^0 [162] or Fe^{3+} [163] in the absence of O_2. Some species are organotrophs [161–163], whereas others gain energy from the oxidation of Fe^{2+} [163]. Many species are thermophiles [162, 163], though some are mesophiles [161]. The genus *Cuniculiplasma* in particular has a single species, *Cuniculiplasma divulgatum*, which is made up of facultatively anaerobic, acidophilic, mesophilic, chemoorganoheterotrophic bacteria [161].

The rare portion of the 16S rRNA gene profile common to most or all replicates of sample T4 includes several of the acidophilic genera, namely *Acidibacter*, *Acidiferrobacter*, *Ferrithrix*, *Leptospirillum*, and *Sulfobacillus*, that were also present in samples T8 and T9. Additionally present were the obligately aerobic acetic acid-producing family of bacteria, *Acetobacteraceae* [164], the candidate genus of amoeba endosymbionts, *Endonucleariba*cter, the extremely acidophilic, iron oxidizing, mesophilic obligate heterotroph *Ferrimicrobium acidiphilum* [157], and unclassified members of the families *Acidimicrobiaceae*, of which *Ferrimicrobium* is a member, and *Solirubrobacteriaceae*. The similarity in taxa found at less than 5% abundance in samples T4, T8, and T9 is further emphasized by the grouping of the replicates of these three samples in ordination space (Figure 3.9).

A previous experiment assessing the microbial composition of the Boom clay deposit (Belgium) by sequencing the 16S rRNA gene found the samples to be dominated by *Proteobacteria*, similar to samples T3, T2, T5, T8, T9, and *Firmicutes*, though some of the *Firmicutes* identified were suggested to be contaminants [78]. Members of the phylum *Proteobacteria* were also found to be dominant members of the microbial community in Spanish bentonite clay deposits in another study, making up between 30% and 100% of total 16S rRNA gene reads [79]. With the exception of *Euryarchaeota* and *Tenericutes*, all phyla detected in the Tsukinuno bentonite clay samples at or above 5% abundance were also detected in the Spanish bentonite samples [79]. In contrast, a Chinese bentonite sample was found to have a microbial community dominated by *Thaumarchaeota*, specifically members of the genus *Nitrososphaera*, though *Proteobacteria* still made up approximately 15% of the

microbial community [80]. All phyla detected in the Tsukinuno bentonite clay samples at or above 5% abundance, with the exception of *Tenericutes*, were also detected in the Chinese bentonite sample [80].

The only ASVs associated with sulfur reduction that were prevalent across the replicates of a sample were ones classified as *Acidithiobacillus ferrooxidans*, the genus *Acidithiobacillus*, and the family *Thermoplasmataceae*, which were prevalent in samples T5, T9, and T4 respectively. All of these bacteria and archaea are facultatively anaerobic and thus are likely using O_2 instead of S^0 as an electron acceptor in the oxic locations from which the samples were taken. No ASVs associated with known SRB were detected. Though the species detected overall in the Tsukinuno bentonite samples through 16S rRNA gene sequencing are capable of some of the forms of metabolism expected to be possible in a DGR, many, especially those associated with sulfate reduction, were not accounted for in the Tsukinuno bentonite clay samples. Performing these same experiments on ancient natural barrier component samples taken from anoxic environments could yield more information on the potential for anaerobic metabolisms, such as sulfate reduction, in these types of samples.

3.7.2 Tsukinuno bentonite-associated cultures

Both the R2A agar and the sulfate reducing medium used to culture microorganisms are complex media and would be expected to support a variety of heterotrophic metabolisms. The sulfate reducing medium is additionally enriched with sodium sulfate to support the growth of sulfate reducing bacteria. The potential for chemoheterotrophy was indeed predicted in all aerobic and anaerobic heterotroph cultures for which a prediction could be made, with the exception of the aerobic heterotroph culture from sample T5, for which the only detected microorganism, a species of *Massilia*, was predicted to be exclusively capable of ureolysis (Figure 3.14). The anaerobic heterotrophs and SRB cultivated from sample T2 were predicted to be capable of fermentation, and the SRB culture had additional evidence for sulfur compound respiration, which could include sulfate reduction. Nitrate and nitrogen reduction potential was additionally predicted in the aerobic heterotroph culture from sample

T7 (Figure 3.14).

Using only three cultivation approaches for a metabolically diverse community, it was expected that only a subset of the ASVs detected in the 16S rRNA gene profiles of the clay samples would be detected in the 16S rRNA gene profiles of the cultures. The occurrence of very few ASVs in the 16S rRNA gene profiles of the cultures was indeed observed, with the microbial profiles of culture biomass each being dominated by one ASV representing ~70-100% of the reads (Figure 3.13). Some cultures had a few additional ASVs that were taxonomically similar to the dominant ASV. Only one ASV present in the 16S rRNA gene profile of a culture was also found in its corresponding clay. This ASV, associated with the genus *Geothrix*, was found in the 16S rRNA gene profile of the anaerobic heterotroph culture of sample T2 at 0.5% abundance, and one of the 40 PCR cycle replicates of this same sample at 0.1% abundance. Many of the organisms detected using 16S rRNA gene sequencing were acidophilic, thermophilic, and used reduced iron and sulfur compounds as an electron source, and these conditions were not met by the cultivation techniques employed.

The sequencing of the 16S rRNA genes from culture biomass DNA extracts revealed that bacteria belonging to four different phyla, *Bacteroidetes*, *Proteobacteria*, *Actinobacteria*, and *Firmicutes*, were isolated on the R2A agar plates incubated under oxic conditions, and additional bacteria from the phyla *Actinobacteria* and *Firmicutes* were isolated on R2A agar plates incubated under anoxic conditions (Figure 3.13). The 16S rRNA gene profile of the one SRB culture from sample T2 indicates that the SRB belonged to the genus *Desulfosporosinus*. This ASV, and no other ASV assigned to the genus *Desulfosporosinus*, were found in the 16S rRNA gene profiles of any of the Tsukinuno bentonite clay samples. The genus *Desulfosporosinus* is made up of seven species which are all obligately anaerobic, spore-forming SRB [165–171]. The oxic conditions in the mine would be expected to preclude the growth of these organisms, although they may have existed in the location from which sample T2 was taken at a time when it was anoxic and remained alive and viable as spores.

3.7.3 Opalinus clay and NOCR samples

The five replicates of the Opalinus clay sample had little overlap in 16S rRNA gene profiles (Figure 3.15). The majority of ASVs detected at or above 5% abundance belonged to the phylum *Proteobacteria*, though one member each of the phyla *Tenericutes*, *Firmicutes*, and *Chloroflexi*, and two members each of the phyla *Bacteroidetes* and *Actinobacteria* were also detected. Of the 18 ASVs detected across all replicates at or above 5% abundance, only two were detected in more than one replicate (Figure 3.15). The first was an ASV classified as *Methylobacterium*, a genus of 19 facultatively methylotrophic species [172], which was found in two replicates of the sample, both at above 30% abundance, and no associated negative controls. An additional ASV classified as *Methylobacterium* was a dominant member of the 16S rRNA gene profile of a third replicate and was also not detected in the associated negative controls. The second prevalent ASV was found in two replicates, both at above 20% relative abundance, and was classified as *Vibrio*, a genus made up of over 100 species that are commonly found in marine coastal waters, sediments, estuaries, and freshwater lakes and rivers [173] that have been associated with food-related illness due to their natural associations with marine plant and animals [173]. This ASV was also detected in a negative PCR control associated with one of the two replicate Opalinus clay samples at 1.8% abundance. Of the remaining ASVs detected at or above 5% relative abundance, the ASV classified as *Afipia*, which was the same *Afipia* ASV detected in most of the Tsukinuno bentonite samples, was the only one also detected in a related negative control.

For each of the three NOCR samples, the two inner layer replicates and the outer layer swab replicate had no overlapping dominant (>5% abundant) ASVs (Figure 3.16). Most of the ASVs detected at or above 5% abundance belonged to the phylum *Firmicutes*, though some representatives of the *Proteobacteria*, *Euryarchaeota*, *Cyanobacteria*, *Bacteroidetes*, and *Actinobacteria* were also detected. Among the rarer ASVs, there were three that were present each in two replicates of the NOCR sample N2, classified as *Coriobacteriales*, *Mycobacterium*, and *Pseudomonas* respectively. None of these ASVs were detected in negative controls associated with these samples. The order *Coriobacteriales* is made up of

commensal species capable of using a wide variety of carbohydrate sources for energy and carbon and of producing metabolites such as lactate [174]. The genus *Mycobacterium* is made up of biofilm-forming heterotrophic species that are found in a variety of environments, but they are most well known for their roles in human disease [175]. The genus *Pseudomonas* also includes opportunistic human pathogens, though the metabolically diverse heterotrophs are also found in soil and water [176]. Two of the ASVs detected in the NOCR samples were assigned to the chloroplast of *Austrotaxus spicata*, which is a species of plant endemic to New Caledonia (a French territory in the South-Pacific) [177]. It is not clear why DNA from this organism was found in these samples.

Similar to the Opalinus clay sample, only two of the ASVs (*Pseudomonas* 6533 and *Planococcaceae* 7786) detected at or above 5% relative abundance in the NOCR samples were also detected in the corresponding negative controls, despite the low consistency between replicate 16S rRNA gene profiles. The lack of consistency between replicate 16S rRNA gene profiles of the NOCR and Opalinus clay samples reduces confidence that any ASVs were specifically associated with low biomass rock and clay cores and not instead contaminant sequences. The similar number of reads sequenced for NOCR and Opalinus clay samples compared to negative controls (Figure 3.8) would support this, although little overlap was observed in the specific ASVs detected in the clay and rock samples compared to the controls. Alternatively, the biomass of the samples could be sufficiently low that biological and technical replicates actually contain DNA from different species.

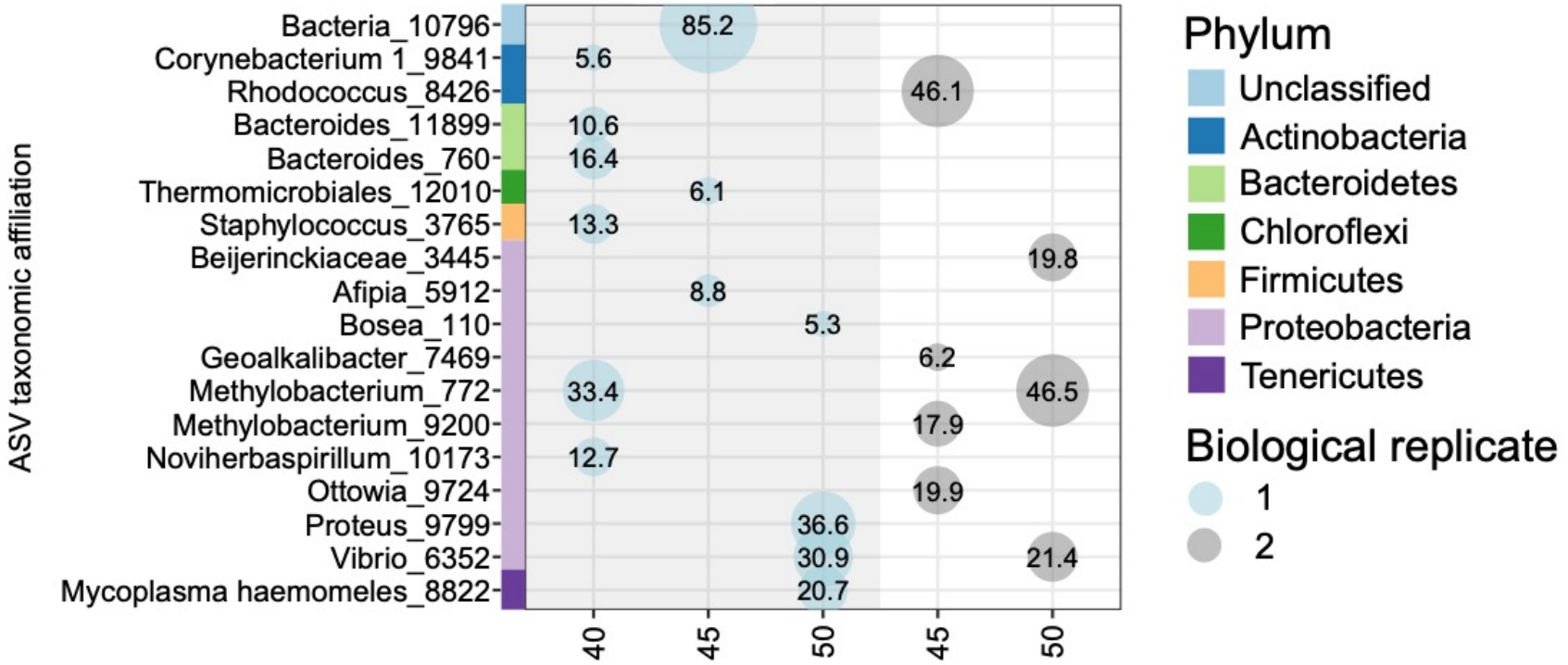

Figure 3.15 Bubble plot showing the 16S rRNA gene profile of the Opalinus clay sample. The labels 40, 45, and 50 indicate the number of PCR cycles used to amplify the DNA samples. Only ASVs at or above 5% relative abundance in a sample are included. Replicates that showed no visible amplicon in an agarose gel after PCR were not included in the sequencing analysis and thus are not included in this plot.

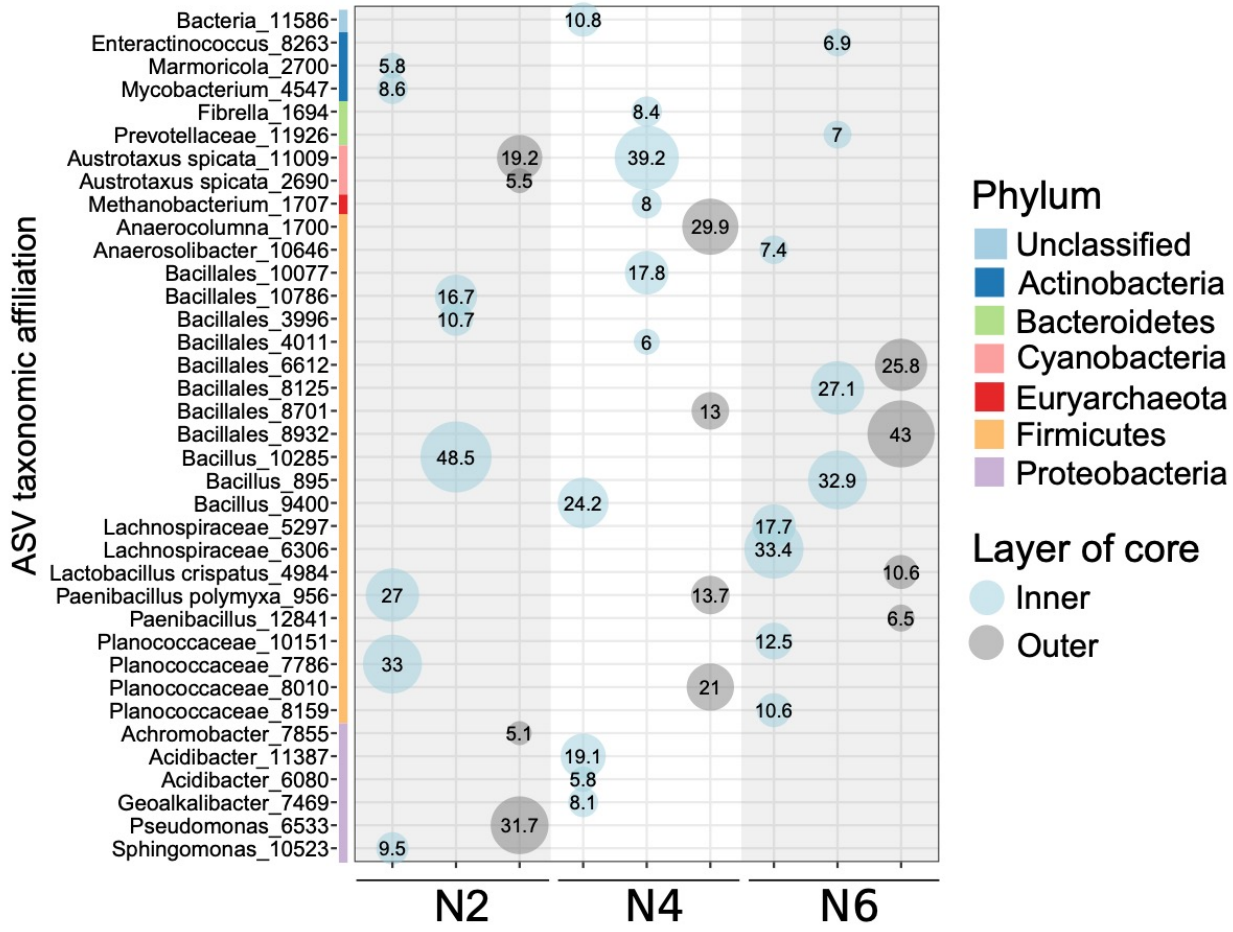

Figure 3.16 Bubble plot showing the 16S rRNA gene profile of the inner and swabbed outer layer of the three NOCR samples. Two biological replicates of each rock sample are included. Only ASVs at or above 5% relative abundance in a sample are included.

3.8 Predicting consistency of 16S rRNA gene profiles before sequencing

Although it is difficult to predict with certainty whether replicate 16S rRNA gene profiles will be consistent before sequencing, it may be possible to gain some insight from amplification data. First, all samples where both biological replicates had amplicons visible on an agarose gel with 4 µL of sample after 40 cycles of PCR, T2, T1, T7, T8, T9, and T4, yielded consistent 16S rRNA gene profiles after sequencing. For these samples, replicates that were amplified with 40, 45, or 50 cycles of PCR had similar 16S rRNA gene profiles (Figures 3.13, 3.15, 3.16). Samples that only had visible amplicons after 45 or 50 cycles of PCR always yielded replicates with inconsistent 16S rRNA gene profiles, although there

were sometimes still abundant ASVs present in all replicates (specifically samples T5 and T10; Figures 3.13, 3.15, 3.16).

It could also be possible to use qPCR to predict if samples would have consistent 16S rRNA gene profiles before sequencing. The six samples with the most consistent 16S rRNA gene profiles between replicates (T2, T1, T7, T8, T9, and T4) all had 16S rRNA gene copy numbers of 6.8×10^3 copies/gdw or higher, and the remaining four Tsukinuno bentonite samples (T3, T5, T6, and T10), the Opalinus clay sample, and the three NOCR samples, which had inconsistent 16S rRNA gene profiles, had a maximum 16S rRNA gene copy number of 3.9×10^3 copies/gdw clay or rock. The DNA from more samples with 16S rRNA gene copy numbers between 3.9×10^3 and 6.8×10^3 copies/gdw would have to be quantified and sequenced to determine a more specific 16S rRNA gene copy number threshold for consistent 16S rRNA gene profiles between replicates.

3.9 Heterogeneity of ancient natural barrier component profiles

Despite originating from similar locations, the Tsukinuno bentonite clay samples varied in moisture content and water activity, and microbial abundance, composition, and diversity. The five samples with 16S rRNA gene profiles dominated by chemolithoautotrophs (T2, T5, T8, T9, and T4) were also associated with the highest water activity and moisture content (Figure 3.3). The remaining five samples with lower water activities and moisture contents were associated primarily with aerobic heterotrophs and fermenting bacteria, and the most prevalent ASVs in the two samples with the lowest consistency in 16S rRNA gene profiles for replicates (T3 and T6) were related to human-associated taxa (Figure 3.13). Statistical analysis further suggests that the differences in profiles among Tsukinuno bentonite samples were driven in part by moisture content and water activity (Figure 3.10), which might also imply microbial growth during long sample shipment delays. The physical and microbial heterogeneity of the samples highlights the importance of studying a variety of different ancient bentonite samples with biogeochemical properties spanning the range of expected properties for DGR-associated bentonite.

Chapter 4
Conclusions and recommendations

Studying the microbiology of undisturbed, ancient clay and rock samples is a useful way to gain insight into what DGR-associated bentonite and host rock microbiomes might be in the future DGR. Although the bentonite clay samples studied were taken from environments with some conditions inconsistent with expected DGR conditions, especially oxygen availability, studying the Tsukinuno bentonite samples, as well as the Opalinus clay and NOCR samples, did provide insight into what microorganisms could be present in a DGR and at what abundance.

The Tsukinuno bentonite samples had a wide range of microbial abundances (Figure 3.5), and a higher average number of 16S rRNA gene copies than the NOCR samples (Mann-Whitney U test; $p<0.05$). Viable aerobic heterotrophs were detected in all Tsukinuno bentonite samples, anaerobic heterotrophs in half of the samples, and SRB were only detected in a single sample with a very low estimated MPN/g of 5. The ability to cultivate microorganisms from each of the Tsukinuno bentonite samples indicates that there were viable cells in these samples, though the cultivation techniques used were expected to only target a portion of the total microbial community. A method of quantifying all living microorganisms in the samples, such as the ATP assay, should be applied to these and future samples to make more accurate estimates of viable microbial biomass in the clay and rock samples.

Applying a DNA sequencing technique to the clay and rock samples revealed a more diverse microbial community than the cultivation approaches did (Mann-Whitney U test, $p<0.05$; Figure 3.12). The 16S rRNA gene profiles were consistent among replicates for several Tsukinuno bentonite samples, but were less consistent among replicates of Opalinus clay and NOCR samples. Though the amplification of samples with 45 and 50 cycles of PCR resulted in the agarose gel-visible amplification of the lowest biomass samples for which

amplification was not visible on an agarose gel after only 40 cycles of PCR, it should be questioned whether conclusions should be made from the 16S rRNA gene profiles of these samples. Samples that only amplified with 45 or 50 cycles of PCR always had less consistent replicate 16S rRNA gene profiles than samples that did have visible amplification after 40 cycles of PCR. These same samples with low consistency between replicates all also had fewer than 3.9×10^3 16S rRNA gene copies/gdw. Despite this, two of the eight samples below this qPCR threshold did have one or two dominant ASVs present in most or all replicates. Because it may not be possible to predict with confidence whether or not a sample will have consistent replicate 16S rRNA gene profiles before sequencing, it is important to always have biological replicates of each sample to assess the validity of the results before drawing conclusions. Due to low consistency between replicate 16S rRNA gene profiles, it was suggested that Tsukinuno bentonite samples T3 and T6, as well as all NOCR and Opalinus clay samples may have 16S rRNA gene profiles that do not reflect the true microbial community of these low biomass samples (Figures 3.13, 3.15, 3.16). This was supported by the observation that many of the most prevalent ASVs across replicates of these samples were human associated. Although a similar number of sequencing reads were obtained for these samples and the negative controls(Figure 3.8), the ASVs detected in these samples rarely overlapped with the ASVs detected in the negative controls.

Samples with consistent 16S rRNA gene profiles between replicates were dominated by one to three ASVs belonging to the same phylum. The five samples with the highest moisture content and water activity (T2, T5, T8, T9, T4; Figure 3.3) were dominated by predicted chemolithoautotrophic acidophiles and heterotrophic archaeal and bacterial taxa. The remaining samples were dominated by aerobic heterotrophic, methylotrophic, or fermenting bacteria.

Cultivation techniques never enriched the dominant species observed in the 16S rRNA gene profiles of DNA extracted and sequenced directly from the clay samples (Figure 3.13), nor did they enrich the rare species, with the exception of a single rare ASV common to a culture

and its corresponding clay (section 3.7.2). This emphasizes the importance of using molecular techniques in addition to cultivation techniques for the quantification and characterization of microbial communities.

The potential for sulfate reduction by SRB in the bentonite clay associated with the DGR is of particular importance to DGR longevity. Cultivation techniques resulted in the enrichment of SRB in only one of the Tsukinuno bentonite samples (Figure 3.5). Sequencing the DNA from biomass taken from this sample revealed that the cultivated SRB was a species of *Desulfosporosinus*. No ASVs assigned to this genus or any other known SRB were detected in the 16S rRNA gene profiles of any clay or rock samples, and the FAPROTAX predictions further supported no sulfate reduction in any of the samples (Figure 3.14). Although known SRB were not detected, ASVs associated with microorganisms capable of sulfur reduction (*Acidithiobacillus ferrooxidans* and members of the family *Thermoplasmataceae*), which could also result in the production of sulfide, were prevalent across the replicates of samples T5, T9, and T4 (Figure 3.13).

The collection of samples studied demonstrated that samples can have a high degree of heterogeneity, even when taken from similar locations. As such, additional natural barrier component analogues should be studied to explore the range of potential microorganisms a future DGR could host. Although microorganisms capable of some of the expected forms of metabolism in a DGR were detected in these samples, others, including SRB, were not as prevalent as might be expected. To address this, the microbial abundance and composition of ancient natural barrier component analogues taken from locations with more DGR relevant conditions than the current samples should be studied. Specifically, studying clay and rock samples from anoxic locations would give more insight into the possibility of the growth of SRB in DGR-relevant environments. Anoxic conditions should be maintained, as best as possible, during the sampling, shipment, and cultivation steps to preserve the viability of strictly anaerobic microorganisms. Additionally, samples should be shipped and stored at a constant temperature of approximately 4°C to maintain the viability of living

microorganisms. It would also be informative to collect more geochemical information about the samples, such as pH and rock or clay composition, to assess the important factors that promote or dissuade the growth of DGR-relevant microorganisms.

Bibliography

1. Canada's used nuclear fuel. *Nuclear Waste Management Organization*. https://www.nwmo.ca/en/Canadas-Plan/Canadas-Used-Nuclear-Fuel. Accessed 5 Mar 2019.

2. Satyanarayana G, Narayana KL, Boggarapu NR. Numerical simulations on the laser spot welding of zirconium alloy endplate for nuclear fuel bundle assembly. *Lasers Manuf Mater Process* 2018; **5**: 53–70.

3. Radiation risk and safety. *Nuclear Waste Management Organization*. https://www.nwmo.ca/en/Canadas-Plan/Canadas-Used-Nuclear-Fuel/Radiation-Risk-and-Safety. Accessed 5 Mar 2019.

4. Weber WJ, Navrotsky A, Stefanovsky S, Vance ER, Vernaz E. Materials science of high-level nuclear waste immobilization. *MRS Bull* 2009; **34**: 46–53.

5. How much is there? *Nuclear Waste Management Organization*. https://www.nwmo.ca/en/Canadas-Plan/Canadas-Used-Nuclear-Fuel/How-Much-Is-There. Accessed 5 Mar 2019.

6. How is it stored today? *Nuclear Waste Management Organization*. https://www.nwmo.ca/en/Canadas-Plan/Canadas-Used-Nuclear-Fuel/How-Is-It-Stored-Today. Accessed 5 Jun 2020.

7. Stroes-Gascoyne S, Hamon CJ, Maak P, Russell S. The effects of the physical properties of highly compacted smectitic clay (bentonite) on the culturability of indigenous microorganisms. *Appl Clay Sci* 2010; **47**: 155–162.

8. Keech PG, Vo P, Shoesmith DW, Jacklin R, Ramamurthy S, Chen J. Design and development of copper coatings for long term storage of used nuclear fuel. *Corros Eng Sci Techn* 2014; **49**: 425–430.

9. King F, Hall DS, Keech PG. Nature of the near-field environment in a deep geological repository and the implications for the corrosion behaviour of the container. *Corros Eng Sci Techn* 2017; **52**: 25–30.

10. Hall DS, Keech PG. An overview of the Canadian corrosion program for the long-term management of nuclear waste. *Corros Eng Sci Techn* 2017; **52**: 2–5.

11. Deep geological repository. *Nuclear Waste Management Organization*. https://www.nwmo.ca/en/A-Safe-Approach/Facilities/Deep-Geological-Repository. Accessed 20 Aug 2020.

12. Abu-Jdayil B. Rheology of sodium and calcium bentonite-water dispersions: effect of electrolytes and aging time. *Int J Miner Process* 2011; **98**: 208–213.

13. Lagaly G, Ziesmer S. Colloid chemistry of clay minerals: the coagulation of montmorillonite dispersions. *Adv Colloid Interfac* 2003; **100**–**102**: 105–128.

14. Shahwan T, Erten HN, Unugur S. A characterization study of some aspects of the adsorption of aqueous Co^{2+} ions on a natural bentonite clay. *J Colloid Interf Sci* 2006; **300**: 447–452.

15. Ballarini E, Graupner B, Bauer S. Thermal–hydraulic–mechanical behavior of bentonite and sand-bentonite materials as seal for a nuclear waste repository: numerical simulation of column experiments. *Appl Clay Sci* 2017; **135**: 289–299.

16. Guo R. Thermal response of a Mark II conceptual deep geological repository in crystalline rock. 2016. Nuclear Waste Management Organization, Toronto, ON.

17. Wersin P, Spahiu K, Bruno J. Time evolution of dissolved oxygen and redox conditions in a HLW repository. 1994. Swedish Nuclear Fuel and Waste Management Co, Stockholm.

18. Müller HR, Garitte B, Vogt T, Köhler S, Sakaki T, Weber H, et al. Implementation of the full-scale emplacement (FE) experiment at the Mont Terri rock laboratory. *Swiss J Geosci* 2017; **110**: 287–306.

19. Cong H, Michels HT, Scully JR. Passivity and pit stability behavior of copper as a function of selected water chemistry variables. *J Electrochem Soc* 2009; **156**: C16.

20. King F. Microbiologically influenced corrosion of nuclear waste containers. *Corrosion* 2009; **65**: 233–251.

21. Balkwill DL, Fredrickson JK, Thomas JM. Vertical and horizontal variations in the physiological diversity of the aerobic chemoheterotrophic bacterial microflora in deep southeast coastal plain subsurface sediments. *Appl Environ Microbiol* 1989; **55**: 1058–1065.

22. Kieft TL, Kovacik WP, Ringelberg DB, White DC, Haldeman DL, Amy PS, et al. Factors limiting microbial growth and activity at a proposed high-level nuclear repository, Yucca Mountain, Nevada. *Appl Environ Microbiol* 1997; **63**: 3128–3133.

23. Leupin OX, Bernier-Latmani R, Bagnoud A, Moors H, Leys N, Wouters K, et al. Fifteen years of microbiological investigation in Opalinus Clay at the Mont Terri rock laboratory (Switzerland). *Swiss J Geosci* 2017; **5**: 345–356.

24. Boylan AA, Perez-Mon C, Guillard L, Burzan N, Loreggian L, Maisch M, et al. H_2-fuelled microbial metabolism in Opalinus Clay. *Appl Clay Sci* 2019; **174**: 69–74.

25. Gaines RH. Bacterial activity as a corrosive influence in the soil. *Ind Eng Chem* 1910; **2**: 128–130.

26. Von Wolzogen Kühr CAH, van der Vlugt LS. Graphitization of cast iron as an electro-biochemical process in anaerobic soils. *Water* 1934; **18**: 147–165.

27. Sarioğlu F, Javaherdashti R, Aksöz N. Corrosion of a drilling pipe steel in an environment containing sulphate-reducing bacteria. *Int J Pres Ves Pip* 2002; **73**: 127–131.

28. Al-Jaroudi SS, Ul-Hamid A, Al-Gahtani MM. Failure of crude oil pipeline due to microbiologically induced corrosion. *Corros Eng Sci Techn* 2010; **46**: 568–579.

29. Yang Y, Khan F, Thodi P, Abbassi R. Corrosion induced failure analysis of subsea pipelines. *Reliab Eng Syst Safe* 2017; **159**: 214–222.

30. Herisson J, Guéguen-Minerbe M, van Hullebusch ED, Chaussadent T. Influence of the binder on the behaviour of mortars exposed to H_2S in sewer networks: a long-term durability study. *Mater Struct* 2017; **50**: 8.

31. Siddiqui DA, Guida L, Sridhar S, Valderrama P, Wilson TG, Rodrigues DC. Evaluation of oral microbial corrosion on the surface degradation of dental implant materials. *J Periodontol* 2019; **90**: 72–81.

32. King F. Microbially influenced corrosion of copper nuclear fuel waste containers in a Canadian disposal vault. 1996. Atomic Energy of Canada Ltd, Chalk River, ON.

33. Gu T, Jia R, Unsal T, Xu D. Toward a better understanding of microbiologically influenced corrosion caused by sulfate reducing bacteria. *J Mater Sci Technol* 2019; **35**: 631–636.

34. Libert M, Bildstein O, Esnault L, Jullien M, Sellier R. Molecular hydrogen: an abundant energy source for bacterial activity in nuclear waste repositories. *Phys Chem Earth* 2011; **36**: 1616–1623.

35. Bagnoud A, Chourey K, Hettich RL, De Bruijn I, Andersson AF, Leupin OX, et al. Reconstructing a hydrogen-driven microbial metabolic network in Opalinus Clay rock. *Nat Commun* 2016; **7**: 12770.

36. Vinsot A, Appelo CAJ, Lundy M, Wechner S, Lettry Y, Lerouge C, et al. In situ diffusion test of hydrogen gas in the Opalinus Clay. *Geol Soc Spec Publ* 2014; **400**: 563–578.

37. Lin LH, Hall J, Lippmann-Pipke J, Ward JA, Lollar BS, DeFlaun M, et al. Radiolytic H_2 in continental crust: nuclear power for deep subsurface microbial communities. *Geochem Geophy Geosy* 2005; **6**: 7.

38. Hernsdorf AW, Amano Y, Miyakawa K, Ise K, Suzuki Y, Anantharaman K, et al. Potential for microbial H_2 and metal transformations associated with novel bacteria and archaea in deep terrestrial subsurface sediments. *ISME J* 2017; **11**: 1915–1929.

39. Nyyssönen M, Hultman J, Ahonen L, Kukkonen I, Paulin L, Laine P, et al. Taxonomically and functionally diverse microbial communities in deep crystalline rocks of the Fennoscandian Shield. *ISME J* 2014; **8**: 126–138.

40. Haveman SA, Pedersen K. Distribution of culturable microorganisms in Fennoscandian Shield groundwater. *FEMS Microbiol Ecol* 2002; **39**: 129–137.

41. Fu B, Jin X, Conrad R, Liu H, Liu H. Competition between chemolithotrophic acetogenesis and hydrogenotrophic methanogenesis for exogenous H_2 /CO_2 in anaerobically digested sludge: impact of temperature. *Front Microbiol* 2019; **10**: 2418.

42. Ye R, Jin Q, Bohannan B, Keller JK, Bridgham SD. Homoacetogenesis: A potentially underappreciated carbon pathway in peatlands. *Soil Biol Biochem* 2014; **68**: 385–391.

43. Pedersen K. Microbial life in deep granitic rock. *FEMS Microbiol Rev* 1997; **20**: 399–414.

44. Bagnoud A, de Bruijn I, Andersson AF, Diomidis N, Leupin OX, Schwyn B, et al. A minimalistic microbial food web in an excavated deep subsurface clay rock. *FEMS Microbiol Ecol* 2016; **92**: fiv138.

45. Bell E, Lamminmäki T, Alneberg J, Andersson AF, Qian C, Xiong W, et al. Biogeochemical cycling by a low-diversity microbial community in deep groundwater. *Front Microbiol* 2018; **9**: 2129.

46. Chivian D, Brodie EL, Alm EJ, Culley DE, Dehal PS, DeSantis TZ, et al. Environmental genomics reveals a single-species ecosystem deep within earth. *Science* 2008; **322**: 275–278.

47. Pedersen K. Metabolic activity of subterranean microbial communities in deep granitic groundwater supplemented with methane and H_2. *ISME J* 2013; **7**: 839–849.

48. Wu X, Pedersen K, Edlund J, Eriksson L, Åström M, Andersson AF, et al. Potential for hydrogen-oxidizing chemolithoautotrophic and diazotrophic populations to initiate biofilm formation in oligotrophic, deep terrestrial subsurface waters. *Microbiome* 2017; **5**: 37.

49. Bell E, Lamminmäki T, Alneberg J, Andersson AF, Qian C, Xiong W, et al. Active sulfur cycling in the terrestrial deep subsurface. *ISME J* 2020; **325**: 184–187.

50. Beal EJ, House CH, Orphan VJ. Manganese- and iron-dependent marine methane oxidation. *Science* 2009; **325**: 184–187.

51. Ettwig KF, Zhu B, Speth D, Keltjens JT, Jetten MSM, Kartal B. Archaea catalyze iron-dependent anaerobic oxidation of methane. *Proc Natl Acad Sci U S A* 2016.

52. Chang YH, Cheng TW, Lai WJ, Tsai WY, Sun CH, Lin LH, et al. Microbial methane cycling in a terrestrial mud volcano in eastern Taiwan. *Environ Microbiol* 2012; **14**: 895–908.

53. Boetius A, Ravenschlag K, Schubert CJ, Rickert D, Widdel F, Gleseke A, et al. A marine microbial consortium apparently mediating anaerobic oxidation of methane. *Nature* 2000; **407**: 623–626.

54. Meulepas RJW, Jagersma CG, Gieteling J, Buisman CJN, Stams AJM, Lens PNL. Enrichment of anaerobic methanotrophs in sulfate-reducing membrane bioreactors. *Biotechnol Bioeng* 2009; **104**: 458–470.

55. Haroon M, Hu S, Shi Y, Imelfort M, Keller J, Hugenholtz P, et al. Anaerobic oxidation of methane coupled to nitrate reduction in a novel archaeal lineage. *Nature* 2013; **500**: 567–570.

56. Valentine DL, Reeburgh WS. New perspectives on anaerobic methane oxidation. *Environ Microbiol* 2000; **2**: 477–484.

57. Bomberg M, Nyyssönen M, Pitkänen P, Lehtinen A, Itävaara M. Active microbial communities inhabit sulphate-methane interphase in deep bedrock fracture fluids in Olkiluoto, Finland. *Biomed Res Int* 2015; **2015**: 979530.

58. Finster K. Microbiological disproportionation of inorganic sulfur compounds. *J Sulfur Chem* 2008; **29**: 281–292.

59. Wu X, Holmfeldt K, Hubalek V, Lundin D, Åström M, Bertilsson S, et al. Microbial metagenomes from three aquifers in the Fennoscandian shield terrestrial deep biosphere reveal metabolic partitioning among populations. *ISME J* 2016; **10**: 1192–1203.

60. Purkamo L, Bomberg M, Nyyssönen M, Kukkonen I, Ahonen L, Itävaara M. Heterotrophic communities supplied by ancient organic carbon predominate in deep Fennoscandian bedrock fluids. *Microb Ecol* 2014; **69**: 319–332.

61. Purkamo L, Bomberg M, Kietäväinen R, Salavirta H, Nyyssönen M, Nuppunen-Puputti M, et al. Microbial co-occurrence patterns in deep Precambrian bedrock fracture fluids. *Biogeosciences* 2016; **13**: 3091–3108.

62. Masurat P, Eriksson S, Pedersen K. Evidence of indigenous sulphate-reducing bacteria in commercial Wyoming bentonite MX-80. *Appl Clay Sci* 2010; **47**: 51–57.

63. Liu D, Dong H, Bishop ME, Zhang J, Wang H, Xie S, et al. Microbial reduction of structural iron in interstratified illite-smectite minerals by a sulfate-reducing bacterium. *Geobiology* 2012; **10**: 150–162.

64. Lantenois S, Lanson B, Muller F, Bauer A, Jullien M, Plançon A. Experimental study of smectite interaction with metal Fe at low temperature: 1. Smectite destabilization. *Clay Clay Miner* 2005; **53**: 597–612.

65. Pedersen K, Bengtsson A, Blom A, Johansson L, Taborowski T. Mobility and reactivity of sulphide in bentonite clays – implications for engineered bentonite barriers in geological repositories for radioactive wastes. *Appl Clay Sci* 2017; **146**: 495–502.

66. Stone W, Kroukamp O, McKelvie J, Korber DR, Wolfaardt GM. Microbial metabolism in bentonite clay: saturation, desiccation and relative humidity. *Appl Clay Sci* 2016; **129**: 54–64.

67. Rajala P, Bomberg M, Kietäväinen R, Kukkonen I, Ahonen L, Nyyssönen M, et al. Rapid reactivation of deep subsurface microbes in the presence of C-1 compounds. *Microorganisms* 2015; **3**: 17–33.

68. Lau MCY, Kieft TL, Kuloyo O, Linage-Alvarez B, Van Heerden E, Lindsay MR, et al. An oligotrophic deep-subsurface community dependent on syntrophy is dominated by sulfur-driven autotrophic denitrifiers. *Proc Natl Acad Sci U S A* 2016; **113**: 927–936.

69. Pedersen K, Motamedi M, Karnland O, Sandén T. Mixing and sulphate-reducing activity of bacteria in swelling, compacted bentonite clay under high-level radioactive waste repository conditions. *J Appl Microbiol* 2000; **89**: 1038–1047.

70. Motamedi M, Karland O, Pedersen K. Survival of sulfate reducing bacteria at different water activities in compacted bentonite. *FEMS Microbiol Lett* 1996; **141**: 83–87.

71. Jalique DR, Stroes-Gascoyne S, Hamon CJ, Priyanto DG, Kohle C, Evenden WG, et al. Culturability and diversity of microorganisms recovered from an eight-year old highly-compacted, saturated MX-80 Wyoming bentonite plug. *Appl Clay Sci* 2016; **126**: 245–250.

72. Urios L, Marsal F, Pellegrini D, Magot M. Microbial diversity of the 180 million-year-old Toarcian argillite from Tournemire, France. *Appl Geochem* 2012; **27**: 1442–1450.

73. López-Fernández M, Fernández-Sanfrancisco O, Moreno-García A, Martín-Sánchez I, Sánchez-Castro I, Merroun ML. Microbial communities in bentonite formations and their interactions with uranium. *Appl Geochem* 2014; **49**: 77–86.

74. Poulain S, Sergeant C, Simonoff M, Le Marrec C, Altmann S. Microbial investigations in Opalinus Clay, an argillaceous formation under evaluation as a potential host rock for a radioactive waste repository. *Geomicrobiol J* 2008; **25**: 240–249.

75. Mauclaire L, McKenzie JA, Schwyn B, Bossart P. Detection and cultivation of indigenous microorganisms in Mesozoic claystone core samples from the Opalinus Clay formation (Mont Terri rock laboratory). *Phys Chem Earth* 2007; **32**: 232–240.

76. Stroes-Gascoyne S, Schippers A, Schwyn B, Poulain S, Sergeant C, Simonoff M, et al. Microbial community analysis of Opalinus Clay drill core samples from the Mont Terri Underground Research Laboratory, Switzerland. *Geomicrobiol J* 2007; **24**: 1–17.

77. Wouters K, Moors H, Boven P, Leys N. Evidence and characteristics of a diverse and metabolically active microbial community in deep subsurface clay borehole water. *FEMS Microbiol Ecol* 2013; **86**: 458–473.

78. Boivin-Jahns V, Ruimy R, Bianchi A, Daumas S, Christen R. Bacterial diversity in a deep-subsurface clay environment. *Appl Environ Microbiol* 1996; **62**: 3405–3412.

79. Lopez-Fernandez M, Cherkouk A, Vilchez-Vargas R, Jauregui R, Pieper D, Boon N, et al. Bacterial diversity in bentonites, engineered barrier for deep geological disposal of radioactive wastes. *Microb Ecol* 2015; **70**: 922–935.

80. Liu H, Dang X, Zhang H, Dong J, Zhang Z, Wang C, et al. Microbial diversity in bentonite, a potential buffer material for deep geological disposal of radioactive waste. *IOP Conf Ser Earth Environ Sci* 2019; **227**: 022010.

81. Engel K, Coyotzi S, Vachon MA, McKelvie JR, Neufeld JD. Validating DNA extraction protocols for bentonite clay. *mSphere* 2019; **4**: e00334-19.

82. Yokoyama S, Kuroda M, Tsutsui M, Sata T, Suzuki K, Enoto H. A comparisons of bentonite from Kawamukai and Umenokida in Tsukinuno mine, Yamagata. *Clay Sci* 2004; **44**: 45–52.

83. Bleyen N, Smets S, Small J, Moors H, Leys N, Albrecht A, et al. Impact of the electron donor on in situ microbial nitrate reduction in Opalinus Clay: results from the Mont Terri rock laboratory (Switzerland). *Swiss J Geosci* 2017; **110**: 355–374.

84. Thury M, Bossart P. The Mont Terri rock laboratory, a new international research project in a Mesozoic shale formation, in Switzerland. *Eng Geol* 1999; **52**: 347–359.

85. Muyzer G, De Waal EC, Uitterlinden AG. Profiling of complex microbial populations by denaturing gradient gel electrophoresis analysis of polymerase chain reaction-amplified genes coding for 16S rRNA. *Appl Environ Microbiol* 1993; **59**: 695–700.

86. Yu Y, Lee C, Kim J, Hwang S. Group-specific primer and probe sets to detect methanogenic communities using quantitative real-time polymerase chain reaction. *Biotechnol Bioeng* 2005; **89**: 670–679.

87. Parada AE, Needham DM, Fuhrman JA. Every base matters: assessing small subunit rRNA primers for marine microbiomes with mock communities, time series and global field samples. *Environ Microbiol* 2016; **18**: 1403–1414.

88. Quince C, Lanzen A, Davenport RJ, Turnbaugh PJ. Removing noise from pyrosequenced amplicons. *BMC Bioinformatics* 2011; **12**: 38.

89. Bartram AK, Lynch MDJ, Stearns JC, Moreno-Hagelsieb G, Neufeld JD. Generation of multimillion-sequence 16S rRNA gene libraries from complex microbial communities by assembling paired-end Illumina reads. *Appl Environ Microbiol* 2011; **77**: 3834–3852.

90. Bolyen E, Rideout JR, Dillon MR, Bokulich NA, Abnet CC, Al-Ghalith GA, et al. Reproducible, interactive, scalable and extensible microbiome data science using QIIME 2. *Nat Biotechnol* 2019; **37**: 852–857.

91. Callahan BJ, McMurdie PJ, Rosen MJ, Han AW, Johnson AJA, Holmes SP. DADA2: high resolution sample inference from Illumina amplicon data. *Nat Methods* 2016; **13**: 581–583.

92. Pruesse E, Quast C, Knittel K, Fuchs BM, Ludwig W, Peplies J, et al. SILVA: a comprehensive online resource for quality checked and aligned ribosomal RNA sequence data compatible with ARB. *Nucleic Acids Res* 2007; **35**: 7188–7196.

93. Davis NM, Proctor DiM, Holmes SP, Relman DA, Callahan BJ. Simple statistical identification and removal of contaminant sequences in marker-gene and metagenomics data. *Microbiome* 2018; **6**: 226.

94. Acinas SG, Marcelino LA, Klepac-Ceraj V, Polz MF. Divergence and redundancy of 16S rRNA sequences in genomes with multiple *rrn* operons. *J Bacteriol* 2004; **186**: 2629–2635.

95. Persson J, Lydmark S, Edlund J, Pedersen K. Microbial incidence on copper and titanium embedded in compacted bentonite clay. 2011. Swedish Nuclear Fuel and Waste Management Co, Stockholm.

96. Zhou GW, Yang XR, Rønn R, Su JQ, Cui L, Zheng BX, et al. Metabolic inactivity and re-awakening of a nitrate reduction dependent iron(II)-oxidizing bacterium *Bacillus ferrooxidans*. *Front Microbiol* 2019; **10**: 1494.

97. Young IE, Fitz-James PC. Chemical and morphological studies of bacterial spore formation: the formation of spores in *Bacillus cereus*. *J Cell Biol* 1959; **6**: 467–482.

98. Willerslev E, Cappellini E, Boomsma W, Nielsen R, Hebsgaard MB, Brand TB, et al. Ancient biomolecules from deep ice cores reveal a forested southern Greenland. *Science* 2007; **317**: 111–114.

99. Tian S, Tian Z, Yang H, Yang M, Zhang Y. Detection of viable bacteria during sludge ozonation by the combination of ATP assay with PMA-miseq sequencing. *Water (Switzerland)* 2017.

100. Kjeldsen KU, Joulian C, Ingvorsen K. Oxygen tolerance of sulfate-reducing bacteria in activated sludge. *Environ Sci Technol* 2004; **38**: 2038–2043.

101. Dolla A, Fournier M, Dermoun Z. Oxygen defense in sulfate-reducing bacteria. *J Biotechnol* 2006; **126**: 87–100.

102. Corvec S. Clinical and biological features of *Cutibacterium* (formerly *Propionibacterium*) *avidum*, an underrecognized microorganism. *Clin Microbiol Rev* 2018; **31**: e00064-17.

103. Brenner DJ, Hollis DG, Moss CW, English CK, Hall GS, Vincent J, et al. Proposal of *Afipia* gen. nov., with *Afipia felis* sp. nov. (formerly the cat scratch disease bacillus), *Afipia clevelandensis* sp. nov. (formerly the Cleveland Clinic Foundation strain), *Afipia broomeae* sp. nov., and three unnamed. *J Clin Microbiol* 1991; **29**: 2450–2460.

104. Moosvi SA, Pacheco CC, McDonald IR, De Marco P, Pearce DA, Kelly DP, et al. Isolation and properties of methanesulfonate-degrading *Afipia felis* from Antarctica and comparison with other strains of *A. felis*. *Environ Microbiol* 2005; **7**: 22–33.

105. Zhang C, Yang Z, Jin W, Wang X, Zhang Y, Zhu S, et al. Degradation of methomyl by the combination of *Aminobacter* sp. MDW-2 and *Afipia* sp. MDW-3. *Lett Appl Microbiol* 2017; **64**: 289–296.

106. Mahalaxmi Y, Sathish T, Prakasham RS. Development of balanced medium composition for improved rifamycin B production by isolated *Amycolatopsis* sp. RSP-3. *Lett Appl Microbiol* 2009; **49**: 533–538.

107. Zhao W, Zhong Y, Yuan H, Wang J, Zheng H, Wang Y, et al. Complete genome sequence of the rifamycin SV-producing *Amycolatopsis mediterranei* U32 revealed its genetic characteristics in phylogeny and metabolism. *Cell Res* 2010; **20**: 1096–1108.

108. Dávila Costa JS, Kothe E, Abate CM, Amoroso MJ. Unraveling the *Amycolatopsis tucumanensis* copper-resistome. *Biometals* 2012; **25**: 905–917.

109. Albarracín VH, Winik B, Kothe E, Amoroso MJ, Abate CM. Copper bioaccumulation by the actinobacterium *Amycolatopsis* sp. AB0. *J Basic Microb* 2008; **48**: 323–330.

110. Pranamuda H, Tokiwa Y. Degradation of poly(L-lactide) by strains belonging to genus *Amycolatopsis*. *Biotechnol Lett* 1999; **21**: 901–905.

111. Pranamuda H, Tsuchii A, Tokiwa Y. Poly (L-lactide)-degrading enzyme produced by *Amycolatopsis* sp. *Macromol Biosci* 2001; **1**: 25–29.

112. Pranamuda H, Chollakup R, Tokiwa Y. Degradation of polycarbonate by a polyester-degrading strain, *Amycolatopsis* sp. strain HT-6. *Appl Environ Microbiol* 1999; **65**: 4220–4222.

113. Nicolaou KC, Sugita K, Baran PS, Zhong YL. New synthetic technology for the construction of N-containing quinones and derivatives thereof: total synthesis of epoxyquinomycin B. *Angew Chemie - Int Ed* 2001; **40**: 207–210.

114. Zmijewski M, Briggs B. Biosynthesis of vancomycin: identification of TDP-glucose: aglycosyl-vancomycin glucosyltransferase from *Amycolatopsis orientalis*. *FEMS Microbiol Lett* 1989; **59**: 129–133.

115. Truman AW, Kwun MJ, Cheng J, Yang SH, Suh J-W, Hong H-J. Antibiotic resistance mechanisms inform discovery: identification and characterization of a novel *Amycolatopsis* strain producing ristocetin. *Antimicrob Agents CH* 2014; **58**: 5687–5695.

116. Al-Tai AM, Ruan JS. *Nocardiopsis halophila* sp. nov., a new halophilic actinomycete isolated from soil. *Int J Syst Bacteriol* 1994; **44**: 474–478.

117. Li MG, Li WJ, Xu P, Cui XL, Xu LH, Jiang CL. *Nocardiopsis xinjiangensis* sp. nov., a halophilic actinomycete isolated from a saline soil sample in China. *Int J Syst Evol Microbiol* 2003; **53**: 317–321.

118. Li WJ, Park DJ, Tang SK, Wang D, Lee JC, Xu LH, et al. *Nocardiopsis salina* sp. nov., a novel halophilic actinomycete isolated from saline soil in China. *Int J Syst Evol Microbiol* 2004; **54**: 1805–1809.

119. Hozzein WN, Li WJ, Ali MIA, Hammouda O, Mousa AS, Xu LH, et al. *Nocardiopsis alkaliphila* sp. nov., a novel alkaliphilic actinomycete isolated from desert soil in Egypt. *Int J Syst Evol Microbiol* 2004; **54**: 247–252.

120. Schippers A, Bosecker K, Willscher S, Spröer C, Schumann P, Kroppenstedt RM. *Nocardiopsis metallicus* sp. nov., a metalleaching actinomycete isolated from an alkaline slag dump. *Int J Syst Evol Microbiol* 2002; **52**: 2291–2295.

121. Kim JW, Adachi H, Shin-Ya K, Hayakawa Y, Seto H. Apoptolidin, a new apoptosis inducer in transformed cells from *Nocardiopsis* sp. *J Antibiot* 1997; **50**: 628–630.

122. Ding ZG, Li MG, Zhao JY, Ren J, Huang R, Xie MJ, et al. Naphthospironone A: an unprecedented and highly functionalized polycyclic metabolite from an alkaline mine waste extremophile. *Chem-Eur J* 2010; **16**: 3902–3905.

123. Li YQ, Li MG, Li W, Zhao JY, Ding ZG, Cui XL, et al. Griseusin D, a new pyranonaphthoquinone derivative from a alkaphilic *Nocardiopsis* sp. *J Antibiot* 2007; **60**: 757–761.

124. Engelhardt K, Degnes KF, Kemmler M, Bredholt H, Fjaervik E, Klinkenberg G, et al. Production of a new thiopeptide antibiotic, TP-1161, by a marine *Nocardiovsis* species. *Appl Environ Microbiol* 2010; **76**: 4969–4976.

125. Gandhimathi R, Seghal Kiran G, Hema TA, Selvin J, Rajeetha Raviji T, Shanmughapriya S. Production and characterization of lipopeptide biosurfactant by a sponge-associated marine actinomycetes *Nocardiopsis alba* MSA10. *Bioproc Biosyst Eng* 2009; **32**: 825–835.

126. Kämpfer P, Kroppenstedt RM. *Pseudonocardia benzenivorans* sp. nov. *Int J Syst Evol Microbiol* 2004; **54**: 749–751.

127. Mahendra S, Alvarez-Cohen L. *Pseudonocardia dioxanivorans* sp. nov., a novel actinomycete that grows on 1,4-dioxane. *Int J Syst Evol Microbiol* 2005; **52**: 593–598.

128. Kohlweyer U, Thiemer B, Schräder T, Andreesen JR. Tetrahydrofuran degradation by a newly isolated culture of *Pseudonocardia* sp. strain K1. *FEMS Microbiol Lett* 2000; **186**: 301–306.

129. Reichert K, Lipski A, Pradella S, Stackebrandt E, Altendorf K. *Pseudonocardia asaccharolytica* sp. nov. and *Pseudonocardia sulfidoxydans* sp. nov., two new dimethyl disulfide-degrading actinomycetes and emended description of the genus *Pseudonocardia*. *Int J Syst Evol Microbiol* 1999; **48**: 441–449.

130. Benson DR, Silvester WB. Biology of *Frankia* strains, actinomycete symbionts of actinorhizal plants. *Microbiol Rev* 1993; **57**: 293–319.

131. Sellstedt A, Richau KH. Aspects of nitrogen-fixing actinobacteria, in particular free-living and symbiotic *Frankia*. *FEMS Microbiol Lett* 2013; **342**: 179–186.

132. Louca S, Wegener Parfrey L, Doebeli M. Decoupling function and taxonomy in the global ocean microbiome. *Science* 2016; **353**: 1272–1277.

133. Beller HR, Chain PSG, Letain TE, Chakicherla A, Larimer FW, Richardson PM, et al. The genome sequence of the obligately chemolithoautotrophic, facultatively anaerobic bacterium *Thiobacillus denitrificans*. *J Bacteriol* 2006; **188**: 1473–1488.

134. Claus G, Kutzner HJ. Physiology and kinetics of autotrophic denitrification by *Thiobacillus denitrificans*. *Appl Microbiol Biotechnol* 1985; **22**: 283–288.

135. Schedel M, Trüper HG. Anaerobic oxidation of thiosulfate and elemental sulfur in *Thiobacillus denitrificans*. *Arch Microbiol* 1980; **124**: 205–210.

136. Sublette KL, Sylvester ND. Oxidation of hydrogen sulfide by *Thiobacillus denitrificans*: desulfurization of natural gas. *Biotechnol Bioeng* 1987; **29**: 249–257.

137. Straub KL, Benz M, Schink B, Widdel F. Anaerobic, nitrate-dependent microbial oxidation of ferrous iron. *Appl Environ Microbiol* 1996; **62**: 1458–1460.

138. Torrentó C, Cama J, Urmeneta J, Otero N, Soler A. Denitrification of groundwater with pyrite and *Thiobacillus denitrificans*. *Chem Geol* 2010; **278**: 80–91.

139. Beller HR. Anaerobic, nitrate-dependent oxidation of U(IV) oxide minerals by the chemolithoautotrophic bacterium *Thiobacillus denitrificans*. *Appl Environ Microbiol* 2005; **71**: 2170–2174.

140. Hutt LP, Huntemann M, Clum A, Pillay M, Palaniappan K, Varghese N, et al. Permanent draft genome of *Thiobacillus thioparus* DSM 505^{T}, an obligately chemolithoautotrophic member of the *Betaproteobacteria*. *Stand Genomic Sci* 2017; **12**: 10.

141. Valdés J, Pedroso I, Quatrini R, Dodson RJ, Tettelin H, Blake R, et al. *Acidithiobacillus ferrooxidans* metabolism: from genome sequence to industrial applications. *BMC Genomics* 2008; **9**: 597.

142. Quatrini R, Appia-Ayme C, Denis Y, Jedlicki E, Holmes DS, Bonnefoy V. Extending the models for iron and sulfur oxidation in the extreme acidophile *Acidithiobacillus ferrooxidans*. *BMC Genomics* 2009; **10**: 394.

143. Drobner E, Huber H, Stetter KO. *Thiobacillus ferrooxidans*, a facultative hydrogen oxidizer. *Appl Environ Microbiol* 1990; **56**: 2922–2923.

144. Pronk JT, Meijer WM, Hazeu W, Van Dijken JP, Bos P, Kuenen JG. Growth of *Thiobacillus ferrooxidans* on formic acid. *Appl Environ Microbiol* 1991; **57**: 2057–2062.

145. Sugio T, Domatsu C, Munakata O. Role of a ferric ion-reducing system in sulfur oxidation of *Thiobacillus ferrooxidans*. *Appl Environ Microbiol* 1985; **49**: 1401–1406.

146. Ng KY, Sawada R, Inoue S, Kamimura K, Sugio T. Purification and some properties of sulfur reductase from the iron-oxidizing bacterium *Thiobacillus ferrooxidans* NASF-1. *J Biosci Bioeng* 2000; **90**: 199–203.

147. Mackintosh ME. Nitrogen fixation by *Thiobacillus ferrooxidans*. *J Gen Microbiol* 1978; **105**: 215–218.

148. Heinhorst S, Baker SH, Johnson DR, Davies PS, Cannon GC, Shively JM. Two copies of form I RuBisCO genes in *Acidithiobacillus ferrooxidans* ATCC 23270. *Curr Microbiol* 2002; **45**: 115–117.

149. Hallberg KB, Hedrich S, Johnson DB. *Acidiferrobacter thiooxydans*, gen. nov. sp. nov.; an acidophilic, thermo-tolerant, facultatively anaerobic iron- and sulfur-oxidizer of the family *Ectothiorhodospiraceae*. *Extremophiles* 2011; **2**: 271–279.

150. Mangold S, Valdés J, Holmes DS, Dopson M. Sulfur metabolism in the extreme acidophile *Acidithiobacillus caldus*. *Front Microbiol* 2011; **2**: 17.

151. Hallberg KB, González-Toril E, Johnson DB. *Acidithiobacillus ferrivorans*, sp. nov.; facultatively anaerobic, psychrotolerant iron-, and sulfur-oxidizing acidophiles isolated from metal mine-impacted environments. *Extremophiles* 2010; **14**: 9–19.

152. Lee EY, Lee NY, Cho KS, Ryu HW. Removal of hydrogen sulfide by sulfate-resistant *Acidithiobacillus thiooxidans* AZ11. *J Biosci Bioeng* 2006; **101**: 309–314.

153. Falagán C, Johnson DB. *Acidibacter ferrireducens* gen. nov., sp. nov.: an acidophilic ferric iron-reducing gammaproteobacterium. *Extremophiles* 2014; **18**: 1067–1073.

154. Wichlacz PL, Unz RF, Langworthy TA. *Acidiphilium angustum* sp. nov., *Acidiphilium facilis* sp. nov., and *Acidiphilium rubrum* sp. nov.: acidophilic heterotrophic bacteria isolated from acidic coal mine drainage. *Int J Syst Bacteriol* 1986; **36**: 197–201.

155. Mohagheghi A, Grohmann K, Himmel M. Isolation and characterization of *Acidothermus cellulolyticus* gen. nov., sp. nov., a new genus of thermophilic, acidophilic, cellulolytic bacteria. *Int J Syst Bacteriol* 1986; **36**: 435–443.

156. Goto K, Mochida K, Kato Y, Asahara M, Fujita R, An SY, et al. Proposal of six species of moderately thermophilic, acidophilic, endospore-forming bacteria: Alicyclobacillus contaminans sp. nov., Alicyclobacillus fastidiosus sp. nov., Alicyclobacillus kakegawensis sp. nov., Alicyclobacillus macrosporangiidus sp. nov.,. *Int J Syst Evol Microbiol* 2007; **57**: 1276–1285.

157. Johnson DB, Bacelar-Nicolau P, Okibe N, Thomas A, Hallberg KB. *Ferrimicrobium acidiphilum* gen. nov., sp. nov. and *Ferrithrix thermotolerans* gen. nov., sp. nov.: heterotrophic, iron-oxidizing, extremely acidophilic actinobacteria. *Int J Syst Evol Microbiol* 2009; **59**: 1082–1089.

158. Coram NJ, Rawlings DE. Molecular relationship between two groups of the genus *Leptospirillum* and the finding that *Leptospirillum ferriphilum* sp. nov. dominates South African commercial biooxidation tanks that operate at 40°C. *Appl Environ Microbiol* 2002; **68**: 838–845.

159. Bogdanova TI, Tsaplina IA, Kondrat'eva TF, Duda VI, Suzina NE, Melamud VS, et al. *Sulfobacillus thermotolerans* sp. nov,. a thermotolerant, chemolithotrophic bacterium. *Int J Syst Evol Microbiol* 2006; **56**: 1039–1042.

160. Battaglia-Brunet F, Joulian C, Garrido F, Dictor MC, Morin D, Coupland K, et al. Oxidation of arsenite by *Thiomonas* strains and characterization of *Thiomonas arsenivorans* sp. nov. *Antonie Van Leeuwenhoek* 2006; **89**: 99–108.

161. Golyshina O V., Lünsdorf H, Kublanov I V., Goldenstein NI, Hinrichs KU, Golyshin PN. The novel extremely acidophilic, cell-wall-deficient archaeon *Cuniculiplasma divulgatum* gen. nov., sp. nov. represents a new family, *Cuniculiplasmataceae* fam. nov., of the order *Thermoplasmatales*. *Int J Syst Evol Microbiol* 2016; **66**: 332–340.

162. Segerer A, Langworthy TA, Stetter KO. *Thermoplasma acidophilum* and *Thermoplasma volcanium* sp. nov. from Solfatara Fields. *Syst Appl Microbiol* 1988; **10**: 161–171.

163. Golyshina O V., Yakimov MM, Lünsdorf H, Ferrer M, Nimtz M, Timmis KN, et al. *Acidiplasma aeolicum* gen. nov., sp. nov., a euryarchaeon of the family *Ferroplasmaceae* isolated from a hydrothermal pool, and transfer of *Ferroplasma cupricumulans* to *Acidiplasma cupricumulans* comb. nov. *Int J Syst Evol Microbiol* 2009; **59**: 2815–2823.

164. Kersters K, Lisdiyanti P, Komagata K, Swings J. The family *Acetobacteraceae*: the genera *Acetobacter*, *Acidomonas*, *Asaia*, *Gluconacetobacter*, *Gluconobacter*, and *Kozakia*. In: Dworkin M, Falkow S, Rosenberg E, Schleifer K, Stackebrandt E (eds). *The Prokaryotes*, 3rd ed. 2006. Springer, New York, NY, pp 163–200.

165. Sánchez-Andrea I, Stams AJM, Hedrich S, Ňancucheo I, Johnson DB. *Desulfosporosinus acididurans* sp. nov.: an acidophilic sulfate-reducing bacterium isolated from acidic sediments. *Extremophiles* 2015; **19**: 39–47.

166. Alazard D, Joseph M, Battaglia-Brunet F, Cayol JL, Ollivier B. *Desulfosporosinus acidiphilus* sp. nov.: a moderately acidophilic sulfate-reducing bacterium isolated from acid mining drainage sediments. *Extremophiles* 2010; **4**: 305–312.

167. Vatsurina A, Badrutdinova D, Schumann P, Spring S, Vainshtein M. *Desulfosporosinus hippei* sp. nov., a mesophilic sulfate-reducing bacterium isolated from permafrost. *Int J Syst Evol Microbiol* 2008; **58**: 1228–1232.

168. Ramamoorthy S, Sass H, Langner H, Schumann P, Kroppenstedt RM, Spring S, et al. *Desulfosporosinus lacus* sp. nov., a sulfate-reducing bacterium isolated from pristine freshwater lake sediments. *Int J Syst Evol Microbiol* 2006; **56**: 2729–2736.

169. Robertson WJ, Bowman JP, Franzmann PD, Mee BJ. *Desulfosporosinus meridiei* sp. nov., a spore-forming sulfate-reducing bacterium isolated from gasolene-contaminated groundwater. *Int J Syst Evol Microbiol* 2001; **51**: 133–140.

170. Stackebrandt E, Sproer C, Rainey FA, Burghardt J, Päuker O, Hippe H. Phylogenetic analysis of the genus *Desulfotomaculum*: evidence for the misclassification of *Desulfotomaculum guttoideum* and description of *Desulfotomaculum orientis* as *Desulfosporosinus orientis* gen. nov., comb. nov. *Int J Syst Bacteriol* 1997; **47**: 1134–1139.

171. Lee YJ, Romanek CS, Wiegel J. *Desulfosporosinus youngiae* sp. nov., a sporeforming, sulfate-reducing bacterium isolated from a constructed wetland treating acid mine drainage. *Int J Syst Evol Microbiol* 2009; **59**: 2743–2746.

172. Patt TE, Cole GC, Hanson RS. *Methylobacterium*, a new genus of facultatively methylotrophic bacteria. *Int J Syst Evol Microbiol* 1976; **26**: 226–229.

173. Ceccarelli D, Amaro C, Romalde J, Suffredini E, Vezzulli L. Vibrio species. In: Doyle M, Diez-Gonzalez F, Hill C (eds). *Food Microbiology: Fundamentals and Frontiers*, 5th ed. 2019. American Society for Microbiology, Washington, DC.

174. Gupta RS, Nanda A, Khadka B. Novel molecular, structural and evolutionary characteristics of the phosphoketolases from bifidobacteria and *Coriobacteriales*. *PLoS One* 2017; **12**: e0172176.

175. Esteban J, García-Coca M. *Mycobacterium* biofilms. *Front Microbiol* 2018; **8**: 2651.

176. Winsor GL, Griffiths EJ, Lo R, Dhillon BK, Shay JA, Brinkman FSL. Enhanced annotations and features for comparing thousands of *Pseudomonas* genomes in the *Pseudomonas* genome database. *Nucleic Acids Res* 2016; **44**: 646–653.

177. Bobrov AVFC, Melikian AP, Romanov MS, Sorokin AN. Seed morphology and anatomy of *Austrotaxus spicata* (*Taxaceae*) and its systematic position. *Bot J Linn Soc* 2004; **145**: 437–443.

Appendix A

Supplemental figures

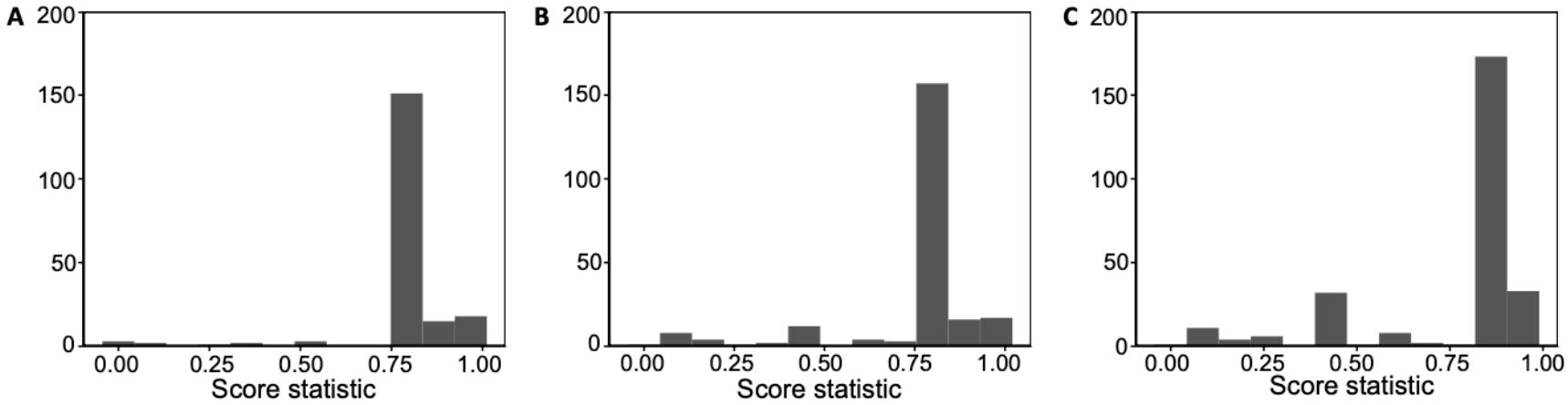

Figure S1 Histograms showing the distribution of score statistics assigned by Decontam [93] to the ASVs detected in the clay and rock sample DNA amplified with 40 (A), 45 (B), and 50 (C) cycles of PCR.

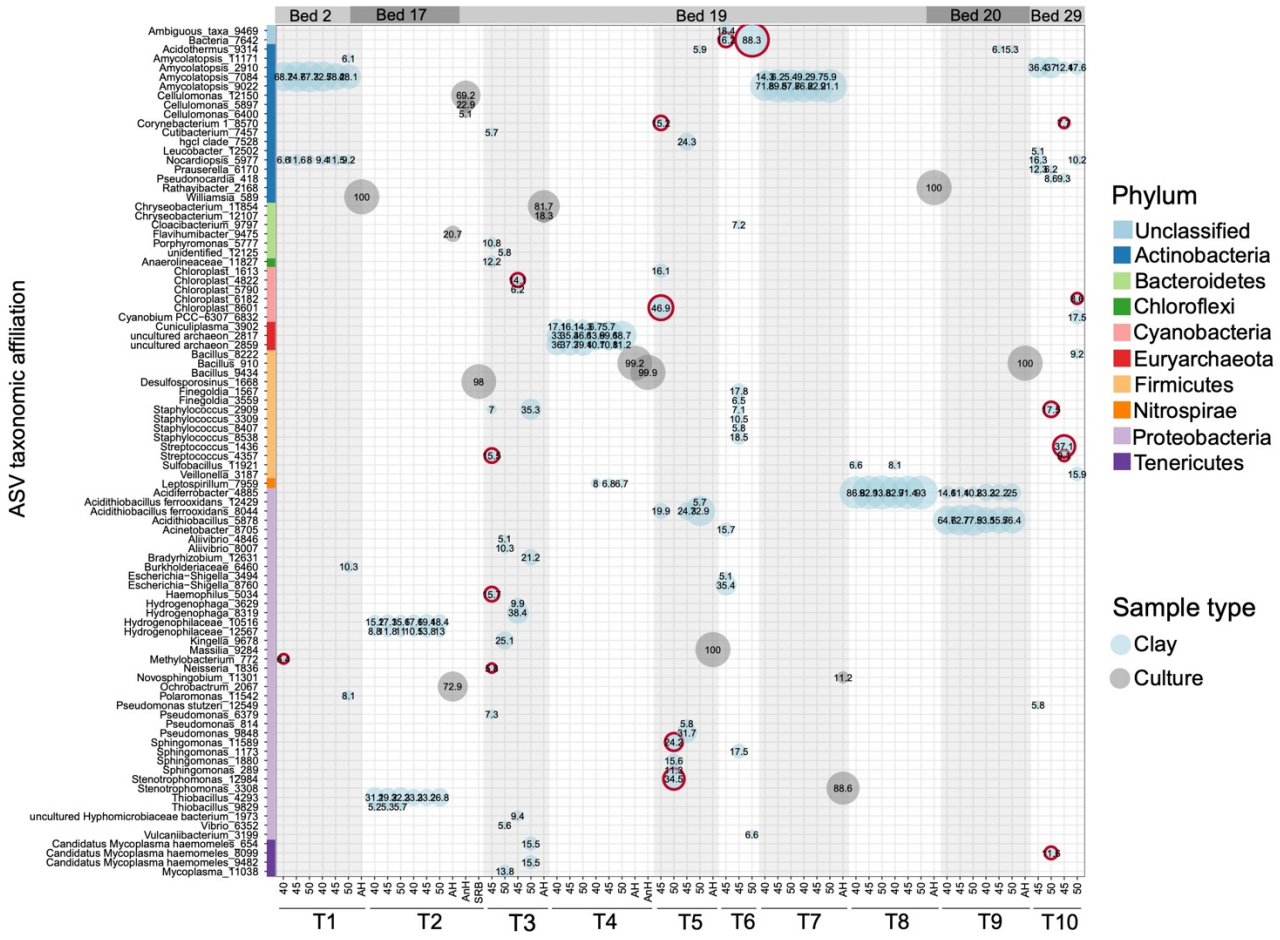

Figure S2 Bubble plot showing the 16S rRNA gene profiles of the ten Tsukinuno bentonite clay samples (blue) and the corresponding aerobic heterotroph (AH), anaerobic heterotroph (AnH), and SRB cultures (grey), with ASVs removed by Decontam [93] with a threshold value of 0.5 indicated (red outline). Only ASVs at or above 5% relative abundance in a sample are included. Up to six replicates were analyzed for each of the ten bentonite samples, comprising of duplicate extractions which were amplified at 40, 45, and 50 cycles of PCR. Samples that showed no visible amplicon in an agarose gel after PCR were not included in the sequencing analysis and thus are not included in this plot. Bed number indicates which bed of the clay deposit each sample was taken from. See Table 3.1 for additional sample information, and Figure 3.13 for a bubble plot with contaminant ASVs removed.

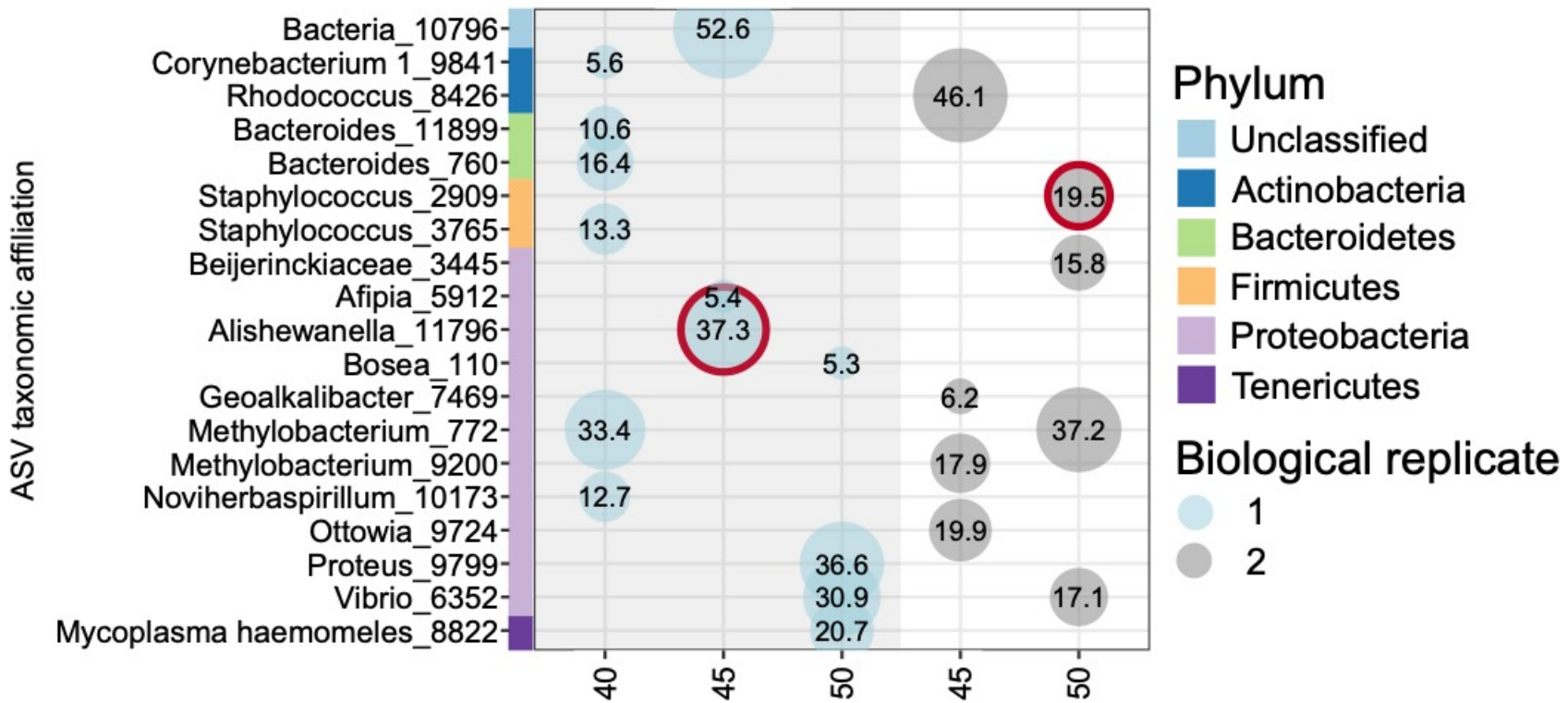

Figure S3 Bubble plot showing the 16S rRNA gene profiles of the Opalinus clay samples, with ASVs removed by Decontam [93] with a threshold value of 0.5 indicated (red outline). Only ASVs at or above 5% relative abundance in a sample are included. The labels 40, 45, and 50 indicate the number of PCR cycles used to amplify the DNA samples. Samples that showed no visible amplicon in an agarose gel after PCR were not included in the sequencing analysis and thus are not included in this plot. See Figure 3.15 for a bubble plot with contaminant ASVs removed.

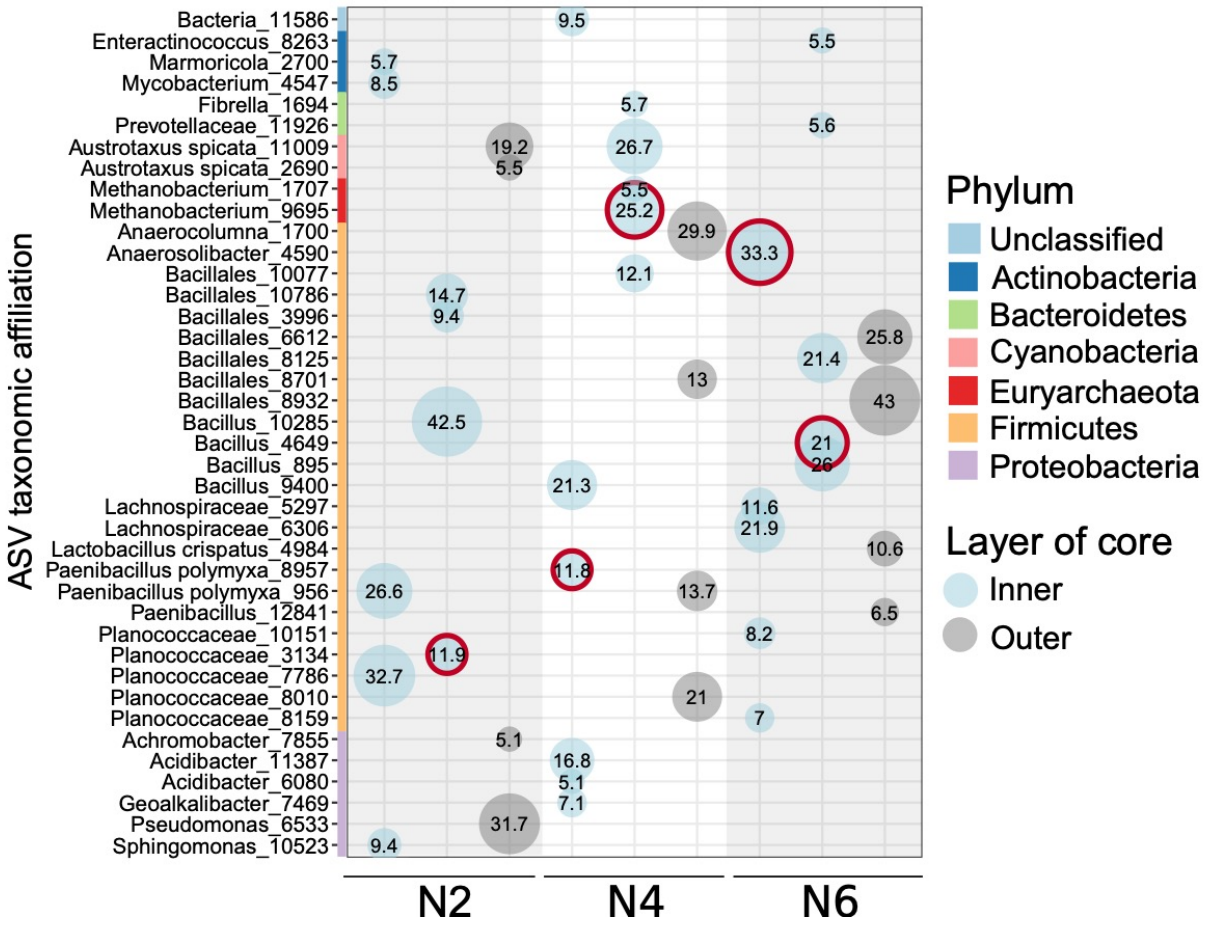

Figure S4 Bubble plot showing the 16S rRNA gene profiles of the NOCR samples, with ASVs removed by Decontam [93] with a threshold value of 0.5 indicated (red outline). Only ASVs at or above 5% relative abundance in a sample are included. See Figure 3.16 for a bubble plot with contaminant ASVs removed.